Rolle der Histonmethyltransferase Suv39h1 in zellulärer Seneszenz und Ras-induzierter Lymphomgenese

DISSERTATION

zur Erlangung des akademischen Grades

d o c t o r r e r u m n a t u r a l i u m
(Dr. rer. nat.)

im Fach Biologie
eingereicht an der

Mathematisch-Naturwissenschaftlichen Fakultät I
der Humboldt-Universität zu Berlin

von

D i p l o m – B i o l o g i n M e l a n i e B r a i g
geboren am 29.04.1978 in Biberach/Riß

Präsident der Humboldt-Universität zu Berlin
Prof. Dr. Christoph Markschies

Dekan der Mathematisch-Naturwissenschaftlichen Fakultät I
Prof. Dr. Christian Limberg

Gutachter: 1. Prof. Dr. rer. nat. Wolfgang Uckert
2. Prof. Dr. med Clemens A. Schmitt
3. Prof. Dr. rer. nat. Reinhold Schäfer

Tag der mündlichen Prüfung: 25. Oktober 2007

Role of the Histone methyltransferase Suv39h1 in cellular senescence and Ras-induced lymphomagenesis

DISSERTATION

to obtain the academic degree

d o c t o r r e r u m n a t u r a l i u m
(Dr. rer. nat.)

in the field of Biology
submitted at the

Faculty of Mathematics and Natural Science I
of the Humboldt University of Berlin

from

M e l a n i e B r a i g (G r a d u a t e i n B i o l o g y)
Born 29.04.1978 in Biberach/Riß

President of the Humboldt University of Berlin
Prof. Dr. Christoph Markschies

Dean of the Faculty of Mathematics and Natural Science I
Prof. Dr. Christian Limberg

Reviewer: 1. Prof. Dr. rer. nat. Wolfgang Uckert
2. Prof. Dr. med Clemens A. Schmitt
3. Prof. Dr. rer. nat. Reinhold Schäfer

Viva voce: 25th of October 2007

This thesis is part of following publication:

Melanie Braig, Soyoung Lee, Christoph Loddenkemper, Cornelia Rudolph, Antoine H.F.M. Peters, Brigitte Schlegelberger, Harald Stein, Bernd Dörken, Thomas Jenuwein and Clemens A. Schmitt:

„Oncogene-induced senescence as an initial barrier in lymphoma-development"

Nature, 2005; Volume 436: 660-665

Meinen Eltern

"Phantasie ist wichtiger als Wissen,
denn Wissen ist begrenzt."

Albert Einstein

Table of contents

I) ABSTRACT (ENGLISH)

Cellular “failsafe” programs like apoptosis or senescence are genetically encoded, stress-responsive mechanisms that ultimately counteract malignant transformation. Acute induction of oncogenic Ras provokes cellular senescence that involves the p16/Retinoblastoma (Rb) pathway to induce a permanent arrest, but the tumor suppressive mechanism *in vivo* still remains questionable. Senescent cells display heterochromatic features on S-phase relevant genes involving methylation of histone H3 on lysine 9 (H3K9me), which may depend on the Rb-associated histone methyltransferase Suv39h1.

In the present thesis it was shown that Eμ-N-Ras transgenic mice harboring targeted heterozygous lesions at the Suv39h1, or the p53 locus for comparison, succumb to invasive T cell lymphomas that lack expression of Suv39h1 or p53, respectively. By contrast, most N-Ras-transgenic wildtype (“control”) animals develop a non-lymphoid neoplasia significantly later. Proliferation of primary lymphocytes is directly stalled by a Suv39h1-dependent, H3K9me-related senescent growth arrest in response to oncogenic Ras, thereby cancelling lymphomagenesis at an initial step. Suv39h1-deficient lymphoma cells grow rapidly but, unlike p53-deficient cells, remain highly susceptible to adriamycin-induced apoptosis. In contrast, only control, but not Suv39h1-deficient or p53-deficient lymphomas senesce after drug therapy when apoptosis is blocked.

These results identify H3K9me-mediated senescence as a novel Suv39h1-dependent tumour suppressor mechanism whose inactivation permits the formation of aggressive but apoptosis-competent lymphomas in response to oncogenic Ras.

Keywords:
Senescence – Ras – Suv39h1 – Histone methylation – Mouse Model – Lymphoma

II) ZUSAMMENFASSUNG (DEUTSCH)

Apoptose und Seneszenz sind stress-responsive, genetisch verankerte „Failsafe“-Mechanismen, welche die Zelle vor maligner Transformation schützen. Onkogenes Ras induziert zelluläre Seneszenz über den p16/Retinoblastoma (Rb)-Signalweg und führt dabei zu einem permanenten Zellzyklusarrest - das tumorsuppressive Potential von Seneszenz *in vivo* bleibt jedoch bis heute fraglich. In seneszenten Zellen ist die Expression von S-Phase relevanten Gene durch die lokale Ausbildung von Heterochromatin, bzw. der Methylierung von Histon H3 an Lysin 9 (H3K9me) blockiert. Dies lässt vermuten, dass Seneszenz ein epigenetische kontrollierter Prozess ist und von Proteinen wie der Rb-assozierte Histonmethyltransferase Suv39h1 reguliert wird.

In der vorliegenden Arbeit konnte gezeigt werden, dass Eμ-N-Ras transgene Mäuse mit heterozygoten Läsionen im Suv39h1 oder p53 Lokus aggressive T-Zell Lymphome entwickeln, die gegen Suv39h1, bzw. p53-Expression selektieren. Im Gegensatz dazu entwickeln N-Ras-transgene Wildtyp-Tiere („Kontrollen“) vorrangig nicht-lymphoide Tumoren und sterben signifikant später. In primären Lymphozyten induziert onkogenes Ras einen Suv39h1-abhängigen, H3K9me-assoziierten Proliferationsarrest und kann dadurch Lymphomgenese verhindern. Suv39h1-defiziente Lymphomzellen wachsen exponentiell und sind, entgegen p53 defizienten Zellen, sensitiv gegenüber Adriamycin-induzierten Zelltod (Apoptose). Jedoch arretieren nur Kontroll-Lymphome unter Therapie *in vitro* wenn Apoptose blockiert ist, nicht aber Suv39h1 oder p53-defiziente Lymphomzellen.

Diese Resultate identifizieren Ras-induzierte Seneszenz als einen neuen, H3K9me-abhängigen Tumorsuppressor-Mechanismus, wobei dessen Inaktivierung die Entwicklung von aggressiven, aber dennoch Apoptose-kompetenten Lymphomen herbeiführt.

Schlagwörter:
Seneszenz – Ras – Suv39h1 – Histonmethylierung – Maus Modell – Lymphome

1) INTRODUCTION

Significance

Cancer is a disease based on intrinsic (epi-) genetic changes that support uncontrolled cell proliferation. To counteract unrestrained growth, cells adopt cellular **"failsafe mechanisms"** that eliminate tumor-prone cells by triggering apoptotic cell death or a permanent growth arrest.
Cellular senescence is known as a permanent cell cycle block that limits the replicative potential of a cell and holds it in an irreversible G1 arrest. It occurs not only as a response to excessive telomere shortening, but also acutely after exposure to cellular stresses like oncogenic signaling, oxidative lesions, or chemotherapy.
Oncogene-evoked senescence mediated by permanent **Ras** signaling requires the tumor suppressor protein p53 and/or the INK4aArf gene products to irreversibly arrest a cell in the G1 phase of the cycle. Consequently, the disruption of those regulators cancels the failsafe machinery and promotes Ras-driven transformation *in vitro*. Ras-induced senescence was shown to involve epigenetic changes that silence S phase promoting genes by Rb-dependent heterochromatin formation, accompanied with methylated lysine 9 on histone H3 (H3K9) and the subsequent recruitment of heterochromatin proteins such as HP1. This suggests that epigenetic factors, e.g. the Rb-bound histone methyltransferase **Suv39h1**, are crucial mediators of the senescence response machinery; and deregulation might impact malignant transformation, likely also *in vivo*.
Understanding the molecular network of uncontrolled proliferation as a key prerequisite of cancer formation has become an issue of intense research and will provide not only deeper insights into the process of tumorigenesis, but will also raise the possibility of developing more effective and specific strategies to treat cancer.

1.1 Cellular senescence and tumor development

Cancer arises as a consequence of cells escaping restrictions that normally limit their uncontrolled expansion. Suppression and elimination of such autonomous cells or their pre-neoplastic precursors are a key property to protect cellular integrity of an organism[1]. Numerous mechanisms, so-called "failsafe programs", exist in a cell that counteract malignant conversion[2].

Apoptosis is the most prominent failsafe mechanism studied so far. In the past decades, various publications uncovered apoptosis as the ultimate rescue from cellular transformation and as the major response to chemotherapy in cancer patients

(reviewed in [3-5]). However, it becomes more and more clear that there are additional programs that presumably control those biological processes. Certain cellular stresses or activated oncogenes do not necessarily force cells to die in a programmed fashion, but rather to exit the cycle and enter a permanent arrest reminiscent of cellular senescence.

1.1.1 Cellular senescence

Decades ago, Hayflick and colleagues invented the term “cellular senescence” as a stable proliferation arrest of human diploid fibroblasts in culture when cells loose their ability to divide caused by the accumulation of cell doublings[6]. Later, excessive telomere shortening was found to be the initiating event leading to the permanent arrest (“replicative senescence”)[6,7], linking the phenomenon to the “growing old” or “aging” of a cell (Figure 1; left). Indeed, senescent cells were reported to accumulate in aging skin fibroblasts of primates[8,9] or in other tissues such as liver or retina[10,11], assuming a putative role for senescence in organismic aging.

In the past years, also intrinsic factors or environmental insults were found to irreversibly block the growth of a cell. Various stimuli like supraphysiological mitogenic signaling, DNA damage or oxidative lesions as well as genetic defects are known to induce this acute form of arrest (“premature senescence”)[12-16] (Figure 1; left).

Features of cellular senescence

Senescence depends on several pathways that result in a permanent growth arrest irreversibly locking the cell in the G1-phase of the cycle[17]. Notably, this senescent arrest differs from a cell cycle arrest in normal, regenerative tissues. In general, oscillating cells in G1 can, before commitment to DNA replication, enter a resting state where they survive for extensive periods of time. Importantly, those cells are capable to re-entering the cycle upon stimulation, whereas a senescent cell remains insensitive to mitogenic signals.

Although senescent cells are viable and remain metabolically active they undergo characteristic changes in morphology turning more flattened and displaying a vacuole rich cytpoplasm[9]. Furthermore, they show an altered gene and protein expression

pattern compared to normal cycling or quiescent cells[9,18]. Upregulation of proteins like p53[15,19], ARF[20,21], p16^{INK4a}[15] or the product of the promyelocytic leukemia gene (PML)[22,23] are main features of a senescent cell (Figure 1; right). In addition, lysosomal activity of the cytoplasmic ß-galactosidase enzyme is increased, which can be detected by a colorimetric assay using X-gal as substrate – currently the gold standard procedure to detect a senescent phenotype[9] (Figure 1; picture).

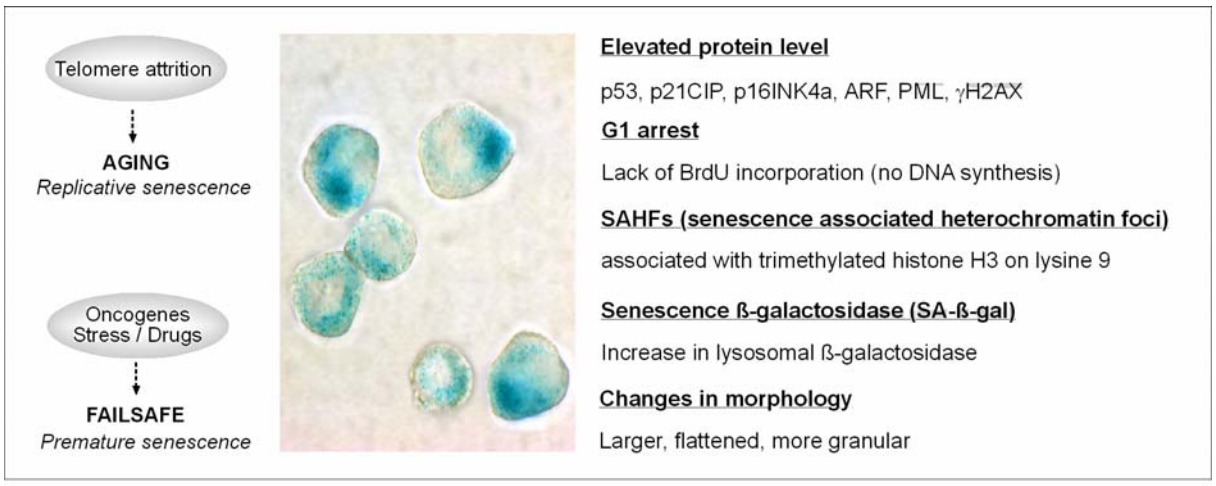

Figure 1: Cellular senescence. Left side: Cellular senescence is induced by excessive telomere shortening ("replicative senescence", top) when cells age or acutely as a failsafe program induced by activated oncogenes, stress like serum starvation, reactive oxygen species (ROS) or chemotherapy ("premature senescence"; bottom). **Right side:** Features of a senescent phenotype. **Picture:** Chemotherapy induces senescence in apoptotically blocked T cell lymphomas. Endogenous ß-galactosidase is increased in senescent cells and can be detected by an enzymatic reaction resulting in a cytoplasmic, blue staining (own data).

Regulators of cellular senescence

Since senescence is characterized by a permanent G1 arrest[17], significant emphasis has been placed on proteins that control cell cycle progression and therefore a senescent phenotype. Indeed, several cell cycle regulators and their connected pathways were shown to mediate a senescence response.

The CDK inhibitor p16^{INK4a} is a critical effector of G1-/S phase transition and was found to be transcriptionally overexpressed during replicative as well as premature senescence[15,24,25]. p16^{INK4a} promotes a G1 arrest by blocking cyclins that are relevant for S phase entry (CDK4/6) by maintaining the Rb protein in its hypophosphorylated, growth-suppressive state. In this activated form Rb associates with several transcription factors, of which the most prominent is E2F, and silences their

transcriptional function on S phase relevant promoters (e.g. cyclin E or A). In addition, also the transcriptional activity of the tumor suppressor p53 significantly increases with the accumulation of cell doublings and upon certain stress stimuli[15,26]. p53 is an essential effector of the cell cycle machinery and induces a broad variety of downstream targets (e.g. the CDK inhibitor $p21^{CIP}$) that contribute to diverse phenotypes, including a senescent cell cycle arrest. p53 is regulated by the alternate reading frame product of the INK4aArf locus ("ARF") that blocks the p53-degrading activity of MDM2 and therefore stabilizes p53. Importantly, also ARF turns to be overexpressed – at least in murine cells – during cellular senescence[21,27].
Taken together, the activation of the $p16^{INK4a}$/Rb axis and/or the ARF/p53[28] pathway promotes the establishment of a stable growth arrest and therefore a senescent phenotype depending on the cell type and the particular stimulus.

Ras, an oncogene that induces senescence

In additional to numerous stimuli like telomere attrition, DNA damage and some chemotherapeutic agents, also oncogenes were shown to induce a senescence-like cell cycle block.
In 1997, Serrano and colleagues unveiled for the first time in rodent and human fibroblasts that acute overexpression of oncogenic Ras provokes a cell cycle arrest reminiscent of cellular senescence *in vitro*[15]. Moreover, Serrano *et al* found an upregulation of proteins like $p16^{INK4a}$, p53 and $p21^{CIP}$, a manifest cell cycle block locking the cells in G1 and an increase in endogenous ß-galactosidase. This hallmark finding underlines the putative senescent phenotype and states that in response to oncogenic Ras-signaling cells acutely undergo senescence to counteract uncontrolled growth. Data from intense research unveils that Ras predominantly involves the MEK/MAP kinase pathway[29] that activates the p16-Rb axis to induce cellular senescence. Hereby, transcription factors from the Ets family were shown to activate the expression of the tumor suppressor protein $p16^{INK4a}$. As discussed above, $p16^{INK4a}$ indirectly promotes the hypophosphorylation of the Rb protein by inhibiting the D-type cyclin-dependent kinases CDK4 and CDK6. This keeps the transcription factor E2F bound to the Rb protein, halts the cell in the G1-phase and prevents S phase entry (Figure 2 and Figure 4).
In contrast to a "conventional" cell cycle arrest on the Rb-governed restriction point, e.g. after serum starvation, the Rb-dependent G1 block representative for

senescence is irreversible and cells are insensitive to any mitogenic stimuli. In this context, it is highly indicative that E2F responsive S phase genes are stably silenced during cellular senescence, likely via local chromatin changes. Indeed, it was shown recently that Ras-induced senescent cells display Rb-mediated "senescent-associated-heterochromatin foci" (SAHFs), transcriptionally silenced heterochromatin regions mapped to E2F responsive promoters and enriched for methylated histone H3 lysine 9 (H3K9)[30]. This supports the hypothesis that senescence is an epigenetically controlled program where S phase promoting genes are repressed by histone methylation.

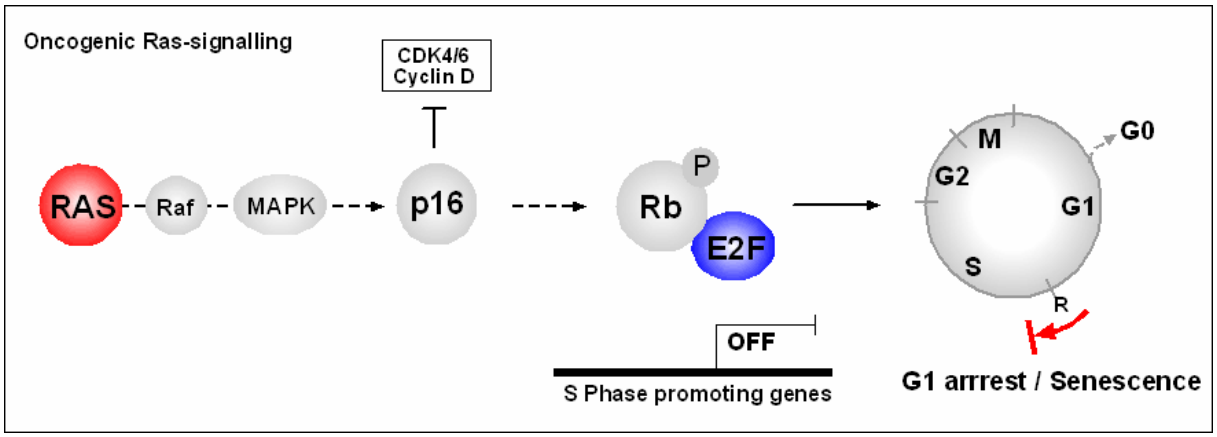

Figure 2: Cellular responses to oncogenic Ras signaling: Excessive mitogenic signaling by oncogenic Ras (red) activates the MAPK pathway that leads to the expression of the tumor suppressor $p16^{INK4a}$. $p16^{INK4a}$ blocks the hyperphosphorylation of Rb by inhibitory binding to the kinase domain of CDK4/6. This keeps E2F transcription factors bound to Rb, while, consequently, S phase relevant genes remain unaffected provoking a permanent cell cycle stop.

1.1.2 Cellular failsafe programs

Oncogenes and the cellular failsafe machinery

As previously outlined, it seems that in response to oncogenic stress cells are able to recruit programs like senescence to ultimately counteract unrestrained proliferation. Those so-called "cellular failsafe mechanisms", like programmed cell death (apoptosis) or senescence, can be recruited upon intra- or extracellular stress stimuli

to get rid of defective cells[2]. In fact, also other oncogenic stresses were shown to induce this cellular failsafe machinery.

The proto-oncogene Myc is a transcriptional regulator that transduces a potent mitogenic stimulus by positively regulating cell cycle regulators but, concomitantly, induces apoptosis in the absence of survival factors[31,32]. Hereby, Myc activates ARF, the "alternative reading frame" product of the INK4aArf locus that directly inhibits the p53 repressor MDM2. This leads to the activation of p53 inducing apoptotic cell death (Figure 3).

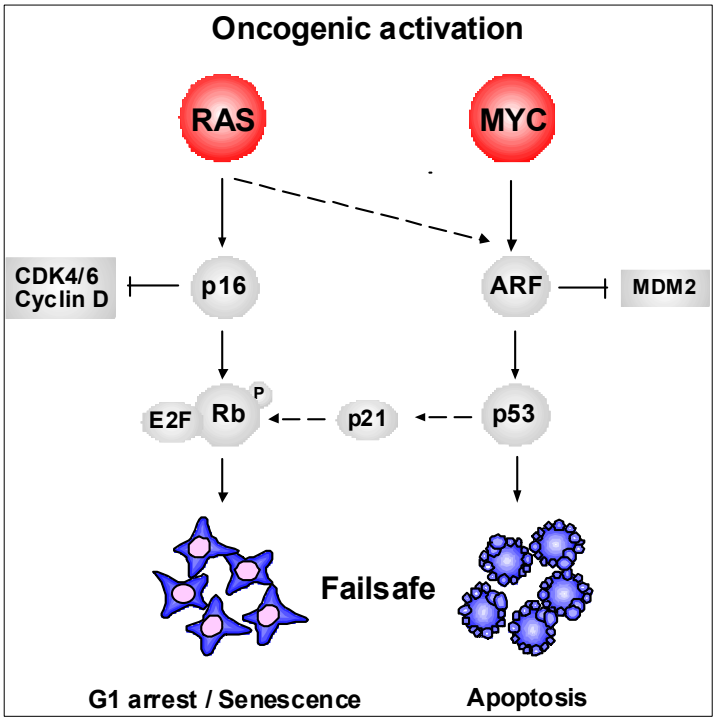

Figure 3: Cellular failsafe programs induced by oncogenic activation: Oncogenic Ras or Myc provoke either a terminal growth arrest (senescence) or programmed cell death (apoptosis) by the activation of the $p16^{INK4a}$ and/or ARF proteins. Ras-induced senescence is controlled via the inhibition of the cyclin dependent kinases 4 and 6 (CDK4/6) either through $p16^{INK4a}$ or alternatively through p53-induced p21. This retains the E2F transcription factor and keeps it bound to Rb, indirectly silencing E2F-responsive promoters of growth promoting S-phase genes. Myc induces apoptosis by the induction of the ARF protein that blocks the p53 inhibitor MDM2. Subsequently, p53 can be activated and induces downstream effector targets that trigger an apoptotic response or a cell cycle arrest.

Furthermore, the adenoviral oncoprotein E1A stimulates prosurvival signaling and permits hyperproliferation; however, E1A fails to transform primary cells because of the induction of p53-dependent cell death (apoptosis)[31,33].

The insufficient regulation of such oncogenic signaling, in particular the cancellation of those failsafe programs, provides a basis for cells to adopt unrestrained growth capabilities and forces malignant transformation.

1.1.3 Tumor development

The development and progression of a tumor is a multistep process that requires numerous genetic or epigenetic alterations leading to a malignancy[34]. Various regulatory programs and anti-cancer mechanisms need to be disrupted before neoplastic transformation can occur. Growth signal independent proliferation, unlimited replicative potential and defects in apoptosis as well as sustained angiogenesis and metastasis are considered the "Hallmarks of Cancer" and display the main features a cell must acquire during tumorigenesis[1].

Malignant transformation

It was a paradigm for years that telomerase activity, together with other cooperative events, is prerequisite for malignant transformation[35-37]. However, the first report in 2002 sufficiently unveiled that simply two oncogenes in combination with p53 inhibition are enough to transform human cells *in vitro* and form, when transplanted into nude mice, tumors *in vivo*[38]. Later, comprehensive data using rodent systems showed that telomerase is not absolutely necessary for malignant conversion. For instance, the functional disruption of p53 or genetic ablation of the INK4aArf locus cooperates with oncogenic Ras to induce malignant transformation. Primary mouse embryonic fibroblasts (MEFs) deficient for p53 or INK4aArf can directly be transformed in response to oncogenic Ras and show features like anchorage-independent growth and a refractile morphology[15], characteristics of a malignant phenotype.

Indeed, the activation of proto-oncogenes and the disruption of tumor suppressors are frequently found as the driving force in human entities. Tumor suppressors like the transcriptional regulator p53, the cell cycle mediators Rb and $p16^{INK4a}$ are often mutated in human cancers. Accompanied with mutated (e.g. Ras) or amplified oncogenes (e.g. Myc) these alterations permit uncontrolled growth and finally lead to a full-blown malignancy[1].

While there are numerous hypotheses discussing what drives tumor formation, it is frequently observed that disruption or cancellation of the cellular failsafe machinery displays an early event during tumorigenesis initiating a malignant phenotype (Figure 4)[39]. Other defects that are acquired during tumorigenesis are considered to be a consequence and are therefore not always necessarily required for transformation[1,2,40,41].

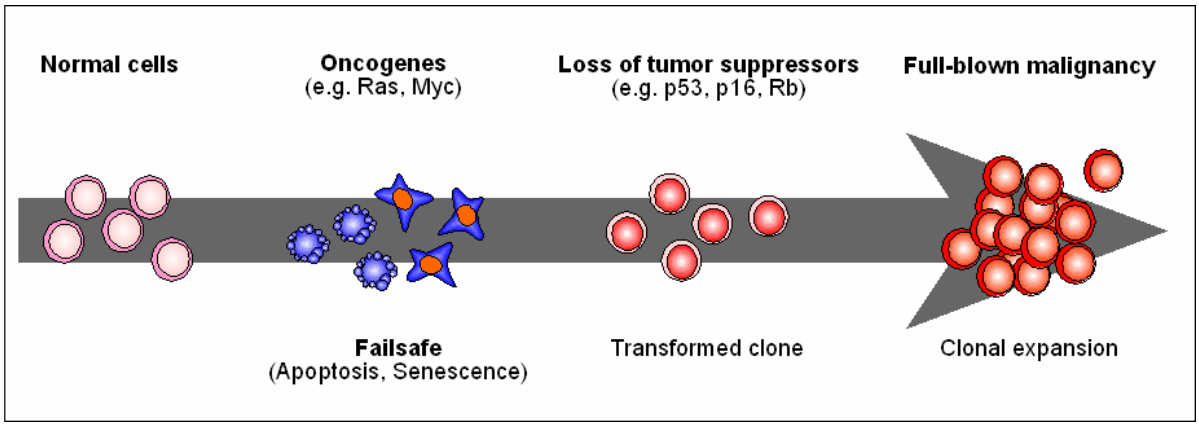

Figure 4: A road to malignant transformation. Loss of tumor suppressors (e.g. p53, ARF, p16, Rb) is required to escape oncogene-induced failsafe programs such as apoptosis or senescence. Their inactivation provides the basis for malignant transformation and therefore promotes tumor formation.

Ras and its role in tumor formation

Studies including transgenic mouse models and carcinogen-induced Ras-tumors in mice suggest a crucial role for oncogenic Ras during tumorigenesis[42-51], but the direct consequence of Ras mutations in human tumors has not been fully understood so far. Currently, there is convincing evidence from *in vitro* studies that oncogenic Ras triggers senescent growth arrest to prevent transformation. Consequently, pre-neoplastic lesions with defined primary Ras mutations would likely undergo a senescent arrest to counteract malignant transformation, while full-blown malignancies have escaped the senescent failsafe machinery. However, those issues remain elusive until now.

Enhanced mitogenic signaling was frequently linked to constitutively activated Ras[52]. At present, it is known that mutated *ras* alleles, predominantly codon 12, 13 or 61, were found in almost one third of human cancers[52]. Moreover, many tumors appear

to be driven by activated signaling of the Ras cascade due to constitutive oncogenic upstream modifications (e.g. the ErbB2 (Her2/neu) receptor activation[53]) or downstream alterations (e.g. constitutive activation of the B-Raf protein).

Ras genes were identified already in the early 1960s as transforming elements of the Harvey and Kirsten rat sarcoma virus[54,55]; however, their oncogenic capacity was first linked to human tumors in the mid 80s[52,56,57]. The mammalian family of *ras* genes consists of three members located on different chromosomes encoding for the independent, but structurally highly related proteins H-Ras, K-Ras and N-Ras[58,59]. Hereby, the *H-* and *K-ras* genes reflect the cellular counterpart of the viral *Harvey* and *Kirsten* genes[54,55], respectively, while N-Ras is missing a viral counterpart and has been found mutated in a human neuroblastoma cell line. Expression patterns of the different isoforms are highly variable during embryonic development and also differ in adult tissues[60-63]. Thus, H-Ras is mainly expressed in brain, muscle and skin, N-Ras predominantly in thymic glands or testis and K-Ras shows its highest expression levels in gut or lung. However, the predicted function in those organs is not fully understood until today.

The *K-ras* gene is mutated in more than 90% of pancreas carcinomas and 50% of colorectal tumors. Also lung and bladder, thyroid and ovarian tumors are frequently mutated in one of the *ras* genes. The mutation leads to the constitutive activation of the Ras protein by rendering it insensitive to GTPases and confers a permanent stimulation of intracellular kinase cascades irrespective of external stimuli. This provokes uncontrolled proliferation and degradation of the extracellular matrix and involves the expression of cell cycle regulators (e.g. cyclin D1) or matrix metalloproteases (e.g. PAI-1) that influence invasiveness and metastasis.

Tumor formation and epigenetics

It is widely believed that the key to all eukaryotic organisms is inherited through the genome and that alterations in the DNA code, e.g. mutations in the *Ras* genes, are the basis for malignancies. Whereas deoxyribonuclein acid (DNA) is considered the ultimate template of life, it seems that there are mechanisms beyond that regulate and transduce genomic information[64].

In the past few years, one just realized that variations on an epigenetic level can potentiate genetic information without affecting DNA sequence. The “Histone code”, proposed in the year 2000 by Strahl and Allis[65], suggests a striking role for DNA-packaging proteins (histones) in changing higher order chromatin structures and regulating accessibility of genomic information[66]. Depending on their modification status, histones and related proteins display crucial regulators that control transcriptional states. Deregulation likely contributes to tumor development since mistargeting of these enzymes contributes to altered transcriptional regulation of tumor promoting or tumor suppressing genes[67].

Given the attractive hypothesis that Ras-induced senescence is an epigenetically controlled process[30] it is conceivable that epigenetic regulators trigger a senescent response, whereas their deregulation might have an impact on tumor formation.

1.2 Histone methylation and Suv39h1

Eukaryotic DNA is folded, twisted and compacted into a complex structure called chromatin. Chromatin condensation relies on the organization of nucleosomes, the basic repeating unit of the chromatin that consists of double stranded DNA wrapped two times around an octamere of the basic core histones H2A, H2B, H3 and H4[68-71]. Nucleosomes are connected to linker histones (H1) that compact and twist the chromatin fiber and associate with non-histone proteins leading to higher chromatin structures.

Transcriptionally active chromosome regions (euchromatin) can be discriminated from inactive parts (heterochromatin) that are highly condensed and contain facultatively or constitutively silenced genes. The dynamic change between euchromatin and heterochromatin relies on the re-organization of the nucleosomes. Remodelling of certain chromosome regions alters the contact between DNA[70] and the core histone complexes, and controls a variety of DNA-based processes like transcription, DNA repair or replication[72].

1.2.1 Histone modifications

Changes in chromatin structure include, besides the depositioning of nucleosomes (ATP-dependent "nucleosome-sliding") through co-factors like Swi/Snf or NURD[73-75], the covalent modification of histone "tails", the amino-terminus of the core histones that protrude from the nucleosome. These post-translational modifications comprising phosphorylation, methylation, acetylation or ubiquitinylation are transduced by certain enzymes and are highly specific for the amino acid position (Figure 5 top and [72]), whereas reversibility of such modifications contributes to the highly dynamic "on-off" switch in chromatin structure.

Covalent modifications of histone tails

Chromatin changes are regulated by pathways that transfer extrinsic signals or internal changes to the nucleus in order to control gene transcription. Accordingly, histone modifications represent a molecular fingerprint of a cell depending on the biological phenotype (Figure 5 bottom).

In a resting cell, growth promoting stimuli result in a global change the in histone modification pattern contributing to a more relaxed chromatin structure on S-phase responsive gene loci. This euchromatic structure is mainly characterized by hyperacetylated histones and methylation of H3 (K4, K36, K79). Contrarily, arrested, non-proliferating cells display mainly heterochromatin structures on growth promoting genes that are less acetylated and predominantly methylated at histone 3 (K9, K20, K27) or histone 4 (K20)[65,76].

Histone acetylation of lysine residues is catalysed by histone acetyltransferases (HATs) and reversed by histone deacetylases (HDACs)[77,78]. Hyperacetylation of histone tails neutralizes the basic histone complex and reduces affinity to DNA, thereby mainly contributing to transcriptional activation. Specific kinases induce the phosphorylation of several histone residues and mediate, like acetylation, gene activation by loosening the contact between nucleosomes, DNA and associated proteins. Not surprisingly, phosphoacetylated serine 10 on histone H3 is found upon mitogenic signaling in nucleosomes of promoter regions of immediate early genes like *c-jun* or *c-fos*[72,78]. Both, histone acetylation and phosphorylation contribute

predominantly to transcriptional activation and represent highly dynamic modifications that instantly can be reversed by enzymes like HDACs or phosphatases.

In contrast, methylation of lysine and arginine residues seems to be of a different nature. Depending on the site, methylation of histone residues can regulate either transcriptional activation or repression. Until recently, methylation seemed to be a permanent epigenetic mark. Specifically, lysine 9 methylation on histone H3 plays an important role and will be outlined in greater detail.

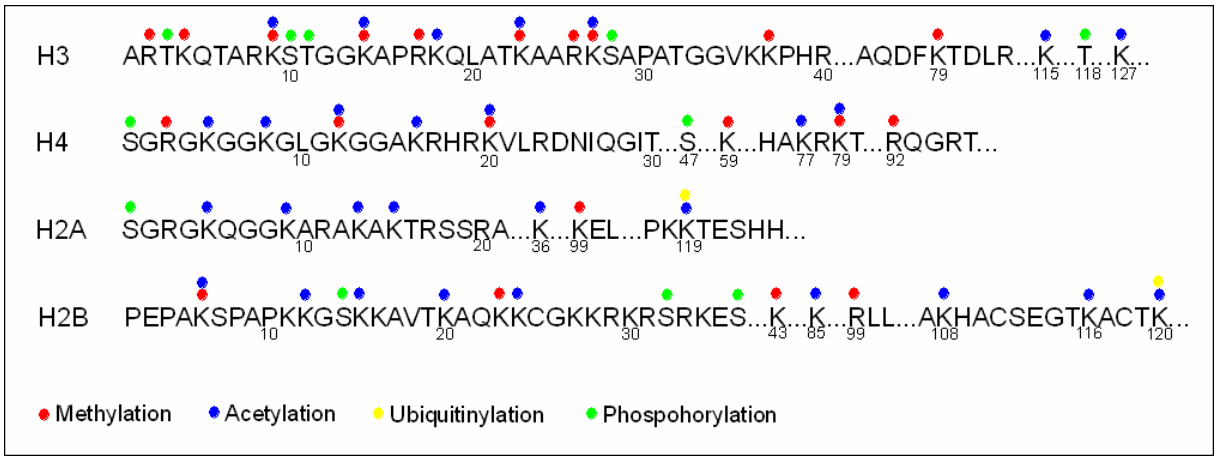

Figure 5: Covalent modifications on histone tails and their biological responses: Top: Putative sites for methylation (red), acetylation (blue), ubiquitinylation (yellow) and phosphorylation (green) on the core histones H3, H4, H2A and H2B[72]. Other modifications like sumoylation or ADP-ribosylation and modifications on the N-terminus of the linker histone H1 are neglected in this context. **Bottom**: Enzymes that catalyze covalent histone modifications of specific residues of histone tails and their biological function. Histone acetylases and kinases confer predominantly transcriptional activation, whereas histone methylation promoted by methyltransferases mediates both silencing and activation of transcription.

	Acetylation	Phosphorylation	Methylation
Enzymes	***Histone acetylases*** **CBP/p300** **MYST** **TAFII250** **HAT1**	***Histone specific kinases*** **Rsk-2** **Aurora-B-kinase** **ATM, ATR, DNA-PK**	***Histone methyltransferases*** **Suv39h1** **Ezh2** **G9a** **Set9**
Biological funtion	**Transcriptional activation** **Replication** **Nucleosome remodelling**	**Transcriptional activation** **Repair** **Apoptosis**	**Transcriptional activation** **Transciptional repression** **X-inactivation** **Imprinting**
Residue	**Lysine (K)**	**Serine (S) / Threonine (T)**	**Lysine (K) / Arginine (R)**

1.2.1 Histone methylation

Histone methylation was first described in the early 60s, however, the linkage between methylation of histones and transcriptional regulation was discovered more than 30 years later. During the last years, exciting new research unveiled the importance of histone lysine methylation in heterochromatin formation, gene silencing and imprinting (reviewed in [79-81]) and is even thought to be relevant for the regulation of non-histone proteins[82].

Histone lysine 9 methylation and gene silencing

Histone lysine methylation appears to be the key mechanism to silence gene transcription on an epigenetic level. Methylation comprises residues on histone H3 (K4, K9, K27, K36), histone H4 (K20)[83-86]. Lysines can be mono-, di- or tri-methylated[87,88] and the particular degree on the histone tail confers different biological outcomes. Of note, lysine methylation depends on the highly selective interplay between other covalent modifications on the nucleosomes or the DNA template[76]. Methylated H3K9 for instance directly antagonizes adjacent H3K4 methylation as well as phosphorylation of serine 10 that would provoke transcriptional activation. In addition, histone methylation can directly be linked to the methylation of DNA, an alternative way repressing the transcription of certain genes. Since DNA methylation itself blocks acetylation of histone residues, a putative feedback loop exists that locally enhances repression and forces heterochromatin formation.

Histone methylation and cancer

Given the fundamental impact of epigenetic processes in the regulation of nearly all biological processes deregulation of epigenetic mechanisms contribute to uncontrolled proliferation and therefore to cancer formation. Intense research in the last years unveiled global changes in DNA methylation and histone acetylation as prerequisite for cancer formation, while therapeutic drugs to restore a normal epigenetic phenotype are currently in pre-clinical studies or already under clinical investigation. Conversely, how histone methylation contributes to tumorigenesis is poorly understood so far. Mice defective in Riz1, a HMT that methylates H3K9, are prone to tumor formation[89] and mutations in the PR-domain of the gene were found

in human breast cancer, melanomas, lung carcinomas or colorectal tumors[90]. However, detailed evidence supporting this data is missing up to now.

1.2.2 The Suv39h HMTs

In the beginning of the 90s, screens for PEV (position effect variegation) in *Drosophila melanogaster* and *S. pombe* identified a subclass of 40 gene loci referred to as the *Su(var)* (suppressor of variegation) group[91,92]. Genes of the *Su(var)* group encode numerous histone deacetylases, protein phosphatases and S-adenosyl methionine synthetases, but also heterochromatin associated proteins (Suv(var)2-5, Su(var)3-7 and Su(var)3-9). Of note, *Drosophila* Su(var)3-9 as well as the *S. pombe* Crl4 display the most powerful PEV modifiers.
In 2000, Rea *et al* identified and isolated for the first time the corresponding human (SUV39H1) and murine (Suv39h1) homologues, respectively[93]. Those enzymes turned out to be histone methyltransferases specific for methylating histone H3 at position 9 (H3K9). Importantly, the selective methylation of H3K9 catalyzed by Su(var) proteins creates a binding site for heterochromatin proteins like HP1 contributing to the propagation of stable heterochromatic regions and putatively to local gene silencing.

Molecular structure and function

Proteins of the SU(VAR)3-9 family members contain two of the most evolutionarily conserved chromatin regulating motifs, the N-terminal “chromo” (chromatin organization modifier) and the C-terminal “SET” domain (Figure 6) .
The SET domain was initially named after the three founding members **S**U(VAR)3-9, **E**(Z) from the polycomb-group and the trithorax-protein **T**RX and is found in more than 140 gene sequences throughout the species. However, there are SET-domain harboring proteins with different and even antagonistic functions, and only a few were linked with histone methyltransferase activity[94,95]. To comprise HMT activity, the combination of the SET domain with adjacent cystein rich regions is required. This is restricted to only a number of SET domain encoding proteins like the SUV39H family members or the yeast homologue Crl4.

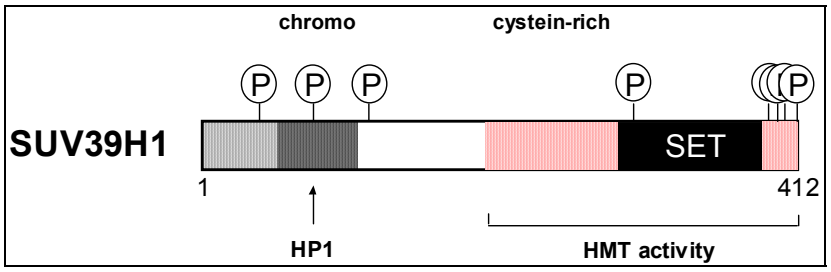

Figure 6: Structure of the human SUV39H1 protein: SU(VAR) proteins contain two highly conserved elements: the SET domain (black) with adjacent cystein-rich sequences (red) that comprise the HMT activity located at the C-terminus of the protein and an N-terminal chromodomain (dark grey) for putative binding partners like HP1.

Members of the SU(VAR)3-9 family are highly conserved from yeast to human and also the correlated function, gene silencing through histone methylation, seems to be evolutionarily preserved. SU(VAR)3-9 proteins have been shown to be restricted to modifying histone H3 at lysine 9 by either mono, di- or trimethylation. H3K9 methylation creates a binding site for heterochromatin proteins like HP1 that contributes to the condensation and compaction of chromatin. Furthermore, HP1 complexes with Suv39h through the chromo-domain and enhances therefore the repressive action on the chromatin region.

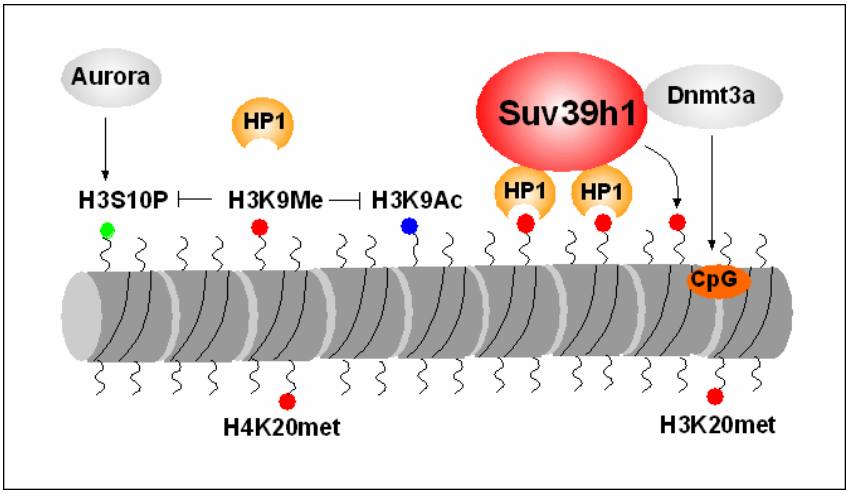

Figure 7: Heterochromatin formation involves the Suv39h1 protein: Suv39h1 locally methylates lysine 9 on histone H3 (red). This recruits heterochromatin proteins like HP1 that bind to the methylated H3K9 mark as well as to Suv39h1 and stabilize heterochromatic chromatin regions. Simultaneously, phosphorylation of serine 10 (green) and acetylation of the H3K9 (blue) is blocked that would otherwise confer a relaxed chromatin structure. DNA methyltransferases (DNMTs) such as Dnmt3a, also linked to Suv39h1, methylate DNA on CpG islands and facilitate therefore stable heterochromatic sites.

Interestingly, acetylation of histone H3 (H3K9ac) or phosphorylation of serine 10 (H3S10ph) via the Ipl1/aurora kinase blocks the transfer of a methyl group to lysine 9[93] (Figure 7). These findings underline the interplay and interdependence of SU(VAR)3-9-dependent H3K9 methylation and other site-specific histone tail modifications like phosphorylation or acetylation. It was also shown that Dnmt1 and Dnmt3a, DNA methyltransferases, interact *in vivo* and *in vitro* with the SUV39H1 HMT and thereby facilitate gene silencing. Since DNMTs, like MeCP2, form complexes with histone deacetylases (HDACs) as well, a putative feedback loop exists that enhances repression by blocking acetylation of histone residues[96-99] (Figure 7).

Two members of this HMT family, human SUV39H1/SUV39H2 and their murine homologues Suv39h1/Suv39h2, will be described as selective H3K9 methyltransferases in more detail.

Suv39h enzymes were shown to be crucial epigenetic regulators in mammalian development[100] and were demonstrated to control chromosomal segregation, local gene repression and S-phase related gene silencing. Despite knockout mice deficient for both Suv39h1 and Suv39h2 are viable, they are born only at sub-Mendelian ratios due to an increased rate of prenatal lethality, and are growth retarded at birth and during adulthood[100]. During embryogenesis, Suv39h1 and Suv39h2 are expressed in various tissues in an overlapping pattern. In contrast, in adult mice, Suv39h2 was found to be mainly expressed in testis[101] suggesting an important role for this isoform in the male germline. Indeed, male Suv39h double knockouts are infertile and spermatogenesis is severely impaired in those animals. Suv39h double null mice are prone to tumor development and highly susceptible for B cell lymphomas, potentially due to segregation defects in mitosis leading to chromosomally instable karyotypes[100]. Primary mouse embryonic fibroblasts (MEFs) isolated from double knockout mice do not show global changes in H3K9 methylation pattern, however H3K9 methylation is completely absent in DAPI-enriched heterochromatic regions. These observations underline the putative role of the Suv39h HMTs as regulators of pericentric heterochromatin regions protecting genomic stability during mammalian development.

As already highlighted, Suv39h proteins interact with a broad variety of chromatin associated proteins and histone modifiers underlining their central role in the

regulation and maintenance in stable heterochromatin regions. Importantly, it was shown that Suv39h1 associates with the tumor suppressor protein Rb on euchromatic regions[102]. Thereby, the Suv39h1/HP1 complex binds hypophosphorylated active Rb by parts of its pocket domain and directs methylation of histone H3. The Retinoblastoma protein, regulated by the cyclin D-inhibitor $p16^{INK4a}$, controls the repression of S phase relevant genes by locking the transcription factor E2F in its inactive state, likely by methylating nucleosomes in the vicinity of the responsive promoters through Suv39h1. This indicates that the Suv39h1-HP1 complex does not only regulate pericentric chromatin regions, but also euchromatic Rb-related genes by focal heterochromatinization (Figure 8).

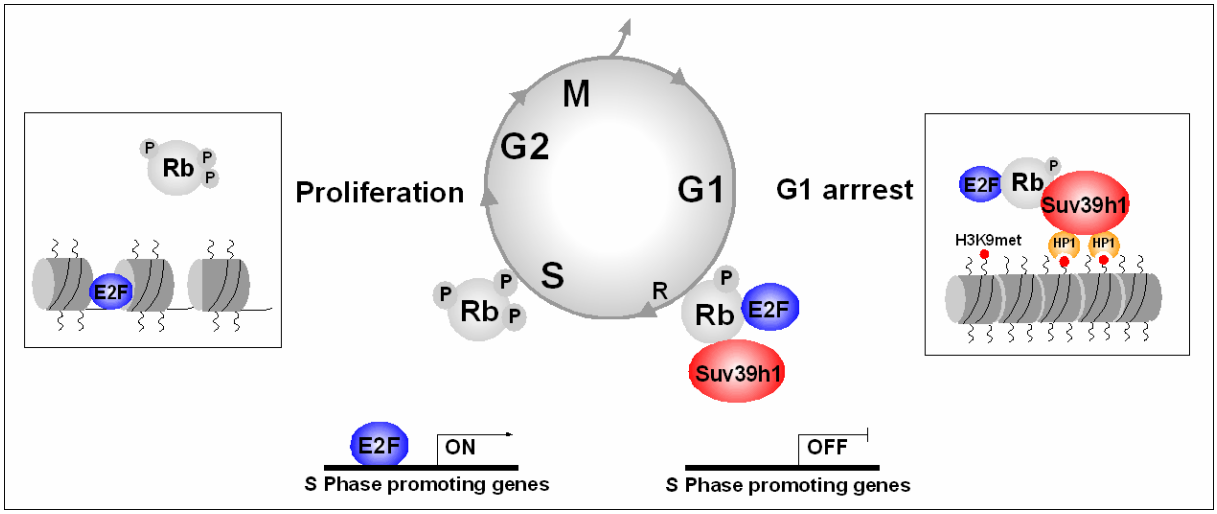

Figure 8: Suv39h1 and cell cycle regulation: Suv39h1 interacts with Rb in its hypophosphorylated and E2F connected form. This suppresses the transcription of S phase relevant genes by local induction of heterochromatin catalyzed by methylation of H3K9.

1.3 Proposed Model

Cellular failsafe mechanisms activated upon permanent oncogenic signaling account for the ultimate rescue from malignant transformation. Oncogenic Ras has been shown to provoke a terminal cell cycle arrest (premature senescence) that is considered a putative tumor suppressor mechanism *in vitro*[15]. Premature senescence is accompanied with accumulation of the tumor suppressor p53[15] and the cell cycle regulator $p16^{NK4a}$[15] that keeps the Retinoblastoma protein in its hypophosphorylated form preventing the transcription factor E2F from transactivating growth promoting

genes. Remarkably, in senescent cells E2F responsive promoters are transcriptionally silenced by the local formation of heterochromatin enriched for methylated histone H3K9 (SAHFs)[30]. This supports the hypothesis that S-phase relevant genes are stably repressed upon Ras activation when cells enter a senescent cell cycle arrest, while these genes might be regulated on an epigenetic level by specific histone modifications. The observation that the Rb-bound histone methyltransferase Suv39h1[102] methylates H3 lysine 9 close to E2F responsive genes[103] proposes Suv39h1 as a key candidate executing Ras-induced senescence on an epigenetic level (Figure 9). Consequently, disruption of Suv39h1 is a candidate moiety that may disable cellular senescence and therefore promote oncogenic transformation. Exploring this and testing whether cancellation of cellular senescence also plays a role in tumor development *in vivo* will be addressed in this work.

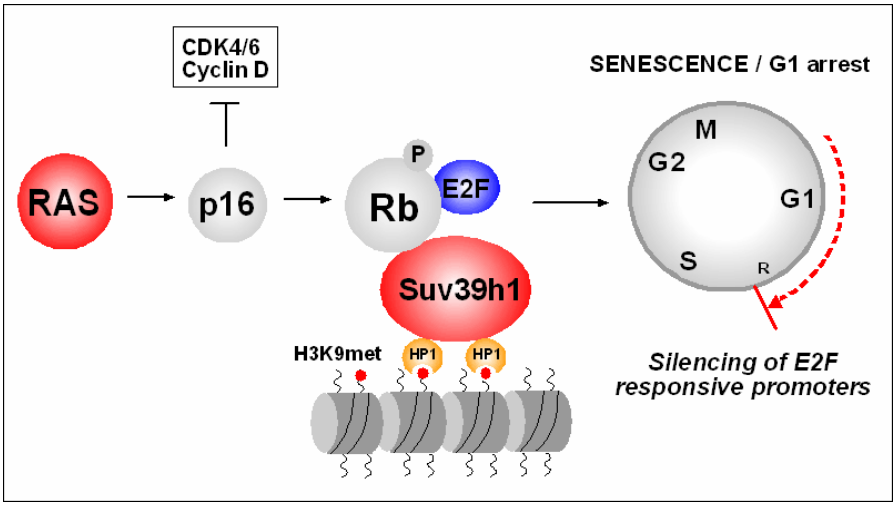

Figure 9: Model: Ras-induced senescence is thought to be a Suv39h1 and therefore H3K9me-controlled mechanism that controls the silencing of E2F responsive promoters by heterochromatin formation.

1.4 Mouse Models

1.4.1 The Eμ-N-Ras transgenic mouse model

In the late 80s, a tremendous effort was undertaken to generate transgenic mice to study the role of oncogenes and their particular impact on tumor development.

People around S. Cory at the WEHI in Melbourne developed a model for transgenic mice constitutively overexpressing a desired oncogene (e.g. Myc or Ras) in the hematopoietic compartment by fusing the oncogene to a tissue-specific promoter, the immunoglobulin (Ig) heavy chain enhancer Eμ. This promoter normally directs the expression of the Ig heavy chain (IgH) in the B-cell lineage suggesting that transgenic mice overexpressing the oncogene develop B cell neoplasia or related diseases. However, in individual transgenic founder lines, the promoter was also found to be transcriptionally active in other cells of the hematopoietic system – e.g. in primary thymocytes or in the myeloid lineage, probably due to the integration environment of the transgene. The N-Ras transgenic mouse[104] was generated by fusing a human mutated cDNA sequence of N-Ras (N-Ras^{V12G}) to an EμSV vector and selected for overexpressed oncogenic Ras in the hematopoietic compartment. Unlike the comparable Eμ-myc transgenic mouse that exclusively develops B cell lymphomas, Eμ-N-Ras transgenic animals form tumors of monocytic origin (histiocytic sarcomas) and sporadically T cell lymphomas.

1.4.2 The Suv39h1 knockout mouse

With the isolation of the first human and murine histone methyltransferases and their suggested role in gene regulation it became attractive to knock out Suv39h1 and its homologue Suv39h2 in a mouse model[93]. The Suv39h1 knockout mouse was generated in the year 2001 by T. Jenuwein and co-workers in Vienna together with a comparable Suv39h2 knockout mouse and an animal that lacks the function of both genes[100]. To obtain mice deficient for the Suv39h1 gene, the murine Suv39h1 locus on the X-chromosome was disrupted by homologous recombination replacing the chromo-domain with a selectable RSV-Neo-cassette and the bacterial LacZ gene. Mice were born at Mendelian ratios, show normal fertility and no impaired viability compared to wildtype mice. Approximately 1/3 of the mice either heterozygous or null for Suv39h1 were susceptible to B cell lymphoma between 9 and 12 months of age.

1.4.3 The p53 knockout mouse

The p53 knockout mouse was generated by Jacks and Weinberg[105] and is not a main part of the present thesis. For details see reference.

2) Material and Methods

2.1 Material

2.1.1 Mouse strains

Mouse	Reference / Genetic background
Eμ-N-Ras transgenic mouse	Haupt et al, Oncogene 1992 WEHI, Melbourne, Australia C57BL/6 x SJL
Suv39h1 knockout mouse	Peters et al, Cell 2001 IMP, Vienna, Austria C57BL/6 x 129 sv
p53 knockout mouse	Jacks et al, Current Biology 1994 Whitehead Institute, Cambridge, USA C57BL/6

2.1.2 Bacteria strains

***E. coli* DH5α**	Invitrogen *Genotype: F-φ80dlcZΔM15Δ(lacZYA-argF)U169 deoR, recA1 endA1 hsdR17 rk-mk+phoA supE44λ- thi-1 gyrA96 relA1*

2.1.3 Cells

Cell type	Medium	Source
NIH 3T3 (Adherent mouse embryonic fibroblast cell line, Cytogenetics: hypertriploid karyotype and 3% polyploidy; deleted in the Ink4Arf locus) ATCC number: CRL-1658	DMEM culture medium	cell line
Phoenix Eco φ^- (Adherent human embryonic kidney cell line 293T, adenovirus-transformed and stably transfected with two plasmids encoding the MML virus sequences “gag”, “pol”, “env”) www.standford.edu/group/nolan.html	DMEM culture medium	cell line
Splenocytes (Primary murine splenocytes isolated from a spleen of a non-transgenic mouse with different genetic backgrounds; suspension cells, require feeder cell culture)	B cell medium + IL-7 (50 pg/ml) + 20% FCS	primary
T-Lymphoma cells (Primary murine Ras-driven T-cell lymphoma cells of different genetic background isolated from the thymus or lymphnode of a terminally sick N-Ras transgenic mouse; suspension cells, require feeder cell culture)	B cell medium	primary

2.1.4 Chemicals and Reagents

Acrylamide/bis	Serva Electrophoresis
Adriamycin (Doxorubicin)	Sigma
Agar Agar	Roth
Agarose	Serva Electrophoresis

Ammoniumpersulfate (APS)	Roth
Ampicillin sodium salt	Roth
Bradford reagent (RotiQuant)	Roth
Bromephenolblue powder	Eurobio
Calciumchloride ($CaCl_2$)	Roth
Chloroform	Merck
Chloroquine diphosphate salt	Sigma
Colcemid KaryoMAX	Gibco Invitrogen
DAPI	Sigma
Dextrose (αD(+)Glucose Monohydrate)	Roth
Diethyl pyrocarbonate (DEPC)	Sigma
diSodiumhydrogenphosphatedihydrate ($Na_2HPO_4x2H_2O$)	Merck
dNTPs	Roth
DTT	Fluka
Ethanol absolute	Roth
Ethidium bromide powder	Roth
Ethylenediaminetetraacetate (EDTA)	Roth
Fetal Calf Serum (FCS)	Biochrom Lot 40Q7441K
Formaldehyde	Roth
G-50 fine Sephadex, DNA grade	Amersham
Glacial acetic acid	Merck
Glucose	Roth
Glutaraldehyde	Roth
Glycerin	Merck
Glycine	Serva Electrophoresis
HCl	Merck
HEPES	Roth
Hexademethrinebromide (Polybrene)	Sigma
Interleukin 7 (recombinant)	RDI Research diagnostics
Isopropanol	Merck
K_3-EDTA	Merck
$KHCO_3$	Merck
L-Glutamine	Biochrom Lot K0283
Magnesiumchloride for PCR	Roche Applied Biosystems
Magnesiumchloride-hexahydrate ($MgCl_2$)	Roth
Methanol	J.T.Baker

Milk powder	Roth
N,N,N´,N´-Tetramethylethylenediamine (TEMED)	Sigma
N,N-dimethylformamide (DMFO)	Roth
N,N-dimethylsulfoxide (DMSO)	Roth
Na-Desoxycholate	Sigma
NH_4Cl	Merck
Nonident 40 (NP-40)	Merck
Paraformaldehyde (PFA)	Sigma
PBS Dulbecco	Biochrom Lot 0699H
PCR buffer (w or w/o Magnesiumchloride)	Roche Applied Biosystems
Penicillin-streptomycin	Biochrom Lot A22139120
Phenol-chloroform isoamylalcohol	Roth
PMSF	Sigma
Potassium ferricyanide ($K_3Fe(CN)_6$)	Sigma
Potassium ferrocyanide ($K_4Fe(CN)_6$ x 3 H_2O)	Sigma
Potassiumchloride (KCl)	Merck
Potassiunacetate (KAc)	Roth
Propidium iodide	Sigma
Protease inhibitors (Complete protease inhibitor mix)	Roche
Puromycin dihydrochloride	Calbiochem
SDS (Sodiumdodecylsulfat)	Roth
Sodium citrate	Sigma
Sodiumchloride (NaCl)	Merck
Sodiumfluoride	Sigma
Sodiumhydroxide (NaOH)	Roth
Sodiumorthovanadate	Sigma
ß-Mercaptoethanol	Roth
Taq polymerase (AmpliTaq)	Roche Applied Biosystems
Tris(hydroxymethyl)aminomethane	Merck
Triton X-100	Merck
TRIZOL reagent	Gibco Invitrogen
Trypan blue solution	Sigma
Trypsin-EDTA (to dilute in 1x PBS or dH_2O)	Biochrom
Trypton/Pepton from casein	Roth
Tween 20	Roth
VectaShield mounting medium (Hard set)	Vector

X-Gal	Roth
Xylene cyanol	Eurobio
Yeast extract	Roth

2.1.5 Enzymes

All restriction enzymes (*BglII, EcoRI, BamHI, NcoI and XbaI*), corresponding buffers and additional reagents (BSA) were obtained from NEB Biolabs.

Proteinase K	Merck
RNase A	Fluka
RNasin Plus RNase Inhibitor	Promega

2.1.6 Oligonucleotides

Oligo	Protocol	Sequence
Suv39h1 fwd 1	Genotyping	5´-GTT GAT GCT TCC TGG TGT GTA GG-3´
Suv39h1 fwd 2	Genotyping	5´-TTT GAG GGG ACG ACG ACA GTA TG-3´
Suv39h1 rev	Genotyping	5´-AAC AGA TGT GGG GTT GGT GGA G-3´
p53 fwd 1	Genotyping	5´-TAT ACT CAG AGC CGG CCT-3´
p53 fwd 2	Genotyping	5´-ACA GCG TGG TGG TAC CTT AT-3´
p53 rev	Genotyping	5´-TCC TCG TGC TTT ACG GTA TC-3´
N-Ras fwd	Genotyping	5´-GCC GCA GAC ATG ATA AGA TAC ATT GAT G-3´
N-Ras rev	Genotyping	5´-AAA ACC TCC CAC ACC TCC CCC TGA A-3´
Suv39h1 cDNA	cDNA	5´-GAA TAC GTT GTA CAC CTG CGA GTT-3´
Suv39h2 cDNA	cDNA	5´-TCA CTT TC ATT TAA CA CCA A-3´
p53 cDNA	cDNA	5´-GAC AGC AAG GAG AGG GGG AG-3´

TBP fwd	RT-PCR	5´-AAC AGC CTT CCA CCT TAT GC-3´
TBP rev	RT-PCR, cDNA	5´-CAT GTT CTG GAT CTT GAA GTC-3´
Suv39h1 fwd	RT-PCR	5´-CGA GTT CTT AAG CAG TTC CAC-3´
Suv39h1 rev	RT-PCR	5´-TGC AGG TTG GGA TCA CAA CTA TGG-3´
Suv39h2 fwd	RT-PCR	5´-CTG CCC AGG ATA GCA TG TT-3´
Suv39h2 rev	RT-PCR	5´-GCT CCG TTT CCT GAC ACT TC-3´
p53 seq PCR fwd	RT-PCR	5´-CTT ACC AGG GCA ACT ATG GC-3´
p53 seq PCR rev	RT-PCR	5´-GCT GGT GAT GGG GAC GGG-3´
p53 seq fwd	Sequencing	5´-GGG CTT CCT GCA GTC TGG-3´
p53 seq rev	Sequencing	5´-CGC TCT CTT TGC GCT CCC-3´
VB10 (136) fwd	TCRR-PCR 1st	5´-AAA CTC TGG GCC ACG ATA CT-3´
DB1 (332) fwd	TCRR-PCR 1st	5´-CAG CCC CTT CAG CAA AGA T-3´
DB2 (385) fwd	TCRR-PCR 1st	5´-CCA AGT TCC TCC CCT CTT TA -3´
JB1 (2464) rev	TCRR-PCR 1st	5´-ATG GGA AGG GAC GAC TCT GT-3´
JB2 (1774) rev	TCRR-PCR 1st	5´-TGA AGT TGA GAG CTG TCT CCT ACT AT-3´
VB10 (218) fwd	TCRR-PCR 2nd	5´-GCA ACT CAT TGT AAA CGA AAC A-3´
DB1 (433) fwd	TCRR-PCR 2nd	5´-GCA TCT TAC CAC CAC CTT GC-3´
DB2 (432) fwd	TCRR-PCR 2nd	5´-GCC CCT CTC AGT CAG ACA AA-3´
JB1 (2408) rev	TCRR-PCR 2nd	5´-CCT AAG TTC CTT TCC AAG ACC AT-3´
JB2 (1765) rev	TCRR-PCR 2nd	5´-GAG CTG TCT CCT ACT ATC GAT TTC C -3´

2.1.7 Expression vectors for retroviral transduction

Plasmids used in the present study are ecotrophic vectors based on the Moloney Murine Leukemia Virus (MMLV) and taken for retroviral transduction of rodent cells. The MSCV (Murine Stem Cell Virus) vector contains the packaging sequence (Ψ^+), the gene of interest in the multiple cloning site (MSC) driven by a PKG (Phosphoglycerate kinase) promoter and a selectable marker (e.g. puromycin resistance) or GFP between the 5´ and 3´LTR. For further details see www.clonetech.com.

Plasmid	Backbone	Insert
MSCV-H-rasV12-puro	MSCV-puro	human mut HrasV12 fcs
MSCV-bcl2-puro	MSCV-puro	murine bcl2 fcs
MSCV-puro	MSCV-puro	-
MSCV-p16-IRES-GFP	MSCV-IRES-GFP	murine p16 fcs
MSCV-AFR-IRES-GFP	MSCV-IRES-GFP	murine ARF fcs
MSCV-IRES-GFP	MSCV-IRES-GFP	-

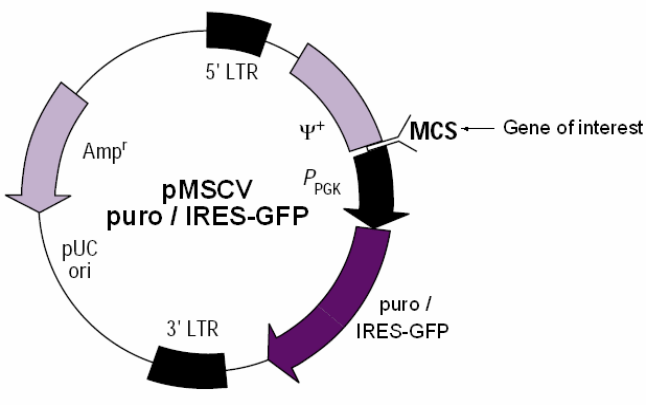

Plasmid map modified from www.clonetech.com

2.1.8 Kits

Kit	Components	Company
cDNA synthesis		
Reverse Transcription Kit	- 5x first strand buffer - 0.1 M DTT - SuperScriptII RT	Invitrogen
Blood smears		
Hemacolor Rapid staining of blood smears	- Fixative solution - Color reagent red - Color reagent blue	Merck

Western blot detection system		
Supersignal West Pico	- Peroxidase solution - Luminol enhancer Solution	Pierce
Sequencing PCR reaction		
BigDye Terminator v.1.1 Cycle Sequencing Kit	- BigDye mix	Applied Biosystems

2.1.9 Antibodies

Primary and secondary antibodies used for WB (Western blot) IF (Immunofluorescence) and IPT (Immunophenotyping)

Antibody	Host / Conjugate	used for	Dilution	Company
Anti-p16INK4a (M-156)	rabbit	WB	1:500	Santa Cruz
Anti-α-tubulin (T5168)	mouse	WB	1:8000	Sigma
Anti-ARF (ab80)	rabbit	WB	1:1000	Abcam
Anti-N-Ras (OP25)	rabbit	WB	1:500	Oncogene
Anti-rabbit IgG	HRP	WB	1:5000	Amersham
Anti-mouse IgG	HRP	WB	1:5000	Amersham
Anti-HP1γ (07-332)	rabbit	IF	1:1000	Upstate
Anti-H3K9me3 (ab8898)	rabbit	IF	1:1000	Abcam
Anti-IgG AlexaFluor594	rabbit	IF	1:2000	Molecular Probes
Anti-CD68	PE	IPT	1:400	Acris
Anti-CD138, CD19	PE	IPT	1μg/test	BD Pharmingen
CD8, CD45R (B220)	PE	IPT	1μg/test	BD Pharmingen
TCRß, CD90.2 (Thy1.2)	PE	IPT	1μg/test	BD Pharmingen
CD117(c-kit), NK1.1	PE	IPT	1μg/test	BD Pharmingen

Anti-CD43, CD86	FITC	IPT	1μg/test	BD Pharmingen
CD11b (Mac1), sIgM	FITC	IPT	1μg/test	BD Pharmingen
CD4, CD5, CD3	FITC	IPT	1μg/test	BD Pharmingen
TCRγσ, GR-1	FITC	IPT	1μg/test	BD Pharmingen

2.1.10 Markers

Marker	Name	Company
Protein		
Molecular weight standard	Roti PRESTAINED	Roth
DNA		
Low molecular weight marker	pBR Mix 328	ROTH
High molecular weight marker	1kb ladder	NEB

2.1.11 Buffers and Solutions

Solutions for DNA preparation	Reagents
DNA lysis buffer	100 mM Tris-HCl, pH 8.5 5 mM EDTA 0.2 % SDS 200 mM NaCl *store at RT*
0.1x TE-buffer	0.1 mM EDTA 10 mM Tris (pH 7.5) *store at RT*

Solutions for Immunofluorescence	Reagents
T-PBS	0.2 % Triton X-100 in 1x PBS *store at RT*
Fixation solution	2 % Paraformaldehyde in 1x PBS *prepare freshly*
Blocking solution	3 drops normal serum in 10 ml T-PBS *prepare freshly*
Normal serum	From Vectastain ABS Kit, Vector

Solutions for Metaphase spreads	Reagents
Fixative solution	Methanol : Glacial acetic acid (3:1) *prepare freshly*

Solutions for Plasmid Mini-Preparation	Reagents
Solution I	50 mM Glucose 25 mM Tris pH 8.0 10 mM EDTA pH 8.0 *store at 4°C*
Solution II	0.2 N NaOH 0.5 % SDS *prepare freshly*
Solution III	25 % 5 M KAc 15 % Acetic acid adjust aq dest to 100 ml *store at 4°C*

Solutions for PCR / RT-PCR	Reagents
6x loading buffer	0.25 % Bromephenol blue 0.26 % Xylene cyanol 30 % Glycerol in aq dest

	store at RT
50x TAE	242 g Tris base
	57.1 ml Glacial acetic acid
	100 ml 0.5 M EDTA (pH 8.0)
	store at RT
DEPC water	0.1 % DEPC in aq dest
	incubate 1 hour at 37°C, autoclave
	store at RT

Solutions for Retroviral TransductionReagents	
2 M $CaCl_2$	5.88 g, ad 20 ml aq dest
	filter 0.2-µm
	store at -20°C
2x HBS (Hepes buffered saline)	280 mM NaCl
	10 mM KCl
	1.5 mM Na_2HPO_4 x $2H_2O$
	12 mM Dextrose
	50 mM HEPES
	adjust pH to 7.05
	adjust to 100 ml with aq dest, filter
	store at -20°C
100 mM Chloroquine	0.516 g Chloroquine diphosphate
	ad 10 ml aq dest
	filter (0.2-µm)
	store at -20°C

Solutions for SA-ß-gal assay	**Reagents**
Fixation solution	2 % Paraformaldehyde in 0.25 %
	Glutaraldehyde in PBS/$MgCl_2$
	prepare freshly
PBS/$MgCl_2$	1 mM $MgCl_2$ in 1x PBS
	store at RT
Staining solution	9.25 ml PBS / $MgCl_2$

	0.5 ml 20x KC solution 0.25 ml 40x X-Gal solution *prepare freshly*
20x Potassium cyanide (KC) stock	20 mg $K_3Fe(CN)_6$ 1.050 mg $K_4Fe(CN)_6$ x $3H_2O$ in 25 ml 1x PBS *store at 4°C in the dark*
40x X-Gal solution	40 mg X-Gal per 1 ml of DMFO *store at -20°C*

Solutions for Sequencing analysis	**Reagents**
Sephadex ready-to-use	5 g / 70 ml aq dest *store at 4°C*

Solutions for Western Blot	**Reagents**
Protein lysis buffer (Lämmli)	1 ml of 0.5 M Tris-HCl, pH 6.8 0.8 ml Glycerol 1.6 ml of 10% SDS 0.4 ml of 14.3M ß-mercaptoethanol 3.8 ml aq dest *store at RT*
Protein lysis buffer (Triton X-100)	2.5 ml Tris base (pH 7.6) (50 mM) 438 mg NaCl (150 mM) 500 µl NP-40 (1%) 1.25 ml 10% NaDesoxycholat (0.25%) 9.2 ml Sodiumorthovanadate (1 mM) 21 mg Sodiumfluorid (10 mM) adjust to 50 ml with aq dest + Protease Inhibitors + 1 mM PMSF *store at 4°C*

SDS sample buffer	1 ml 0.5 M Tris-HCl (pH 6.8)
	0.8 ml Glycerol
	1.6 ml 10% SDS
	0.4 ml 14.3 M ß-mercaptoethanol
	0.4 ml of 1 % Bromephenol blue
	store at -20°C
0.5 M Tris-HCl pH 6.8	6 g Tris base
	60 ml dH_2O
	adjust to pH 6.8, adjust with aq dest to
	100 ml, *store at RT*
1.5 M Tris-HCl, pH 8.8	27.23 g Tris base
	80 ml dH_2O
	adjust to pH 8.8, adjust with aq dest to
	100 ml, *store at RT*
10x Electrode running buffer (pH 8.3)	30 g Tris base
	144 g Glycin
	10 g SDS
	adjust with aq dest to 1l
	store at RT
Anode I buffer	18.15 g Tris base
	50 ml Methanol
	adjust 500 ml aq dest
	store at RT
Anode II buffer	1.51 g Tris base
	50 ml Methanol
	adjust to 500 ml with aq dest
	store at RT
Katode buffer	1.51 g Tris base
	1.44 g Glycin
	adjust to 500 ml with aq dest
	store at RT
10x TBS	100 ml 1 M Tris pH 8.0
	300 ml 5 M $NaCl_2$
	store at RT
1x TBS-Tween (TBS-T)	0.2 % Tween 20 in TBS
	store at RT

Blocking buffer	5 % dry milk in 1x TBS-T prepare freshly or *store at 4°C (1 day)*
Washing buffer	0.5 % Dry milk 0.2 % Tween 20 in 1x TBS *store at RT*

Standard solutions	**Reagents**
PBS (Phosphate-buffered-saline)	8 g NaCl (137 mM) 0.2 g KCl (2.7 mM) 1.44 g Na_2HPO_4 (10 mM) 0.24 g KH_2PO_4 (2mM) adjust to 800 ml with aq dest set pH 7.4 adjust to 1l with aq dest *store at RT*
ACK red blood cells lysis buffer	8.29 g NH_4Cl (150 mM) 1.0 g $KHCO_3$ (1 mM) 200 µl 0.5 M EDTA (0.1 mM) adjust to 800 ml with aq dest, adjust to pH 7.3, adjust 1 l aq dest, filter sterile *store at 4°C*

2.1.12 Media

Cell culture	**Medium**
DMEM	Dulbecco´s modified Eagle medium + Glucose 4500 mg/L + L-Glutamine + Pyruvate

	Gibco Invitrogen
	s*tore at 4°C*
IMDM	Iscove's modified Eagle's media
	+ L-Glutamine
	+ HEPES 25 mM
	Gibco Invitrogen
	s*tore at 4°C*
Culture medium	DMEM
	+ 10% FCS
	+ Penicillin-streptomycin (100 U/ml)
	s*tore at 4°C*
B cell medium	DMEM + IMDM (1:1)
	+ 10% FCS
	+ Penicillin-streptomycin (100 U/ml)
	+ 4 mM L-Glutamine
	+ 25 μM ß-mercaptoethanol
	store at 4°C
Freezing medium	FCS + 10 % DMSO
	s*tore at 4°C*

Bacteria culture	**Medium**
LB-Medium (Luria-Bertani)	10 g Trypton
	5 g Yeast Extract
	10 g NaCl
	adjust to 1 l with aq dest (pH 7.2-7.5)
	store at 4°C
LB-Medium + Ampicillin	50 μg/ml Ampicillin in LB (liquid)
	100 μg/ml Ampicillin in LB (plates)
LB-bacteria plates	10 g Trypton
	5 g Yeast Extract
	10 g NaCl
	15 g Agar Agar
	adjust to 1 l with aq dest (pH 7.2 - 7.5)
	store at 4°C

2.1.13 Equipment

All instrumentation/material not listed in detail is standard lab equipment

Cell culture Equipment	**Company**
Cell culture dishes, sterile (different sizes)	TPP
Centrifuge tubes, sterile (different sizes)	TPP
Serological pipettes, sterile (different sizes)	Falcon Becton Dickinson
“Mr. Frosty” Freezing box	Nalgene Cryo 1°C Freezing Container
Neubauer cell-counter chamber (Improved 0.025 mm, Depth 0.1mm)	Superior Marienfeld
Syringes for single-use, sterile (different sizes)	- Braun, Omnifix, BS Plastic
Needles for single-use, sterile (different sizes)	Neoject
Disposable scalpel for single-use, sterile	Feather
Polystyrene tubes for FACS analysis (5 ml)	BD Falcon
Cryotubes, sterile PK-100 (1.2 ml)	Simport Plastics
Frosted slides (76 x 26 mm)	Engelbrecht
Nylon Mesh (35 μm)	Sefar
Rotilabo Filter sterile (0.45 μM PVDF)	Roth
Rotilabo Filter sterile (0.22 μM PVDF)	Roth
Microscopy Immersion Oil	Merck

Mouse dissection Equipment

- Dissecting board and pins, sterilized
- Scissors and forceps of different sizes and sharpness, sterilized
- Scalpels, sterile

Cytospin Equipment	Company
- Centrifuge (Rotina 35R)	Hettich
- Inserts (1670) and Plastics (1668)	Hettich

Western Blot Equipment	Company
Western blot chamber for SDS-PAGE	C.S.B. Scientific CO
Western blot semidry blotting apparatus (Transblot Semidry Transfer Cell)	BIORAD
Whatman paper (3 MM)	Schleicher-Schuell
PVDF membrane (Immobilon-P)	Millipore
X-O-mat films LS	Kodak

Standard Equipment	Company
Centrifuges	Eppendorf Centrifuge 5417R Eppendorf Megafuge 1.0 R
PCR machine	Mastercycler Eppendorf
Photometer	Eppendorf BioPhotometer 8.5 mm
Microscope	Zeiss Telaval 31
Flow cytometry	Becton Dickinson FACSCalibur
Fluorescence microscope	Zeiss Axioplan
Flow Hood Typ UVF 6.18S	BDK
Incubator	Heraeus cytoperm 2
UV detection system	Biometra T13 UV table and BioDoc CCD-Camera + Software

2.2 Methods

For equipment and solutions not listed in detail see Material section.
As an additional reference see also Sambrook & Russel: `Molecular Cloning´Vol 1-3, CSHL Press or www.MolecularCloning.com

2.2.1 Mouse work and statistics

Transgenic and knockout mice were kept under standardized S2-conditions based on the common GV-SOLAS* and FELASA** guidelines. General mouse work like daily animal care, breeding and offspring separation was carried out in collaboration with the animal facility of the Campus Virchow Hospital, Charité Universitätsmedizin Berlin.
All mouse strains used in this thesis were backcrossed into a C57BL/6 background. In order to obtain Ras-transgenic mice with defined genetic lesions, Eμ-N-Ras-transgenic animals were intercrossed to Suv39h1 knockout and p53 +/- mice, respectively. Tagging of the offspring was carried out according to standard protocols and the genotype was assessed by locus-specific PCR as described. For detailed information about the Eμ-N-Ras-transgenic mouse, Suv39h1 and p53 knockout mice see introduction section (1.4), references and commonly available information (www.ncbi.nlm.gov).
Mice were monitored at least twice a week for any sign of sickness or tumor development. Time to death was defined as the latency between birth and a terminal stage of disease (symptoms like severe weight loss, hyperventilation and palpable hepatosplenomegaly) or sudden death.

Statistical comparison of Kaplan-Meier curves is based on the log-rank test. For comparisons of means and standard deviations (“s.d.” denoting a significant *P*-value of < 0.05) the unpaired *t*-test was applied. All error bars represent the “s.d”.

** GV-SOLAS = Society for Laboratory Animals*
*** FELASA = Federation of European Laboratory Animal Science Associations*

2.2.2 Cell culture

2.2.2.1 Thawing of cells

Reagents, solutions and material

- Frozen cells in -80°C or LiN_2
- Pre-warmed DMEM culture medium or B cell medium
- Feeder cells (for lymphoma cells or splenocytes) in conditioned B cell medium

Cells were thawed quickly at 37°C (e.g. in a water bath) and transferred dropwise to 10 ml medium. After centrifugation (1200 rpm, 5´, RT), supernatant was discarded and pellet was resuspended in 1 ml medium. Cells were plated in an appropriate cell number on culture dishes or feeder cells (see 2.2.2.4).

2.2.2.2 Freezing of cells

Reagents, solutions and material

- All cell types
- Freezing medium (4°C)
- 1x PBS
- 1x Trypsin
- DMEM culture medium or B cell medium
- 1.0 ml cryotubes
- "Mr. Frosty" freezing box (stepwise cool down of cells; 1°C in 1´)

Adherent cells:

After medium was removed from the culture plate, cells were washed with 1x PBS, detached with 1 ml Trypsin (37°C; 5´) and resuspend in fresh DMEM medium.

Suspension cells:

Cells were directly harvested from the culture plate.

After centrifugation (1200 rpm, 5´, RT), supernatant was removed and pellet was resuspended in ice-cold freezing medium (1 ml freezing medium/cryotube/~1-2x 10^6 cells). Cells were immediately transferred to ice and subsequently placed into the "Mr. Frosty" box at -80°C (4h). For long term storage, cells were transferred to LiN_2.

2.2.2.3 Culture of adherent cells: NIH 3T3 and Phoenix cells

Reagents, solutions and material

- NIH 3T3 fibroblasts or Phoenix cells
- Pre-warmed DMEM culture medium
- 1x PBS
- 1x Trypsin

NIH 3T3 fibroblasts or Phoenix cells were plated in DMEM medium and cultivated under standard conditions (37°C, 5% CO_2, 95% humidity) until they reached confluency. Cells were split by the following procedure: medium was removed and cells were washed with 1x PBS. 1 ml of Trypsin was added until cells detached (37°C). After resuspending the cells in culture medium, cells were re-seeded in the desired density (1:2 – 1:10) onto new cell culture plates containing fresh medium.

2.2.2.4 Preparation of feeder cells

Reagents, solutions and material

- NIH 3T3 fibroblasts
- Pre-warmed DMEM culture medium
- 1x PBS
- 1x Trypsin
- Pre-warmed B cell medium

NIH 3T3 fibroblasts were seeded in DMEM culture medium and grown for 1-2 passages. When they reached 70-80% confluency, cells were irradiated with 20Gy (3000rad) and incubated under standard conditions for another 12 hours. Afterwards, cells were split according to standard procedures and resuspended in fresh B cell medium. Cells were counted by trypan blue exclusion (see 2.2.8.1) and re-seeded at a density of 1 x 10^6 cells for each 10 cm plate. Medium was changed every 2-3 days when feeder plates were not used until they got flattened or vacuole rich. Medium enriched with growth promoting factors of irradiated 3T3 cells (12 to 24 hours after plating feeder cells) was used as “conditioned medium” for lymphoma/splenocyte culture (non-conditioned medium will slow down proliferation or arrest primary cells).

2.2.2.5 Culture of mouse T lymphoma cells and splenocytes

Experiments rely on good quality of primary cells and therefore on good culture conditions. Cells were only used at a viability of more than 50 % and at low passages (to prevent selection for clones that have gained mutations by long-term culture).

Reagents, solutions and material

- Freshly isolated / thawed lymphoma cells (low passage) *or* splenocytes
- Feeder cells (irradiated NIH 3T3 feeder layer) in conditioned B cell medium
- Conditioned B cell medium from feeder cells for media change

Lymphoma cells or splenocytes were plated at a subconfluent density (~ 70%) on a well conditioned 3T3 feeder layer and cultivated under standard conditions (37°C, 5% CO_2, 95% humidity). Cells were grown until they grew too dense or medium turned too acidic. For splitting, about 1/3 of the cell suspension was removed (cultivated on new feeder plates with conditioned medium, frozen or discarded) and fresh conditioned B cell medium was added. Feeder cell plates were changed after ~ 1 week of culture or when feeder turned too old. For this, the plate was gently rinsed to remove lymphoma cells sticking on the feeders and suspension was centrifuged at 1200 rpm for 5´ (RT). A few ml of the supernatant were retained to resuspend the cell pellet and cell suspension was subsequently transferred to a new plate of feeders with conditioned B cell medium. Splitting was considered as one passage.

2.2.3 Dissection of mice

2.2.3.1 Whole body dissection of mice

Reagents, solutions and material

- Tumor bearing mouse *or* non-transgenic wildtype mouse
- Small box with dry ice, filled with a few ml of H_2O
- 70% Ethanol
- Mouse preparation equipment

After euthanizing the mouse with CO_2, animal was rinsed with ethanol and pinned down on a dissecting board with the belly facing up. Mouse was opened using an inversed “T”-cut: skin anterior to the urethral tract was held with forceps and the skin along the ventral midline was cut from the groin to the chin (careful not to damage the muscle wall underneath). Next, incision was made down near the knee on both sides of the animal and skin was reflected back. Transparent peritoneal wall was cut carefully, body cavity was opened up and reflected back to have access to the structures underneath. After removing the diaphragm on the bottom of the breast, the sternum was opened by lifting it up with forceps and cutting along each side up to the girdle to have access to the thoracic organs. For further steps see next sections.

2.2.3.2 Dissection of tumor bearing mice

Reagents, solutions and material

- N-Ras transgenic mouse of the respective genotype
- Small box with dry ice, filled with a few ml of H_2O
- 70% Ethanol
- Mouse preparation equipment and equipment for blood smears
- Cold 1x PBS
- 4 % Formaldehyde in 1x PBS

Mouse was sacrificed and opened according to the procedure above. Peripheral blood for bloodsmears was obtained by cutting a small piece of tail or by intracardial aspiration. Before cutting the peritoneum, lymphnodes that are located subcutaneously or in the connective tissue between muscles were checked. After opening the peritoneum, abdominal organs were checked for any anatomical abnormalities (right place of the organ, size and color). To open the sternum, diaphragm was punctured and cut along each side up through the cervical girdle, avoiding any damage to the thoracic organs underneath. Organs in the thorax were checked intensely. If at any time point organs were enlarged or showed abnormal features, they were cut with scissors and forceps, released from the connected tissue and rinsed in cold 1x PBS. After measuring the size, parts of the organ and the mouse body were conserved (2.2.3.4) and single-cell suspensions were prepared for cell culture assays (2.2.3.3).

2.2.3.3 Preparation of cells of the lymphoid system

Reagents, solutions and material

- Freshly prepared organs of the respective mouse
- Mouse preparation equipment
- Cold 1x PBS
- Sterile frosted glass slides
- Sterile nylon mesh (35 μm)
- ACK red blood cells lysis buffer
- 25 gauge needle and syringe
- Anticoagulant (7.5 % K_3-EDTA)

Preparation of spleen, thymus or lymphoma cells

Spleen, thymus or lymphnodes were washed, placed into cold 1x PBS and gently minced between two glass slides using the frosted side of the slides. Mixture was resuspended by repeated pipetting. To obtain a single-cell suspension, mixture was filtered through a sterile membrane and centrifuged at 1200 rpm for 5´ (RT). To get rid of red blood cells, pellet was resuspended in 3 ml of ACK lysis buffer and incubated at RT for 5´. Before centrifugation (1200 rpm, 5´, RT), 27 ml of B cell medium were added for neutralization. Procedure was repeated if red blood cells remained. Cells were frozen or immediately used for further experiments.

Preparation of bone marrow cells

Hind limbs were prepared by gently preparing the skin and muscles from the hip, leg and the area around. Femora and tibiae were separated from the body at the hip joint and at the base of the feet. Remaining muscle and connective tissue were removed with scissors and limbs were rinsed in cold 1x PBS. Bone marrow cells were collected in cold 1x PBS by flushing the tibiae and femora with 1x PBS using a 25 gauge needle to expel the bone marrow. Procedure was repeated at least five times. Mixture was resuspended by repeated pipetting and filtered according to the protocol above. Cells were frozen or immediately used for further experiments.

Preparation of peripheral blood cells

Peripheral blood was obtained by intracardial aspiration immediately after euthanasia of the mouse. To get blood out of the ventricle, a 25 gauge needle was used to

puncture the heart through the peritoneum and diaphragm. Blood was aspirated and transferred to a reaction tube including 50 µl K_3-EDTA to prevent coagulation. After centrifugation (1200 rpm, 5´, RT), lysis of red blood cells was performed as described above. Cells were frozen or immediately used for further experiments.

2.2.3.4 Conservation of mouse organs

Reagents, solutions and material

- Mouse organs / tissue / whole body of mouse
- 4 % Formaldehyde in 1x PBS
- LiN_2

Organs or tissues were fixed in 4 % formaldehyde for 24 hours (RT). After transferring them to 1x PBS, fixatives were kept at RT for long-term storage. Alternatively, snap frozen samples were prepared by transferring the organ in LiN_2 for a few minutes. For long-term storage samples were stored at -80°C.

2.2.4 Molecular Biology

2.2.4.1 Preparation of genomic DNA

Reagents, solutions and material

- Mouse tissue / organs / cell pellet etc
- DNA lysis buffer
- Proteinase K
- Phenol-chloroform isoamylalcohol
- 3M KAc
- Absolute Ethanol
- 70% Ethanol
- 0.1x TE-buffer
- Photometer

Tissue or cell pellet was lysed using 450 µl DNA lysis buffer and 50 µl Proteinase K (55° over night). After centrifugation (14 000 rpm, 10´, RT), supernatant was transferred to a new Eppendorf cup and 500 µl phenol-chloroform mixture were added. After vortexing and spinning (14 000 rpm, 10´, RT), supernatant was transferred to a new Eppendorf cup. Procedure was repeated once before precipitating the DNA by adding 2x vol. of absolute ethanol and 1/10 vol. 3M KAc. After incubation at -20°C over night, DNA was centrifuged (14 000 rpm, 20´, 4°C) and washed twice with 1 ml of 70% ethanol. Pellet was air-dried until ethanol was completely evaporated. DNA was dissolved in 10-100 µl of 0.1x TE-buffer for at least 24 hours at 4°C. DNA was measured in a Photometer (260/280 nm) using TE-buffer as the reference. DNA is pure at a ratio (260/280nm) of < 1.8; higher values result from e.g. ethanol. A faster but less pure way omitting the phenol-chloroform step was used to purify tail DNA of mice precipitating DNA with isopropanol.

2.2.4.2 Polymerase chain reaction

Reagents, solutions and material

- Genomic DNA or cDNA (100-500 ng/µl)
- 10x PCR buffer incl 15 mM $MgCl_2$ *or* 10x PCR buffer and 25 mM $MgCl_2$
- dNTP mix (10 mM each)
- Respective primer (stock 10 µM)
- Taq Polymerase (5 U/µl)
- dH_2O

A PCR reaction was prepared according to the following protocols (1x):

Mix for genotyping PCR	**Suv39h1**	**p53**	**N-Ras**
dH_2O	15.15µl	15.1µl	18.5 µl
10x buffer incl $MgCl_2$	2.5 µl	2.0 µl	2.5 µl
Primer1 fwd	0.8 µl	0.4 µl	1.2 µl
Primer2 fwd	1.0 µl	0.4 µl	-
Primer rev	0.3 µl	0.8 µl	1.2 µl
dNTP	1.0 µl	0.4 µl	0.4 µl
DMSO	2.5 µl	-	-
Taq Polymerase	0.5 µl	0.2 µl	0.2 µl
DNA	1.0 µl	1.0 µl	1.0 µl

Mix for Sequencing- / RT-PCR	p53 seq	Suv39h1	Suv39h2
dH_2O	38.85 µl	38.1 µl	38.1 µl
10x buffer w/o $MgCl_2$	5.0 µl	5.0 µl	5.0 µl
$MgCl_2$	2.0 µl	3.0 µl	3.0 µl
Primer fwd	1.0 µl	1.0 µl	1.0 µl
Primer rev	1.0 µl	1.0 µl	1.0 µl
dNTP	0.4 µl	1.0 µl	1.0 µl
Taq Polymerase	0.75 µl	0.4 µl	0.4 µl
RT-first strand product	1.0 µl	2.0 µl	2.0 µl

Cycling conditions were used for amplification of the desired product as follows:

Conditions	Suv39h1 genotyping		p53 genotyping	
1 Denaturation	95°C	5 min	95°C	5 min
2 Denaturation	95°C	60 sec	95°C	30 sec
3 Annealing	56°C	60 sec	62°C	60 sec
4 Elongation	72°C	90 sec	72°C	60 sec
5 Elongation	72°C	10 min	72°C	5 min
6 Hold	4°C	∞	4°C	∞
repeat steps 2-4	*34 x*		*33 x*	

Conditions	N-Ras genotyping		p53 PCR sequencing	
1 Denaturation	95°C	5 min	95°C	5 min
2 Denaturation	95°C	60 sec	95°C	45 sec
3 Annealing	64°C	60 sec	62°C	60 sec
4 Elongation	72°C	90 sec	72°C	90 sec
5 Elongation	72°C	5 min	72°C	5 min
6 Hold	4°C	∞	4°C	∞
repeat steps 2-4	*31 x*		*37 x*	

Conditions	Suv39h1 RT-PCR		Suv39h2 RT-PCR	
1 Denaturation	95°C	3 min	95°C	3 min
2 Denaturation	95°C	60 sec	95°C	30 sec
3 Annealing	60°C	60 sec	66°C	60 sec
4 Elongation	72°C	60 sec	72°C	60 sec
5 Elongation	72°C	5 min	72°C	5 min
6 Hold	4°C	∞	4°C	∞
Repeat steps 2-4	*34 x*		*34 x*	

DNA products were loaded on an agarose gel and run according to the protocol above. Bands were visualized using UV light considering the following fragment sizes:

Suv39h1 geno	wt 417 bp / mut 588 bp	**Suv39h1 RT-PCR**	743 bp
p53 geno	wt 450 bp / mut 600 bp	**Suv39h2 RT-PCR**	100 bp
N-Ras geno	Transgene 200 bp	**TBP**	681 bp

2.2.4.3 Agarose gel electrophoresis

Reagents, solutions and material

- PCR products in 6x DNA loading buffer
- 1 kb ladder or pBr marker
- Agarose
- 1x TAE
- 1% Ethidium bromide
- Equipment for gel electrophoresis

Agarose gels were prepared according to the following procedure: agarose was dissolved in 1x TAE at the desired concentration and boiled in a microwave until the solution looked crystal clear. Ethidium brodmide was added in the appropriate concentration. After casting the gel, hardening occurred within 10-15´. Gel chamber was filled with 1x TAE and aliquots of the PCR samples including the corresponding amount of loading buffer were loaded into the slots. To determine DNA length of the fragments, an appropriate standard marker was used. Depending on the size of the supposed bands, gel was run 45´ (100-160V). DNA was visualized by UV-light.

2.2.4.4 Preparation of RNA

Reagents, solutions and material

- Low passage lymphoma cells (up to 10^7 cells)
- TRIZOL reagent
- Chloroform
- Isopropanol
- 75% Ethanol
- DEPC H_2O
- Photometer

To homogenize tissue or cell fractions, cells were centrifuged at 1200 rpm for 5´ (RT). Medium was removed and pellet was resuspended by gently pipetting in 1 ml of TRIZOL reagent. After incubation (5´ at RT), 200 µl of chloroform were added to separate RNA from proteins and DNA. Suspension was vortexed for 15´´ and

incubated 3´ at RT. After centrifugation, (12 000 g for 15´, 4°C), RNA that remains in the colorless aqueous phase was transferred to a new tube. To precipitate RNA, 500 µl of isopropanol were added to the samples, incubated for 10´ at RT and centrifuged again at 12 000 g for 15´ (4°C). Supernatant was removed and pellet was washed with 1 ml of 75% Ethanol. After centrifugation at 7500 g for 10´ (4°C), supernatant was discarded and pellet was air-dried until ethanol was completely evaporated. RNA was re-dissolved in DEPC H_2O and incubated for 10´ at 55°C before measuring RNA in a photometer (260/280nm) using DEPC H_2O as a reference. RNA is pure at a 260/280 ratio of < 1.8. In general, RNA was stored at -20°C and for long-term storage at -80°. All buffers, solutions, tips and other equipment were RNase free. In addition, only DEPC-treated H_2O was used. For RNA of lymphoma cells, only cells after passage 2 were taken to avoid contamination with bystander cells. Lymphoma cells were plated 2-3 hours on a plate without feeders to exclude feeder cells in the RNA prep.

2.2.4.5 cDNA synthesis for RT-PCR or sequencing reactions

Reagents, solutions and material

- Extracted RNA of lymphoma cells
- Corresponding primer for cDNA synthesis (2 mole) *or* Oligo(dT) (500 ng)
- DEPC dH_2O
- 5x first strand buffer
- 0.1 M DTT
- dNTP mix (10 mM each)
- 1 U RNasin enzyme
- 200 U SuperScript Reverse Transcriptase

1µg of RNA and 1µl of primer (or Oligo(dT)) were mixed and adjusted with dH_2O to 12µl. Samples were incubated for 10´ at 70°C to destroy RNA secondary structures and transferred to ice for cool down (5´). The following mix was prepared for each sample: 4µl first strand buffer, each 1µl DTT, dNTPs and RNasin. Mix was incubated for 60´ at 42°C, while after 2´ pre-heating 1µl SS-RT was added. Reaction was stopped at 70°C (15´) and transferred to 4°C for 10´. cDNA was stored at -20°C.

2.2.4.6 Sequencing reactions

Reagents, solutions and material

- Genomic DNA or cDNA (500 ng-1μg DNA)
- Big Dye
- Specific 3´ and 5´ sequencing primer (10 μM)
- dH_2O
- Ready-to-use Sephadex (5g/70ml) to prepare G50 columns
- Sequencing equipment

For the sequencing reaction, the following mix was set up: 0.5–1 μg DNA, 0.4 μl 5´ or 3´ primer and 4.0 μl Big Dye. Mix was adjusted to 10 μl with dH_2O. Samples were mixed well before a PCR was run using the following cycling conditions:

Conditions Sequencing			
1 Denaturation	95°C	3 min	
2 Denaturation	95°C	30 sec	
3 Annealing	50°C	15 sec	
4 Elongation	60°C	4 min	*Repeat steps 2-4 25x*

Subsequently, the PCR product was purified using sepharose-gradient centrifugation. For this, 700 μl of ready-to-use Sephadex was loaded into a G50-column and centrifuged at 3000 rpm for 2´ (RT). After exchanging the receiver tube, the PCR product was loaded onto the Sephadex column and centrifuged at 3000 rpm (2´, RT). Purified PCR product was sequenced at the HU Berlin (Department of Genetics).

2.2.4.7 T-cell receptor rearrangement PCR (TCRR-PCR)

Reagents, solutions and material

- Genomic DNA (100-500 ng/μl) of low-passage lymphoma cells
- 10x PCR buffer (incl $MgCl_2$)
- dNTP mix (10 mM each)
- Primer (200 nM each; 10 μM stock) for the 1st and 2nd PCR, respectively
- Taq Polymerase (5 U/μl)
- dH_2O

A 1st PCR reaction mix was prepared to amplify any rearrangements of the T-cell receptor ß-chain including the variable (V), diverse (D) and joining (J) gene regions:

Mix for TCRR-PCR	
dH_2O	37.5µl
10x buffer (incl $MgCl_2$)	5.0 µl
VB1 fwd, DB1 fwd, DB2 fwd	each 1.0 µl
JB1 rev, JB2 rev	each 1.0 µl
dNTP	1.0 µl
Taq Polymerase (1U)	0.2 µl
DNA	1.0 µl

After vortexing, cycling conditions as outlined below were used to run the 1st PCR. For the 2nd PCR reaction a mix according to the 1st approach was set up using the corresponding primers and an aliquot (2.0 µl) of the 1st PCR product. After the 2nd PCR using the conditions below, the product was loaded onto a 1.5% agarose gel and DNA bands were visualized by UV light.

Conditions	**1st PCR reaction**		**2nd PCR reaction**	
1 Denaturation	95°C	30 sec	95°C	5 min
2 Annealing	59°C	4 min		
3 Elongation	72°C	2 min		
4 Denaturation	95°C	10 sec	95°C	10 sec
5 Annealing	59°C	1 min	61°C	1 min
6 Elongation	72°C	30 sec	72°C	30 sec
Repeat steps 4-6	*33x*		*34x*	
7 Elongation	72°C	5 min	72°C	5 min

2.2.5 Protein Biochemistry

2.2.5.1 Western Blot

Western Blotting was performed using a 15 % SDS-PAGE-system and a semi-dry blotting technique.

Reagents, solutions and material

- Cell pellets for protein lysis (freshly prepared or frozen)

- Protein lysis buffer (Triton-X-100)
- Protease inhibitors
- Rotimark Bradford Reagent
- BSA (stock 1 μg/μl in dH_2O)
- Tris-HCl pH 6.8 and pH 8.0
- dH_2O
- 30% Acrylamide/bis 37 5:1 mixture
- 20% SDS
- TEMED and 10% APS
- Isopropanol
- Sample buffer (SDS reducing buffer)
- 10x electrode running buffer
- Western Blot equipment
- Low or high molecular weight standards (Roti Prestained Marker)
- PVDF-membrane (Immobilon-P)
- Methanol
- Whatman paper
- Anode buffer I & II and cathode buffer
- Semi-dry blotting apparatus
- 1x TBS-T (TBS-Tween 20)
- 5 % non-fat milk (in 1x TBS-T)
- Washing buffer
- First and corresponding secondary antibody diluted in TBS-T-milk
- Pierce supersignal detection system (Solution I and II)
- Kodak X-O-mat films LS

Preparation of a 15 % SDS-PAGE

Glass plates were cleaned well with Ethanol before they were set in the casting apparatus. A 15 % separating gel (10ml) was set up mixing the following solutions:

- 2.35 ml aq dest
- 5.0 ml 30% Acrylamide mix
- 2.5 ml 1.5 M Tris pH 8.8
- 50 μl 20% SDS

50 μl APS and 5 μl TEMED were added to the gel mixture, vortexed and casted between the spacers of the prepared glass plates. To prevent evaporation, a few drops of isopropanol were carefully added on top. Polymerization occurred within 10´.

Isopropanol was removed from the separating gel and rinsed with water. Meanwhile, a 4 % stacking gel was prepared (5 ml):

- 3.4 ml aq dest
- 0.83 ml 30 % Acrylamide mix
- 0.63 ml 1.5 M Tris pH 8.8
- 25 µl 20 % SDS

Again, 50 µl APS and 5 µl TEMED were added to the stacking gel mixture, vortexed and pipetted on top of the separating gel. A comb with the desired number of slots was inserted. Polymerization occurred within 10´. After removing the comb, slots were rinsed with dH_2O and the gel was inserted into the gel running box.

Protein isolation (whole cell protein extracts)

Cells were washed once in 1x PBS and centrifuged at 1200 rpm for 5´ (RT). Cell pellet was resuspended in protein lysis buffer (vol=3x volume of cell pellet) and incubated 40´ on ice. To separate cell debris from proteins, lysates were centrifuged (14 000 rpm, 20´, 4°C) and supernatant containing the proteins was transferred to a new tube. Protein concentration was determined by a standard Bradford assay (see next section) and lysates were kept at -20°C or -80°C for long term storage.

Protein measurement (Bradford´s protein micro assay)

A ready-to-use Bradford solution was prepared by diluting Bradford reagent 1:4 with dH_2O using 1 ml per cuvette and sample. A BSA standard curve was set up using the following concentrations: no BSA, 1, 2, 4, 6, 8 and 10 µg BSA including 1 µl of the protein lysis buffer each (corresponding to the volume of the protein lysate that is measured afterwards). To create a standard curve, the absorbance of the individual BSA-samples were determined in a photometer at a wavelength of 595 nm against the no BSA-control. The curve was depicted in a linear regression (R2 values close to 1.0). For the individual protein lysates, each 1 µl was pipetted into 1 ml of the pre-diluted Bradford solution and measured in accordance to the standard curve.

Preparation of the protein samples

Protein samples were thawed on ice. Volume for the desired protein concentration was calculated and the respective amount of loading buffer (sample buffer) was added before the samples were boiled for 5´ at 95°C.

Running the gel

Gel box was filled with 1x electrode buffer. Boiled protein samples were loaded into the slots using 15µl of a molecular weight standard (Rotimark Prestained) as a marker. Gel was started at a voltage of 70-90 V until dye front reached the front of

the separating gel. Gel was run at a voltage of 130-180 V until dye front was close to the bottom. After disassembling the gel apparatus, stacking gel was carefully removed and separating gel was immediately used for further blotting.

Semi-dry blotting procedure

An Immobilon blot membrane and six pieces of Whatman paper were cut in the size of the gel and semi-dry blotting chamber was cleaned. Membrane was activated with methanol for a few seconds, rinsed with dH_2O and soaked in Anode II buffer. A semi-dry blotting "sandwich" was set up in the following order:

- 2 Whatman papers soaked in Anode I buffer
- 1 Whatman paper soaked in Anode II buffer
- Activated Immobilon blot membrane
- Gel
- 3 Whatman papers soaked in Cathode buffer

Air bubbles were removed and sandwich was blotted for 60´ at 1.2 mA per cm^2 gel. Afterwards, blotting apparatus was disassembled and membrane was labeled.

Antibody incubation

Labeled membrane was blocked for 30´ at RT in blocking solution under gentle agitation. Meanwhile, the first antibody was prepared in an appropriate dilution. Membrane was incubated either 4 hours (RT) or over night (4°C) under gentle agitation. Afterwards, antibody solution was saved (and re-used when stored at 4°C) and membrane was washed 3x 5´ in washing buffer. Subsequently, the membrane was incubated for 60´ with the corresponding secondary antibody (RT) under gentle agitation followed by three washing steps (3x 15´). Next, the two components of the Luminol detection kit were diluted 1:1 in the dark and transferred onto the wet membrane. After 1-2´ incubation, membrane was wrapped in a transparent cover and put into a cassette. Membrane was exposed to an X-O-Mat LS film for 1´-60´, depending on the individual antibodies and the amount of protein.

2.2.5.2 Immunofluorescence

Reagents, solutions and material

- Splenocytes
- Cytospin equipment
- Freshly prepared fixation solution
- T-PBS

- Blocking solution (normal serum in T-PBS according to the secondary antibody)
- Primary antibodies and respective secondary antibody (in blocking solution)
- VectaShield Mounding medium for fluorescence (hard set)

Cells were harvested at the appropriate time point, centrifuged (1200 rpm, 5´, RT) and washed once in 1x PBS. Cell number and viability were assessed by trypan blue exclusion (see 2.2.8.1) to adjust cell number to a final concentration of 200 000 cells / ml. 500μl were transferred to a slot of the cytospin plastic and centrifuged at 700 rpm for 8´ (15°C). Supernatant was carefully removed by aspiration and cells were fixed by a freshly prepared fixation solution. After incubation (15´, RT), slides were washed three times in 1x PBS and permeabilized in T-PBS for 30´ (RT). Cells were incubated in the first antibody over night (4°C). Slides were washed three times in 1x T-PBS (5´) and subsequently incubated with the corresponding secondary antibody for 60´ (RT). After extensive washing in T-PBS (3x 15´), slides were mounted and fluorescence was detected under the microscope. Slides were stored in the dark at 4°C.

2.2.6 Immunology

2.2.6.1 Immunophenotyping

Reagents, solutions and material

- Lymphoma cells (low passage) *or* freshly prepared lymphoid or liver cells
- Positive and negative control (spleen, thymus or bone marrow of a wt mouse)
- 1x PBS
- Desired fluorescence-conjugated FACS antibodies
- FACS equipment

At least 10^6 cells (freshly isolated or cultured) as well as the proper antibody-controls were centrifuged (1200 rpm, 5´, RT) and washed in 1x PBS. Pellet was resuspended in 100 μl 1x PBS including the diluted antibodies and incubated on ice for 30´ in the dark. Afterwards, cells were washed in 1x PBS, filtered through a 35 μM nylon mesh and transferred to ice for immediate analysis by flow cytometry.

2.2.7 Stable transductions

2.2.7.1 Retroviral transduction

Protocol corresponds to the transfection of a 10 cm Phoenix cell plate for the collection of 4 x 3 ml of retroviral supernatant for one 10 cm plate of primary cells. For more virus protocol was scaled up.

Reagents, solutions and material

- Low passage Phoenix cells (<20)
- Low passage lymphoma cells *or* freshly isolated splenocytes
- Retroviral plasmid DNA (including an appropriate marker)
- Ecotrophic helper plasmid DNA
- dH_2O
- 2M $CaCl_2$
- 2x HBS pH 7.05
- Chloroquine (stock 100 mM, final 25 μM)
- 1x PBS
- Polybrene (stock 4 mg/ml, final 4 μg/ml), an transduction enhancer
- Conditioned B cell medium (filtered to prevent contamination with feeder cells)
- IL-7 for splenocytes (pre-stimulation with 50pg/ml 2-6 hours before transduction)
- FACS equipment *or* puromycin (stock 300 μg/ml, final 2.5 μg/ml)

Calciumphosphate Transfection of Phoenix cells

Low passage Phoenix cells were grown in a 10 cm plate to a maximal density of 70%. 20μg retroviral plasmid DNA, 15μg helper plasmid DNA and 62.5μl $CaCl_2$ were mixed in a FACS tube and adjusted with sterile water to 500μl. After adding 500μl 2x HBS dropwise under constant agitation (air bubbles), DNA precipitation occurred within 5´ at RT (mixture gets milky and cloudy). Meanwhile, old medium of Phoenix cells was exchanged. Subsequently, 9 ml DMEM medium containing 25 μM Chloroquine and the precipitate (1 ml) were added. After 12 hours incubation under standard conditions, medium including the precipitate was removed from the Phoenix cells. Cells were washed carefully with 1x PBS and 3 ml of conditioned B cell medium were added to collect the first virus supernatant after 24 hours.

Preparation of retroviral supernatant and transduction procedure

The *first virus supernatant* was harvested after 24 hours by aspiration and filtered through a 0.45 μm filter. A well growing cell population (lymphoma cells or IL-7 pre-stimulated splenocytes) at a subconfluent density was pelleted by centrifugation (1200 rpm, 5´, RT) and resuspended in the virus supernatant including 4 μg/ml Polybrene. New medium (3 ml) was added to the Phoenix cells for the next round of transduction. Afterwards, cells were incubated and grown under standard conditions. After 8 hours of incubation, the *second virus supernatant* was harvested according to the procedure above, supplemented with Polybrene and added to the lymphoma or splenocyte culture. After spinoculation of the plates (1500 rpm, 10´, 32°), cells were incubated and grown until the next round of transduction. In addition, new medium (3 ml) was added to the Phoenix cells for the next round of transduction. The *third and fourth virus supernatants* were collected 12 hours and 8 hours later according to the procedure above (see first two rounds of transduction).

12 hours after the last transduction, medium was removed from the cells by centrifugation and cell pellet was resuspended in fresh conditioned B cell medium. Lymphomas and splenocytes were grown for approximately 24 hours to allow cells to express the gene of interest. For cells transduced with GFP-plasmids, percentage of positive cells was determined by flow cytometry (FACS) using a non-transduced control. For cells transduced with an antibiotic marker (puromycin), cell population was selected with puromycin (3 d) until non-transduced cells were completely dead.

2.2.8 Cell Viability, Apoptosis and Senescence

2.2.8.1 Assessment of cell number and cell viability (Trypan blue)

Reagents, solutions and material

- All cell types
- Trypan blue solution (diluted in 1x PBS)
- Neubauer counting chamber

Cells were harvested, centrifuged (1200 rpm, 5´, RT) and cell pellet was resuspended in a small volume of 1x PBS (e.g. 100 μl). The trypan blue solution was

added 1:1 and cells were incubated for 1´. An aliquot was transferred to the Neubauer chamber and checked for equal distribution of the cells in all four big quadrants. If more samples were counted, the trypan blue solution was added shortly before counting and cells were placed on ice. Dead cells were blue, viable white.

For viability assessment and cytotoxicity assays

At least 200 cells were counted in total (dead and alive). Percentage of viability was indicated as the ratio of living cells to the whole cell number.

For total cell number and growth analysis

All viable cells in 16 quadrants of the big 4-square-field were counted and number of living cells in culture was assessed by the following calculation: total number of cells alive in 16 quadrants x dilution factor x 10^5 x ml.

2.2.8.2 In vitro drug cytotoxicity

Reagents, solutions and material

- Low passage lymphoma cells
- Conditioned B cell medium
- Adriamycin ADR (= Doxorubicin, stock diluted in B cell medium, 50 μg/ml)
- Trypan blue solution (diluted in 1x PBS)
- Neubauer counting chamber

Lymphoma cells of a well growing population were harvested and a small aliquot was taken to check viability. 2x 10^5 – 3x 10^5 lymphoma cells were seeded in duplicates onto a 12 well plate in fresh conditioned B cell medium without feeder cells. The following Adriamycin concentrations were used: 0.5 μl/ml, 0.1 μl/m, 0.05 μl/ml, 0.01 μl/ml and an untreated control. Cells were incubated for 24 hours under standard culture conditions. After centrifugation (1200 rpm, 5´, RT), viability was assessed using trypan blue exclusion. Cell viability of the ADR-treated samples was indicated by normalization to the untreated control.

2.2.8.3 Growth curve analysis

Reagents, solutions and material

- Low passage lymphoma cells on feeder cells *or* splenocytes on feeder cells

- Conditioned B cell medium
- Trypan blue solution (diluted in 1x PBS)
- Neubauer counting chamber

Equal amounts of lymphoma cells (1x 10^4) or retrovirally transduced splenocytes (1x 10^3) were seeded in well conditioned B cell medium onto a 24- and a 12-well plate, respectively. Growth of the cell population was assessed on a daily basis counting viability by trypan blue exclusion. To set equal conditions, the same feeder cells and the same conditioned medium were used. Cells were plated at a density of ~ 60-70 % and split onto a bigger plate when necessary.

2.2.8.4 Therapy-induced senescence

Reagents, solutions and material

- Low passage lymphoma cells overexpressing Bcl2
- Adriamycin ADR (= Doxorubicin, stock diluted in B cell medium, 50 μg/ml)

A lymphoma population retrovirally transduced with Bcl2 was seeded at a low density (~ 60 %) on fresh feeder plates (each individual lymphoma onto two plates). One plate was incubated with 0.1 μg/ml Adriamycin for 5 days without changing medium; the second plate was kept as untreated control. Cells were harvested after 5 days for senescence assays. If feeder cells died or looked flattened and shapeless, lymphoma cells were kept in the old medium and transferred onto new feeder plates.

2.2.8.5 SA-ß-galactosidase assay

Reagents, solutions and material

- Senescent lymphoma cells or splenocytes and their corresponding controls
- PBS with 1 mM $MgCl_2$ (pH 5.5)
- Cytospin equipment
- Freshly prepared fixation solution
- Staining solution
- DAPI (1 mg/ml stock solution, final 1 μg/ml)
- VectaShield Mounting medium for florescence (hard set)

Cells were harvested at the indicated time point. After centrifugation (1200 rpm, 5´, RT), cells were washed in 1x PBS. Cell number and viability were assessed by trypan blue exclusion to adjust the cell number to a final concentration of 200.000 cells / ml. 500 µl were transferred to a slot of the cytospin insert and centrifuged at 700 rpm for 8´ (15°C). Supernatant was carefully removed by aspiration. Cells were fixed immediately in freshly prepared fixation solution in order to avoid drying of the slide. After incubation (15´, RT), fixative was removed and cells were washed twice in PBS/$MgCl_2$. Staining solution was added dropwise and slides were incubated in a humidified atmosphere at 37°C in the dark (10-16 hours depending on the experiment). Afterwards, slides were gently washed with 1x PBS and mounted while still wet. Slides were analyzed under the microscope and stored at 4°C.

2.2.8.6 FACS analysis of senescent cells

Reagents, solutions and material

- Senescent lymphoma cell population and its respective control
- 1x PBS
- FACS equipment

A small aliquot (~ 10^5) of senescent lymphoma cells were harvested, washed with 1x PBS and resuspend in cold 1x PBS. Cell growth and granularity was determined by flow cytometry (FSC/SSC) analysis. Senescent cells were viable and bigger compared to the untreated population resulting in a visible shift in size and granularity.

2.2.9 Chromosomal stability

2.2.9.1 Metaphase spreads

Reagents, solutions and material

- Lymphoma cells (low passage)
- Conditioned B cell medium

- 200x KaryoMAX Colcemid stock solution (10 µg/ml final concentration)
- 0.075 M (=0.56 %) KCl solution
- Fixative solution (methanol / glacial acetic acid)
- Dry and clean microscope glass slides
- DAPI (1 mg/ml stock solution, final 1µg/ml)
- VectaShield Mounting medium for fluorescence (hard set)

Lymphoma cells (~ 10^6-10^7) were grown to approximately 80% confluency. Cells were harvested and seeded onto a new plate in conditioned B cell medium containing Colcemid. To enrich for metaphases cells were cultured for 120´ under standard conditions. After incubation, lymphoma cells were centrifuged (1200 rpm, 10´, RT) and supernatant was carefully removed. 1 ml supernatant was kept to resuspend cell pellet by vortexing. 10 ml of pre-warmed (37°C) KCl solution was added dropwise together with 1 ml of fixative to prevent cell clumping. After vortexing, cells were incubated for 20´ at 37°C and centrifuged (1200 rpm, 10´, RT). Again, supernatant was discarded, cells were resuspended in 1 ml remaining supernatant and fixed with 10 ml of warm (RT) fixative solution while vortexing. Afterwards, cells were centrifuged (1200 rpm, 10´, RT) and supernatant was carefully removed. Fixation step was repeated four times until pellet was brightly white and cells were resuspended in ~ 500 µl fixative solution. Glass slides were positioned on a tray in a humidified atmosphere (boiling water) at a 30° angle and a few drops of the cell suspension were applied from about 50 cm height onto each slide. Slides were dried at RT. Subsequently, slides were stained with a DAPI solution for 2´ and rinsed with dH_2O. After mounting the slides in DAPI-free mounting solution, at least 50 metaphase spreads per individual case were analyzed by fluorescence microscopy. Metaphase preps were stored in the fixative solution at -20°C or 4°C.

2.2.10 Bacteria work

2.2.10.1 Transformation of bacteria

Reagents, solutions and material

- Competent *E. coli* (DH5α)

- Plasmid DNA (500 ng-1μg)
- Pre-warmed LB plates (Ampicillin)

Competent bacteria were thawed on ice using 100 μl for each transformation. Bacteria were mixed with the desired plasmid DNA and incubated 30´ on ice. Bacteria were heat shocked at 42°C for 1´ and immediately transferred to ice (5´). 1 ml of pre-warmed LB medium w/o Ampicillin was added and bacteria were incubated for 60´ at 37°C under gentle agitation. Bacteria were centrifuged (3000 rpm, 5´, RT) and pellet was carefully resuspended in ~50 μl LB. Suspension was plated on LB agar plates and incubated over night at 37°C. Colonies were monitored and picked within one week when stored at 4°C.

2.2.10.2 Plasmid DNA Mini-Preparation of bacteria cultures

Reagents, solutions and material

- Bacteria plate from the transformed DH5α with the plasmid of interest
- Pre-warmed LB medium including Ampicillin (1 μg/ml)
- Ice-cold Solution I including 100 μg/ml RNase A
- Freshly prepared solution II
- Ice-cold Solution III
- Absolute and 70% Ethanol
- dH_2O

Individual colonies were picked from the bacteria plate and incubated in 2 ml + Ampicillin each over night (37°C) with gentle agitation. Bacteria suspension was transferred to a new Eppendorf cup, centrifuged at 14 000 rpm (1´, 4°C) and pellet was lysed by adding 100 μl ice-cold sol I. Afterwards, 200 μl of freshly prepared sol II were added and after gentle inversion incubated on ice for 5´. 150 μl of ice-cold sol III were added and bacteria were incubated 20´ on ice. After centrifugation (14.000 rpm, 10´, 4°C), supernatant was transferred to a new Eppendorf cup and 1 ml of absolute ethanol was added to precipitate DNA. After vortexing and centrifugation (14 000 rpm, 10´, 4°C) the pellet was washed with 1 ml of 70% Ethanol and centrifuged again (14 000 rpm, 10´, 4°C). Pellet was air-dried and DNA was dissolved in ~30 μl dH_2O. DNA concentration was measured and checked by standard enzyme digestion.

2.2.11 Experimental setting

All mouse strains in the present study were backcrossed to a C57BL/6 background and used only > generation F8.

To assess the role of Suv39h1 in Ras-driven lymphomagenesis, male Eμ-N-Ras-transgenic mice were intercrossed either to female Suv39h1 +/- or to female p53 +/- mice, respectively. Hereby, breeding was set in a 1:2 ratio (male: female) using mice between 10 to 20 weeks of age. Females did not exceed more than five pregnancies. After birth of the offspring, mice were separated and genotyped using standard protocol procedures. Due to the X-linked Suv39h1 locus mice deficient for a functional Suv39h1 (hereafter "Suv39h1 -") are either male Suv39h1 y/- or female Suv39h1 -/- (crossing N-Ras Suv39h1 +/- to Suv39h1 +/-). Mice heterozygous for Suv39h1 are always female. To monitor time-to-death latencies, transgenic mice of the respective genotypes were monitored at least twice a week for any signs of sickness like hyperventilation, severe weight loss as well as palpable lymphnodes or unusual behavior. At stages of terminal sickness, mice were sacrificed and the tumors were prepared as described elsewhere. For further analysis single cell preparations or fixed tissue were taken for functional experiments (Figure 10).

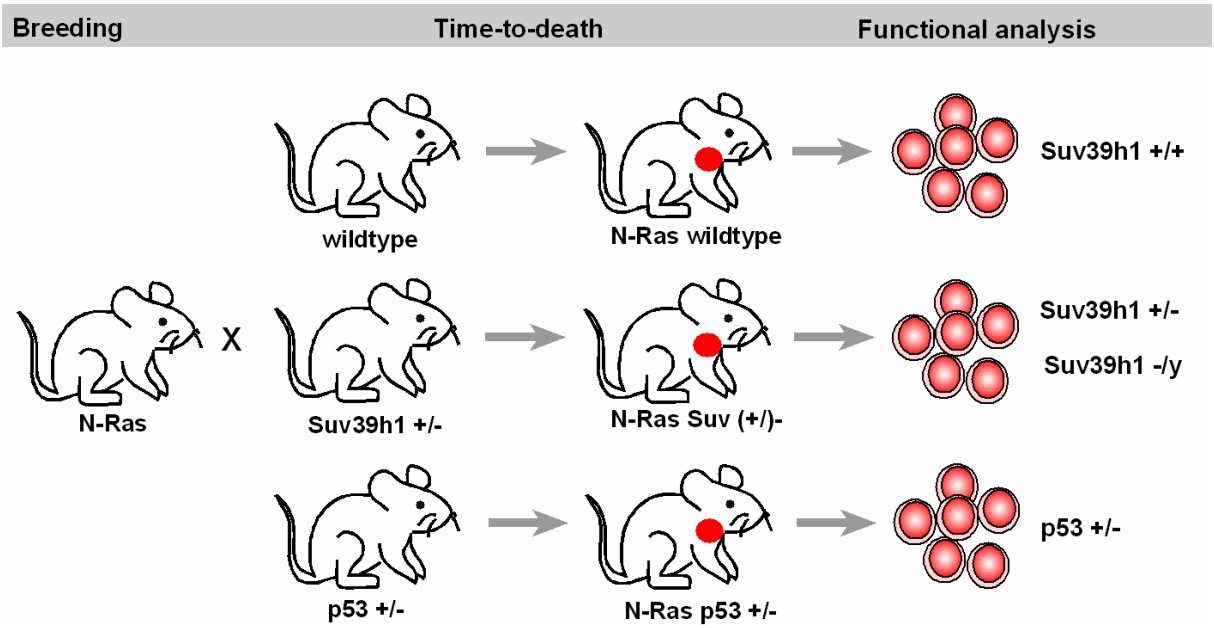

Figure 10: Experimental outline. Mice with different genetic background were monitored for time-to-death latencies and tumors were isolated for subsequent analysis.

3) RESULTS

Results from collaborations are outlined when discussing the respective data

- Immunohistochemistry / Immuncytochemistry (p16, ARF, CD3, CD11b)
- Ki67 staining
- Preparation of paraffin-embedded slides (formalin-fixed tissue)

done by Dr. Christoph Loddenkemper and Simone Spieckermann

- GFP enrichment assay

done by Dr. Soyoung Lee (main part)

- General mouse care and genotyping

done by Bianca Teichmann, Ines Schildhauer, Claudia Kalla and Katja Lankisch

Hypothesis

Oncogenic Ras induces a terminal cell cycle arrest (premature senescence) that is capable of preventing malignant conversion *in vitro*[15]. It involves tumor suppressors like p53[15], p16[15] or the Retinoblastoma protein and changes in higher order chromatin structures[30]. The Rb-bound histone methyltransferase Suv39h1 might therefore represent a crucial effector that controls Ras-provoked tumorigenesis, likely by mediating cellular senescence.
The **Eμ-N-Ras transgenic mouse** provides an *in vivo* model for hematological malignancies that are driven by oncogenic Ras[104]. Intercrossing a **Suv39h1 knockout mouse[100]** allowed us to study the impact of Suv39h1 in Ras-induced tumorigenesis and to investigate the role of Suv39h1 in regulating premature senescence as an initial barrier in tumor development.

3.1 Mouse models

3.1.1 Validation

N-Ras transgenic mouse

Expression status of oncogenic Ras in Eμ-N-Ras transgenic mice

The Eμ-N-Ras transgenic mouse model is characterized by the constitutive overexpression of oncogenic Ras in the blood forming compartment. Basis for this model is a human N-Ras^{G12D} construct linked to the promoter of the immunoglobulin heavy chain enhancer "Eμ". This ensures the permanent expression of oncogenic N-Ras in the B cell lineage, but also in other cells of the hematopoietic compartment like thymocytes or myeloid cells[104].
To validate this model, either Ras-transgenic or non-transgenic mice were compared for their expression of human N-Ras in the hematopoietic system. For this, whole cell protein lysates of spleen and thymus of either pre-neoplastic N-Ras (n=3) or non-transgenic wildtype animals (n=3) were prepared and tested in a Western blot analysis for N-Ras levels. A representative blot is shown in Figure 11.

The results clearly reveal that human N-Ras is overexpressed in the spleen and thymus of Ras-transgenic mice ("N-Ras"), while, contrarily, no endogenous N-Ras expression was detectable in the spleen or thymus of the non-transgenic animal

("wildtype"). The findings confirm the proposed genotype and the functionality of the Eμ-N-Ras transgenic mouse on a protein level.

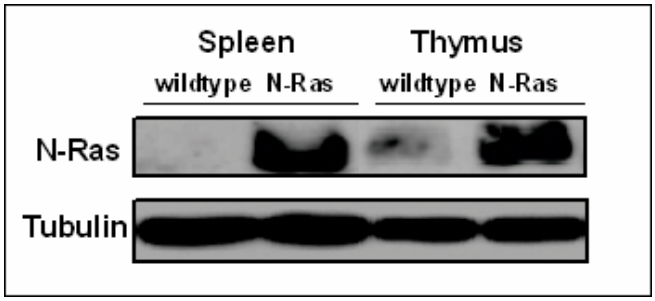

Figure 11: N-Ras is overexpressed in lymphoid organs of N-Ras-transgenic mice. Western blot analysis of N-Ras transgenic spleen and thymus compared to the respective wildtype organs. Lymphoid compartments were isolated from a 10 week old non-transgenic wildtype mouse and a pre-neoplastic N-Ras mouse of the same age. 80 µg whole cell lysates were loaded on a 15 % SDS-gel and the membrane was probed with either an anti-Ras antibody (detecting human N-Ras of 21 kDa size; diluted 1:500) or anti-tubulin (detects murine α-tubulin of 50 kDa size; diluted 1:8000). The experiment was carried out with three individual animals (n=3).

Suv39h1 knockout mouse

Status of Suv39h1 in Suv39h1 knockout animals

The Suv39h1 knockout mouse is genetically disrupted in the Suv39h1 gene locus and therefore lacks the respective histone-methyltransferase activity in all organs and tissues[100].

To test for the functional ablation of Suv39h1, protein expression patterns of mice with different genetic Suv39h1 background were examined. However, since there are currently no antibodies available that recognize murine Suv39h1 and are functional (as tested for the present thesis), the Suv39h1 protein status could not be determined in those animals.

Therefore, we switched to a more genetic test system that confirms the successful disruption of the Suv39h1 locus.

X-linked Suv39h1 was targeted using a conventional lacZ-neo approach. According to the insertion size of the introduced sequence (bacterial lacZ gene/neo-cassette), a PCR specific for the Suv39h1 gene locus was set up that amplifies a mutant fragment larger than the normal wildtype product.

Using tissue DNA (tail) of Suv39h1 proficient (+/+), heterozygous (+/-) and deficient (y/-) animals (n=3 each genotype) the PCR proves that Suv39h1 was successfully disrupted on a genetic level (Figure 12; top). Mice wildtype for Suv39h1 (Suv +/+ or Suv y/+) display the wildtype band; knockout mice (Suv -/- or Suv y/-) the mutated gene segment. In this context, female heterozygous animals (Suv39h1 +/-) show two bands - one for the wildtype and one for the mutated allele.

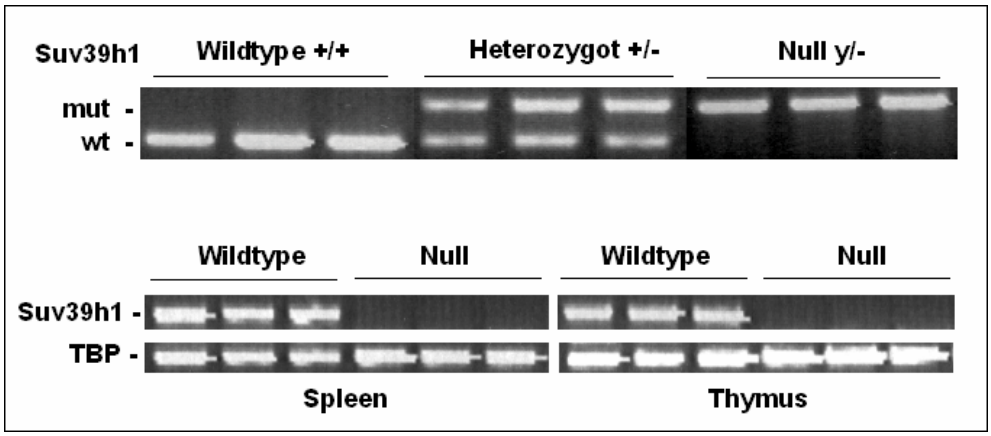

Figure 12: Suv39h1 is genetically disrupted in Suv39h1 k.o. mice. Top Altered Suv39h1 status in mice with different Suv39h1 status. DNA of Suv39h1 +/+, +/- and y/- animals (each n=3) were tested in an allele-specific PCR to detect either wildtype or mutant Suv39h1 in normal tissue (tail) of the mice. **Bottom** mRNA level in the hematopoietic system of Suv39h1 +/+ or Suv39h1 y/- mice. RNA from spleen and thymus was tested in a RT-PCR approach for expression levels of Suv39h1 using TATA-box-binding protein (TBP) as a housekeeping gene control (n=3 animals each approach)**.**

Moreover, mRNA levels were investigated to determine not only the genetic, but also the functional targeting of Suv39h1 in the knockout mouse. With reference to the project outline that examines the role of Suv39h1 in Ras-driven lymphomagenesis, only organs from the hematopoietic system were tested. RNA of spleen and thymus of either Suv39h1 +/+ or y/- animals (n=3) was isolated and gene specific cDNA was transcribed to test for the Suv39h1 message in a semi-quantitative RT-PCR approach (Figure 12; bottom).

As expected, in all Suv39h1 y/- mice no Suv39h1 mRNA was detectable in spleen and thymus compared to Suv39h1 +/+ control animals using TATA-box-binding protein as a reference. This renders the Suv39h1 knockout functionally as “null” and confirms the genotype as proven in hematopoietic organs like spleen and thymus.

Impact of Suv39h1 on differentiation and proliferation of hematopoietic cells

Suv39h1 knockout mice display normal viability and fertility and do not exhibit any apparent immunphenotype or susceptibility to hematological tumors compared to wildtype mice[100]. According to these observations, no significant difference in hematopoietic differentiation would be expected. However, for the present study it was crucial to investigate in more detail whether loss of Suv39h1 function might provoke a pre-neoplastic state by influencing proliferation or differentiation of hematopoietic cells.

Accordingly, the differentiation status of several hematopoietic compartments of Suv39h1 deficient mice was investigated to address any variation or shift in the lymphoid, myeloid or hematopoietic stem cell population compared to Suv39h1 proficient animals. Therefore, spleen, thymus, peripheral blood and bone marrow cells of three individual mice per genotype (Suv39h1 +/+ and Suv39h1 y/-) at the age of four months were isolated and tested in a standard immunophenotyping flow cytometry approach. Single cell suspensions of the respective organs were double-stained with matched pairs of FITC or PE-conjugated antibodies recognizing specific antigens on lymphocytes (T/B cells), myeloid cells (monocytes/macrophages), progenitor cells (hematopoietic stem cells) or others like natural killer cells.

Each individually stained cell population was measured by flow cytometry and the viable fraction in the forward side scatter analysis (FSC/SSC) was blotted in a dual-color dot blot. A detailed summary of the antibodies used is listed in Table 1. FACS parameters (detectors & amps for FL1/FL2) and compensation status were set before using the respective negative (isotype) and positive control for each antibody. Dot blots were gated uniformly using the same quadrant stats for each antibody pair distinguishing negative, single and double positive cell populations. For statistical evaluation values were calculated in percentage (%).

Representative blots of spleen, thymus, blood and bone marrow in the relevant double stainings are pointed out in Figure 13. The comparative overview in the four compartments show nearly identical patterns suggesting no overt difference in the immunphenotype when comparing non-transgenic Suv39 +/+ to Suv -/- animals.

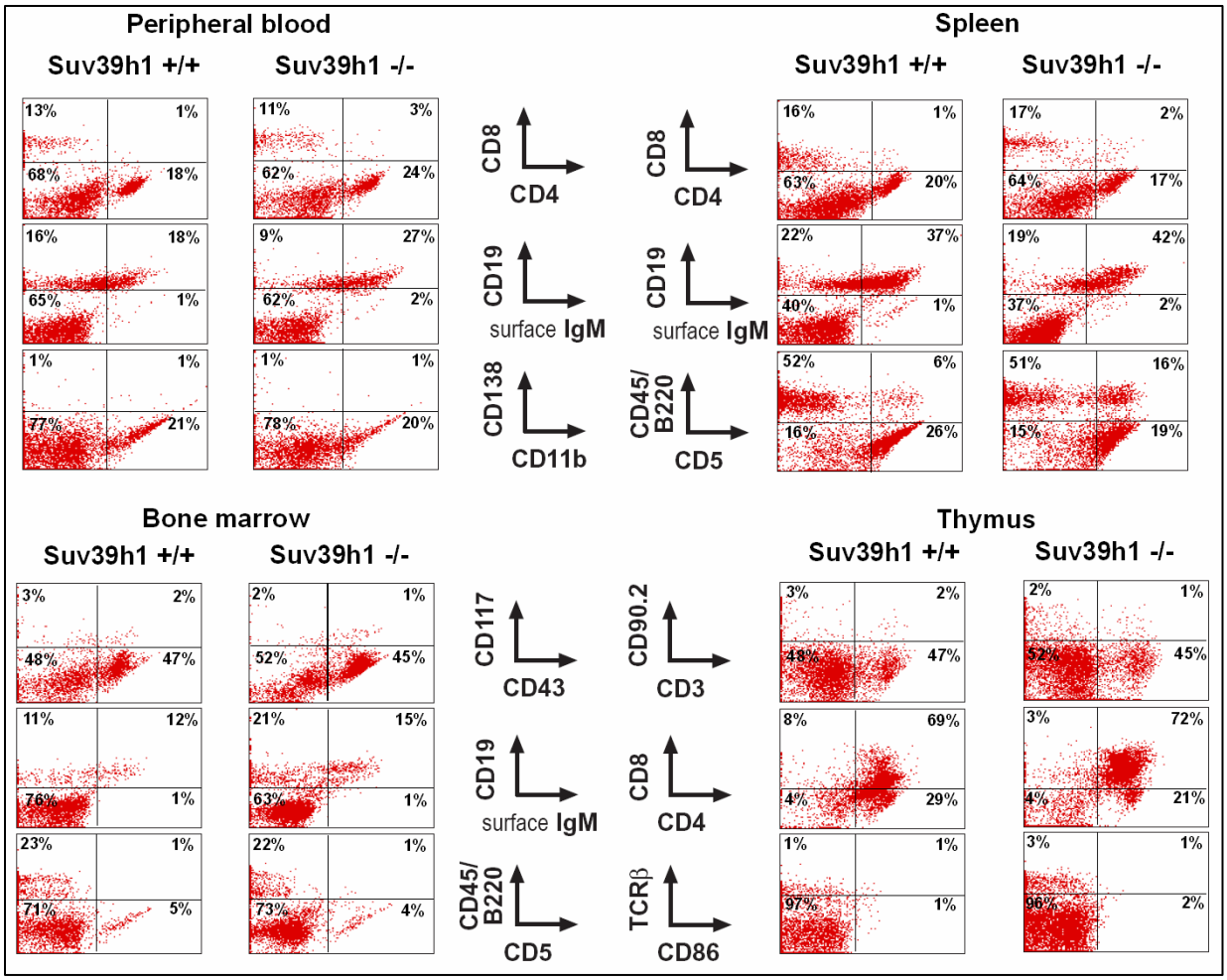

Figure 13: Suv39h1 does not impact on hematopoietic differentiation. Immunophenotyping analysis of the hematopoietic differentiation status in Suv39h1 knockout mice (n=3) and wildtype control mice (n=3) matched to the same age of about four months. Spleen, thymus and bone marrow were isolated and peripheral blood cells were obtained by intracardial aspiration. Two-color flow cytometry was performed using antibodies detecting myeloid or lymphoid markers and markers on hematopoietic progenitor cells (1 µg/test). % indicates the average of n=3. For a summary see T1.

The detailed summary (Table 1) considering all individual mice points out the variability in percentages for the indicated antibodies. Again, no obvious difference was found in the respective compartments in Suv39h1 proficient and deficient animals.

This unveils that in mice lacking functional Suv39h1 the susceptibility for hematological tumors is not increased and loss of Suv39h1 in a non-transgenic context does not drive proliferation or differentiation in these cells.

Haematological differentiation and Suv39h1 status

Antigen/	Bone marrow		Thymus	
Immunophenotype	Suv39h1+/+	Suv39h1-/-	Suv39h1+/+	Suv39h1-/-
B-cell antigens				
CD5	+	+	+ (var)	+
CD19	+	++	(+/-) (var)	(+) (var)
CD19+/ surface IgM+	(+)	+	- (var)	- (var)
CD45 (B220)	++	++	(+) (var)	(+) (var)
CD138	(+/-)	(+/-)	(+/-)	(+) (var)
T-cell antigens				
CD3	- (var)	(+) (var)	++	+
CD4+CD8-	(+)	(+)	++ (var)	+
CD4-CD8+	(+)	(+)	(+) (var)	(+)
CD4+CD8+	(+/-)	(+/-)	+++ (var)	+++
TCRβ	++ (var)	+++	++	++
TCRγ/δ	(+/-) (var)	(+)	(+) (var)	(+)
Myeloid antigens				
CD11b	++	+++	(+) (var)	+ (var)
GR-1	+++	+++	+ (var)	+ (var)
Natural killer cell antigens				
NK1.1	+	+	+ (var)	+ (var)
Progenitor antigens				
CD117 (c-kit)	(+)	(+)	(+) (var)	(+/-) (var)
Others				
CD43	+++	+++	++	++ (var)
CD68	-	-	(+/-)	(+/-) (var)
CD86	(+/-) (var)	(+/-) (var)	(+) (var)	(+)
CD90.2 (Thy1.2)	+	+	++ (var)	++

Table 1: Summary of hematological differentiation in Suv39h1 proficient and deficient mice. The table indicates the percentage of positive cells in the respective compartment outlined in Figure 14 as followed: "-" < 0.5%; "(+/-)" 0.5 to < 1.5%; "(+)" 1.5 to < 5%; "+" 5 to < 15%; "++" 15 to < 45%; "+++" > 45 %; "(var)" means high variability (at least half of the mean). **Top:** Calculation for bone marrow and thymus using the indicated antibodies **Bottom:** Calculation for Spleen and peripheral blood using the indicated antibodies.

Haematological differentiation and Suv39h1 status

Antigen/ Immunophenotype	Spleen		Peripheral blood	
	Suv39h1+/+	Suv39h1-/-	Suv39h1+/+	Suv39h1-/-
B-cell antigens				
CD5	++	+++	++	+++
CD19	+++	++	++	++
CD19+/ surface IgM+	++	++	++	++
CD45 (B220)	++	+++	++ (var)	++ (var)
CD138	(+/-)	(+/-)	(+/-)	(+/-)
T-cell antigens				
CD3	++ (var)	+	++	++ (var)
CD4+CD8-	++	++	++	++
CD4-CD8+	+	++	+	+
CD4+CD8+	(+) (var)	(+/-)	(+/-)	(+/-) (var)
TCRβ	++	++	++	++
TCRγ/δ	(+/-) (var)	(+)	+	+
Myeloid antigens				
CD11b	(+)	(+)	++	++
GR-1	+	+	++	+
Natural killer cell antigens				
NK1.1	+	++	(+) (var)	+
Progenitor antigens				
CD117 (c-kit)	(+) (var)	(+/-) (var)	(+/-)	(+) (var)
Others				
CD43	++	++ (var)	+++	+++
CD68	(+/-)	(+/-)	(+/-) (var)	(+/-) (var)
CD86	-	-	(+/-) (var)	(+) (var)
CD90.2 (Thy1.2)	++ (var)	++ (var)	+++	+++

3.2 Phenotype of Ras-transgenic mice with different Suv39h1 status

3.2.1 Impact of Suv39h1 in Ras-induced tumorigenesis *in vivo*

Alterations in the Suv39h1 locus accelerate Ras-induced tumorigenesis *in vivo*

Overall survival: Kaplan-Meier `Time-to-death´ latencies in Ras-transgenic mice

To assess the role of Suv39h1 in Ras-driven hematological neoplasia, Eμ-N-Ras mice were intercrossed with animals harbouring targeted deletions in the Suv39h1

locus. The offspring, comprising N-Ras-transgenic Suv39h1 heterozygous (+/-), Suv39h1 null (y/- males; -/- females) and Suv39h1 control mice (+/+), was monitored for tumor development and sacrificed when a terminal state was reached. “Time-to-death” latencies were plotted in Kaplan-Meier format to monitor overall survival (Figure 14).

Transgenic mice with no additional lesions in the Suv39h1 locus (N-Ras controls; black; n=63) displayed a slow progression of tumor disease while still appearing healthy and entered a terminal state at a median age of 235 days. Strikingly and in stark contrast to this observation, N-Ras Suv- animals (orange; n=7) lacking functional Suv39h1 entered a comparable state significantly earlier at a median age of 66 days (P=0.0004). Remarkably, those mice died only a few days after the first signs of sickness. Surprisingly, Ras mice harboring only one mutated allele of Suv39h1 (Suv39h1+/-; red; n=17) succumbed to a terminal stage nearly at the same time as Suv- animals. This already leads to the presumption that defects in the Suv39h1 locus accelerate tumorigenesis in N-Ras-transgenic mice, even in a heterozygous context where only one allele of Suv39h1 is affected.

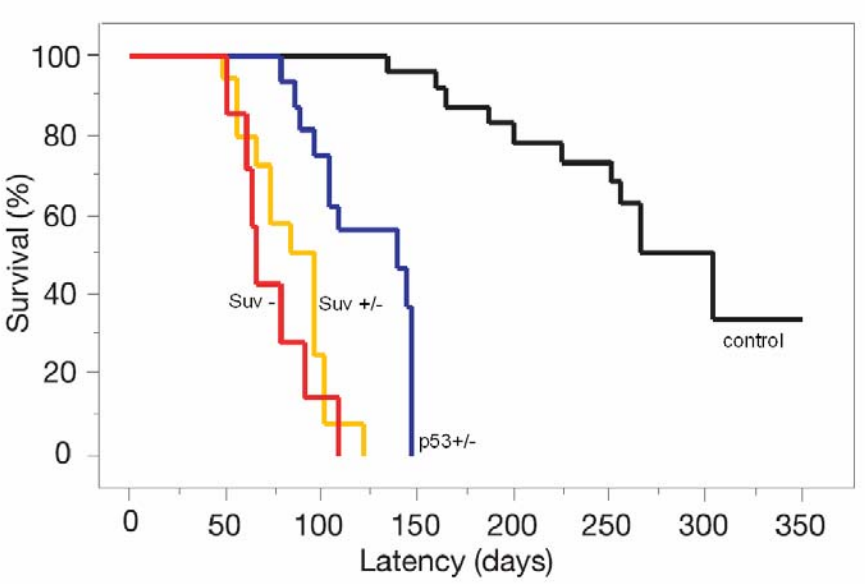

Figure 14: Suv39h1 and p53 defects accelerate Ras-driven tumorigenesis. Kaplan-Meier “Time-to-death” latencies of N-Ras transgenic Suv null (female Suv -/- and male Suv -/y, n=7; red line), female Suv +/- (n=17, orange line) and p53 +/- mice (n=19; blue line) and pooled N-Ras wildtype controls with no additional genetic lesion (n=63; black line). N-Ras controls (305 days) comprise the “late death” group; Suv nulls (66 days), Suv +/- (80 days) and p53 +/- (141 days) make up the “early death” group (median time-to-death values in brackets).

To validate these observations, N-Ras p53 heterozygous animals were generated intercrossing N-Ras transgenics with mice harbouring distinct lesions in the p53 locus. In this model it is likely that p53 defects have an impact on tumor formation since p53 plays a crucial role in Ras-driven tumorigenesis *in vitro*[15] as well as in myc-driven lymphomagenesis *in vivo*[106]. The statistics confirm this hypothesis as Ras p53 +/- mice (blue; n=19) became sick (median time-to-death 141 days) almost as fast as animals with lesions in the Suv39h1 locus. As shown in Figure 14, they display significant differences in the "time-to-death" latencies (p=0.02) compared to controls. Of note, no signs of tumor were observed in non-transgenic animal deficient for Suv39h1 or heterozygous for p53 during a time period of more than one year.

Taken together, the results conclude a strong role for Suv39h1 and p53 in N-Ras-driven tumorigenesis *in vivo* since defects in those genes markedly show an impact on tumor formation in the context of oncogenic Ras.

Suv39h1 defects permit aggressive T cell lymphomas in response to oncogenic Ras

The overall survival data discussed above shows that impaired Suv39h1 or p53 function accelerates cancer formation *in vivo* and underscores a potential role for both players in response to activated Ras signaling in the chosen model.
To phenotypically assess and characterize Ras-induced neoplasia in the different genetic backgrounds, tumor bearing animals were sacrificed at time of terminal sickness and dissected for any sign of tumor. The respective infiltrated organs or conspicuous tissue sections were prepared and used for further analysis. Therefore, parts of the organ were fixed for pathological questions and single cell suspensions were generated from the remaining tissue.
Mice that died early, comprising Suv39h1 deficient, p53+/- and - to a small percentage - also control animals, were younger than 180 days (< 180 days) and grouped into the so-called **"early-death-group"**. Mice that died later (> 180 days after birth) were summarized in the **"late-death-group"**.

In the following section several questions will be addressed assessing the phenotype of N-Ras-driven entities of the early compared to the late death group: Common

macropathology, histology and hematological features as well as the immunphenotype.

Experiments with the “early death group” always comprise a representative number of all Suv39h1 and/or p53 genotypes; samples from “late death group” include only N-Ras control animals. Of note, it should be mentioned that the small fraction of N-Ras control mice (without any additional genetic lesions) that also succumbed to the “early death phenotype” were analysed in the upcoming paragraphs as well.

Macropathology, histology and hematology of Ras-driven neoplasms

Macropathological assembling revealed that at terminal stages of disease animals of the early death group showed heavy splenic and thymic enlargement, while other organs like liver seemed to be unaffected. Contrarily, mice from the late death group displayed dramatically enlarged livers and spleens, but only rare thymic involvement (Figure 15 left).

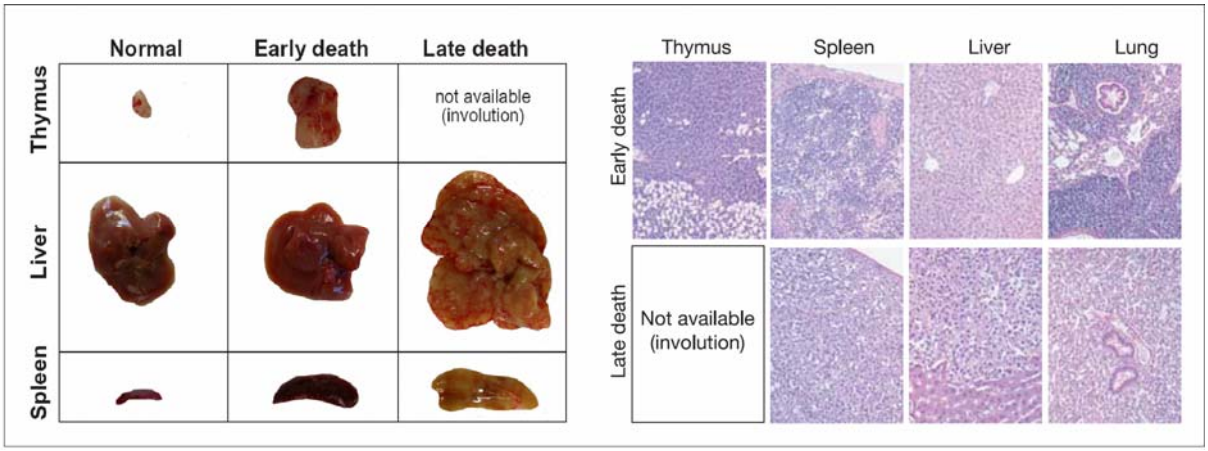

Figure 15: Macropathology and histopathology of Ras-induced tumors. Left: Animals of the early and late death group display different macropathological features. Representative photographs of spleen, thymus and liver of the late and early death group at the same scale. Normal organs for comparison. Note that the thymus is not available in mice older than about 200 days (involution). **Right:** Different phenotypical characteristics in Ras-transgenic mice of different genotype. H&E (Hematoxylin/Eosin) staining of representative organs of Ras-transgenic mice. Formalin-fixed thymus, spleen, liver and parts of the lung were embedded in paraffin and cut in 7 µm kryosections to stain with H&E *(Loddenkemper et al).* Note that the thymus is not available in mice older than about 200 days (involution). Arrows indicate representative areas of lymphoblastic infiltration (early death) or histiocytic populations (late death).

Furthermore, to address histological features of these organs, formalin-fixed and paraffin-embedded sections were stained with hematoxylin/eosine *(Loddenkemper et al).* Results of representative pictures are outlined in Figure 15 (right).
The staining unveils that mice from the early death group suffer from a massive lymphoblastic infiltration in thymus and spleen even in non-lymphoid organs like the lung, whereas the liver remains unpathological. In contrast, late death animal display infiltrated histiocytic populations in spleen and liver, while non-lymphoid organs were only rarely affected.

To determine the hematological status in the periphery, blood smears were performed using a drop of blood by intracardial aspiration from mice at stages of terminal illness. The staining according to the Wright's protocol (Figure 16) uncovered that the lymphoblastic phenotype of the early death group is accompanied by a drastic leukaemic burden visible by an immature blastic population (stained in deep purple), whereas blood smears of the late death group are exclusively normal and non-pathological.
Those histological and hematological examinations suggest that defects in the Suv39h1 or p53 provoke different tumor phenotypes in response to oncogenic Ras and alterations in the respective loci might promote the early-death lymphoblastic phenotype. In addition, the results identify the early death phenotype as more aggressive underscoring the time-to-death latencies observed *in vivo* and assume that loss of Suv39h1 or p53 cancels a tumor suppressive program that leads to an accelerated death.

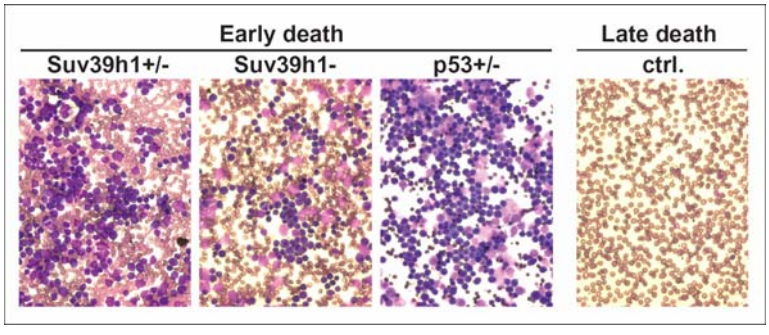

Figure 16: Mice of the early death group show a severe leukemic burden. Representative blood smears of N-Ras transgenic mice (Wright's stain). Peripheral blood was obtained from early and late death animals of the indicated genotypes by intracardial aspiration at a terminal stage of disease.

Immunophenotype of Ras-induced tumors

Taken together, previous data show that N-Ras transgenic mice with defects in the Suv39h1 or p53 locus succumb to an aggressive lymphoblastic phenotype and die significantly earlier compared to N-Ras control mice that suffer at a later timepoint from a non-invasive histiocytic-like invasion.

To study the immunophenotype of those entities, single-cell suspensions of freshly prepared tissues were stained in a dual-color immunophenotyping approach with a T lymphoid marker as well as with a marker detecting antigens on myeloid cells.
Therefore, thymus preparations of early death mice (5 each genotype) or late death liver cell isolates (5 individual samples) were stained with a marker for T cells (CD90.2-FITC) and macrophages (CD11b-PE) using the respective fluorescence-conjugated antibodies. The viable fraction in the forward sidescatter analysis was plotted in a dot blot to determine positive and/or negative populations. Representative pictures are shown in Figure 18 (left; upper picture).
The results highlight clear immunophenotypical discrimination between the early and the late death group. Cells isolated from early death animals showed a distinct positive population for the T cell maker CD90.2, while cell populations from the late death group were exclusively positive for the myeloid antigen CD11b and negative for the T cell marker.

In addition, immunohistochemistry for T cell and macrophage markers was performed to validate the findings above. Formalin-fixed and paraffin-embedded slides of either infiltrated lung or liver were stained with an anti-CD3 antibody, a common T cell marker, and with an antibody against the myeloid marker CD11b *(Loddenkemper et al)*.
The results (Figure 17; right) confirm the previous immunophenotyping experiments. While CD3 staining is positive in the lung sections of early death animals and correspond histologically to the infiltrated lymphoblastic population, stainings of the lungs of late death animals remain negative. Contrarily, when liver sections of late death mice were probed with the myeloid marker CD11b, the histiocytic population turned positive, whereas - according to the pathological phenotype – early death liver sections remain negative.

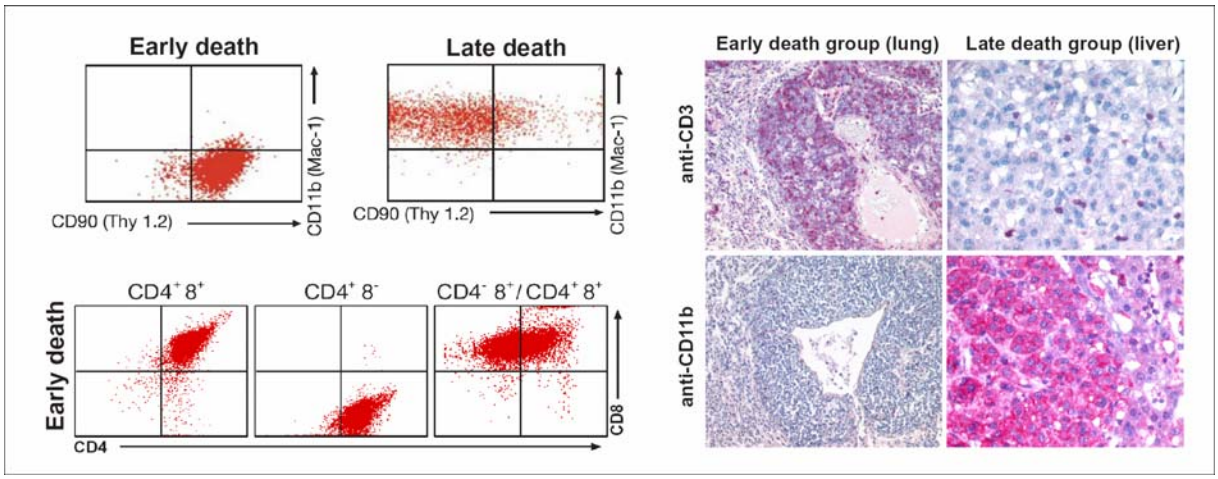

Figure 17: Mice of the early and late death group display different immunological phenotypes. **Left top:** Immunophenotyping analysis of early death tumors (thymus of a N-Ras Suv39h1 deficient mouse) versus late death neoplasms (liver of an N-Ras control animal). Two-color flow cytometry of the indicated cell populations for myeloid (anti-CD11b-PE) and T cell markers (anti-CD90.2-FITC). **Left bottom:** Immunophenotype of N-Ras controls, Suv nulls and p53 null lymphomas (5 each genotype). Two-color flow cytometry using an anti-CD8-PE and CD4-FITC antibody recognizing cytotoxic and helper T cells. Similar distribution of the individual lymphomas is discussed in the text. **Right:** *In situ* immunohistochemistry of early and late organs (liver / lung) from formalin-fixed paraffin-embedded slides (7 µm) stained for the myeloid marker CD11b and the T cell marker CD3 *(Loddenkemper et al)*

This reveals that early death mice develop a clear T cell phenotype in contrast to late death animals showing a histiocytic phenotype from macrophage origin.

To characterize the T cell lymphoblastic population of early death mice in more detail, all early samples used in the previous approach were stained with a fluorescence-conjugated antibody recognizing antigens on either T helper cells (CD4-FITC) or cytotoxic T cells (CD8-PE). Flow cytometry was performed according to the procedure described in the last paragraph. Representative blots are pointed out in Figure 17 (left lower picture) and unveil similar distribution patterns of T cell subtypes in the different genotypes (see following table).
Since T cell lymphomas are of different origin throughout the genotypes it seems that N-Ras drives the early death phenotype without any preference for a T cell subpopulation.

	ctrl.	Suv39h1-null	p53-null
$CD4^+8^+$	2	3	2
$CD4^+8^-$	1	1	0
$CD4^-8^+/CD4^+8^+$	2	1	3

Taken together, the immunophenotyping revealed that upon oncogenic Ras signaling in the hematopoietic system, defects in the Suv39h1 or p53 locus provoke a T lymphoblastic phenotype, whereas without any additional defects a myeloid disease develops.

Tumor characteristics: Proliferation and clonality of early death lymphomas

Previous experiments showed that in response to oncogenic Ras defects in the Suv39h1 or p53 locus permit an aggressive tumor-like phenotype, whereas animals without any additional genetic lesion succumb mainly to a milder form of histiocytic-like disease. However, it needs to be investigated whether the altered Suv39h1 or p53 status drives a clonal tumor or simply the hyperproliferation of T cells. Hence, growth parameters and clonality were assessed in early death T cell isolates.

To determine growth parameters, paraffin-embedded sections of the spleen derived from early death phenotypes were stained with the proliferation marker Ki67 *(Loddenkemper et al)*. Spleen sections from late death animals were taken as controls. Representative pictures are shown in Figure 18; upper part).

The results of the immunohistochemistry revealed that proliferation is markedly increased in all of the early samples. Hereby, 77% (Suv39h1 defective; early control) and up to 90% (p53 -/-) were positive for the staining. This underlines the aggressive and fast growing T cell lymphoblastic phenotype. Contrarily, in the late death group, only 10% turned positive characterizing a less invasive malignancy contributing to a longer overall survival of N-Ras control animals.

However, in principal, also a non-malignant, benign cell population can proliferate due to permanent external growth factor supply or intrinsic stimuli. Those hyperproliferating tissues are characterized by a polyclonal cell population. Accordingly, it is necessary to test if the T lymphoblastic population is from monoclonal origin displaying a tumor entity.

Therefore, DNA of the early death group was tested for T cell receptor ß (TCRß) rearrangement in a two-step PCR analysis. During T cell maturation in the thymus, the TCR is rearranged by V-D-J recombination and in a normal thymus diverse variants of the TCRß chains are present. In contrast, a tumor population is derived from a clone that expresses only one distinct rearranged TCRß chain. In this approach, the rearrangement of the variable region (V) of the TCRß to any diverse (D) or joining (J) segment can be detected. A normal thymus population results in various DNA fragments of different sizes, a monoclonal population in distinct bands.

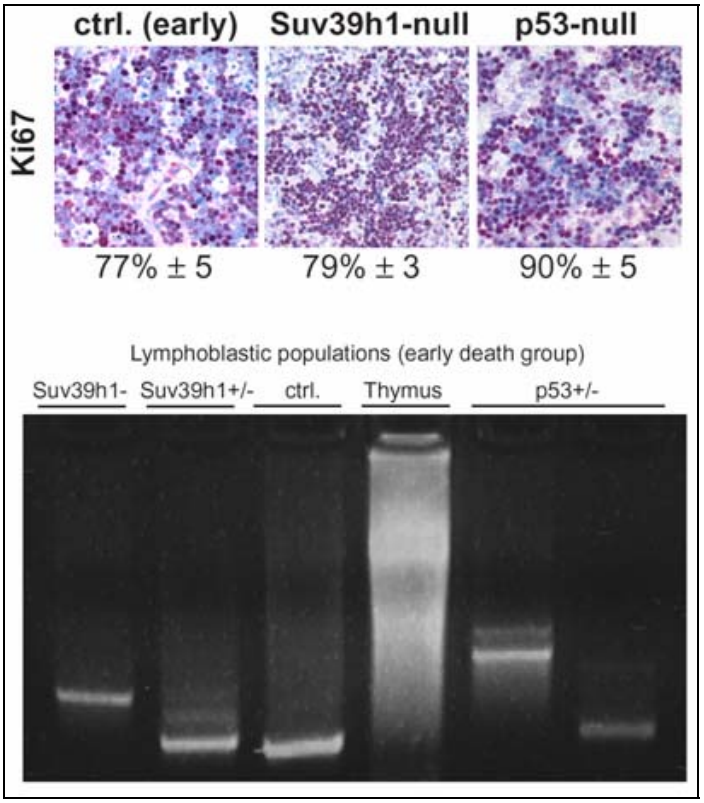

Figure 18: Tumor characteristics in terminally early death tumors. **Top:** Proliferation status. Formalin-fixed and paraffin-embedded sections (7µm) of the spleen were stained for the Ki67 protein of animals of the indicated genotypes (n=3). Quantification values (100 cells) of three individual samples of each genotype were averaged (in %) and blotted including standard deviations (*Loddenkemper et al)*. **Bottom:** Clonality of the lymphoblastic T cell population (T-cell receptor ß-rearrangement). DNA was isolated to determine the V-D-J recombination status in the T cell tumor population using a multiplex 2-step PCR protocol. The representative picture includes the individual genotypes (control, Suv39h1 heterozygous and null, n=1; p53 heterozygous, n=2) and the positive control (thymus of a non-transgenic wildtype animal).

As outlined in Figure 18 (lower part), the polyclonal thymus population of a non-transgenic wildtype mouse expresses a huge arsenal of different TCRß chains (smear), whereas thymus DNA isolated from early death mice results in sharp bands, independent of the different genotypes. This argues for a monoclonal population of N-Ras early death animals rendering the respective entities as T cell lymphomas.

In summary, these results unveil that in mice with an altered Suv39h1 or p53 status oncogenic Ras provokes aggressive tumors from T lymphoid origin which do not develop (besides a small fraction) in a N-Ras driven wildtype background. The data strongly argue for a crucial role of Suv39h1 and p53 controlling Ras-induced tumorigenesis *in vivo*.

3.3 Molecular signature of Suv39h1 deficient lymphomas

3.3.1 Oncogenic Ras and the Suv39h1 status

Ras selects against Suv39h1 expression during tumor formation

In the previously described experiments it was shown that altered expression of Suv39h1 or p53 accelerate oncogene-driven tumorigenesis in N-Ras transgenic mice, likely by disabling a failsafe mechanism that normally protects against Ras-induced lymphomagenesis. Notably, this was observed not only for N-Ras Suv39h1-mice, but also for animals with a heterozygous Suv39h1 +/- background. Since those Suv39h1 +/- mice show almost identical time-to-death latencies and do not differ in their phenotype it is highly suggestive that Ras may select against Suv39h1 during lymphoma formation. Likewise, since functional loss of p53 correlates with accelerated tumorigenesis *in vivo* and *in vitro,* p53 function might also be lost in N-Ras transgenic p53 heterozygous animals in this model.

Status of Suv39h1 and p53 in Suv39h1- and p53-deficient lymphomas

To investigate whether oncogenic N-Ras selects for Suv39h1 or p53, allele-specific PCR was performed to detect wildtype and mutant Suv39h1 and p53, respectively.

For this, genomic DNA from low-passage lymphoma cells was isolated and set in a polymerase chain reaction with the corresponding normal tissue DNA (tail) from the mouse. DNA of MEFs (mouse embryonic fibroblasts) was taken as a standard and N-Ras controls from the early death group served as cell type control.

According to the Knutson's hypothesis, Ras selected for the remaining wildtype p53 allele in heterozygous p53 +/- mice during lymphomagenesis, resulting in a "loss of heterozygosity" (LOH) in 4/5 lymphoma samples tested (Figure 19 top; picture in the middle). These are predicted data since in different already published models a p53 LOH is detectable *in vivo* as well as *in vitro*.
However, in Suv39h1 heterozygous lymphomas the wildtype allele was still detectable (Figure 19; picture in the middle; n=4) on a genomic level. This assumes no gross deletions in the Suv39h1 locus during Ras-driven lymphomagenesis. Remarkably, when those tumor samples were tested for mRNA expression levels of Suv39h1 in an RT-PCR approach, no transcript was detectable in any of the cases tested (n=12; Figure 19 top; upper picture). These data suggest that in those animals oncogenic Ras likely selects for cells where the remaining Suv39h1 wildtype allele maps to the inactivated X-chromosome (Barr-body) and is therefore inactivated already before tumor formation. Therefore, former Suv39h1 heterozygous lymphomas can be declared functionally as "null" lymphomas.

In line with the previously described observations these data uncover that Ras promotes lymphomagenesis by selectively disrupting a functional Suv39h1 message or wildtype p53. Accordingly, these players seem to be important mediators of Ras-induced tumorigenesis, also *in vivo*.

Further examination was made to investigate if Suv39h1 loss can potentially protect p53 LOH during Ras-driven lymphomagenesis.
Therefore, N-Ras mice heterozygous for p53 (N-Ras 53+/-) were intercrossed with Suv39h1 +/- mice in order to obtain N-Ras p53+/- Suv- (2 cases) or N-Ras p53+/- Suv+/- (1 case) animals (see scheme Figure 19 bottom; upper picture). Subsequently, the offspring was monitored for time-to-death latencies and tested for the status of p53 and Suv39h1. N-Ras control lymphomas from the early death group served as cell type control.

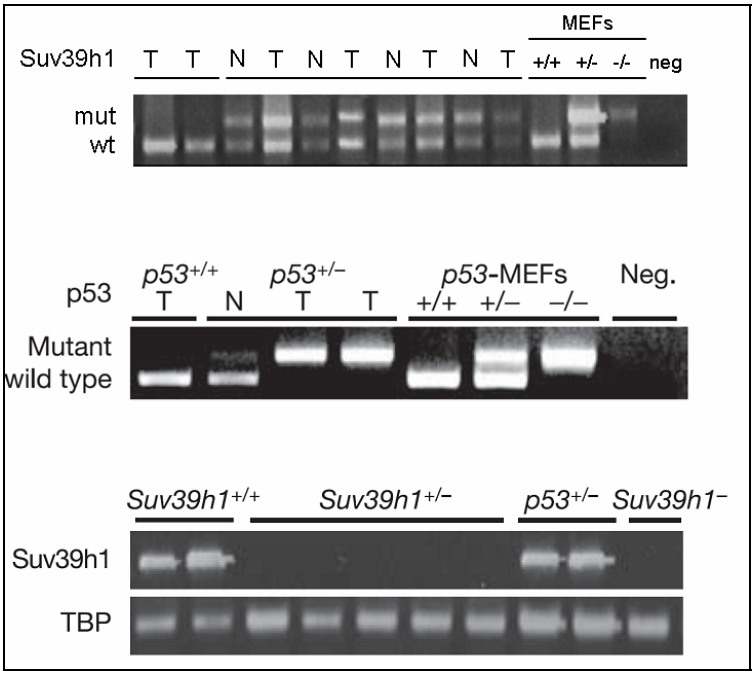

Figure 19: Cells select against Suv39h1 or p53 during lymphomagenesis. Top: Status of Suv39h1 or p53 in Ras-driven Suv39h1 or p53 heterozygous lymphoma cells. Suv39h1 +/- (n=4; upper) or p53 +/- (n=5; middle) lymphomas were tested in an allele-specific PCR to detect the wildtype or mutant Suv39h1/p53 allele in tumor (T) or the corresponding normal tissue (N) for comparison. As an internal control mouse embryonic fibroblasts of the respective genotype were used. mRNA level in Suv39h1 heterozygous lymphoma cells (n=5; lower): RT-PCR for Suv39h1 and TATA-box-binding protein (TBP) as a control. **Bottom:** Breeding scheme (upper; see also text). Suv39h1 RT-PCR (middle) and genomic p53 PCR (lower) were preformed as described above. DNA or RNA of lymphoma cells derived from p53+/- animals either Suv+/- or Suv-.

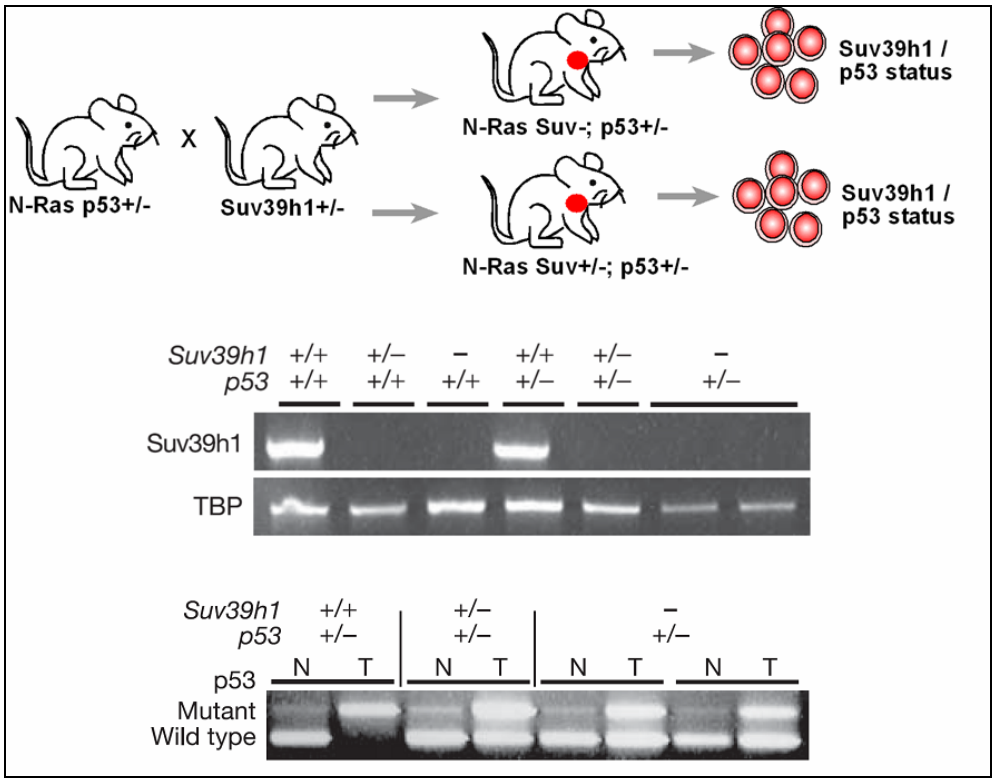

As expected, all animals succumb to a terminal state of disease at approximately the same time as the early death group and showed identical features. T lymphoma cells were isolated and tested either in an allele-specific PCR or an RT-PCR approach for p53 or Suv39h1, respectively.

Impressively, data revealed that Ras selected against Suv39h1 since no mRNA transcripts were detectable in any lymphoma; however the p53 wildtype was retained (Figure 19 bottom; lower picture). According to these results it is highly conceivable that in response to oncogenic Ras loss of Suv39h1 protects from co-inactivating p53. It seems that selection against Suv39h1 is quite an early event, while a p53 LOH occurs later (see time-to-death Kaplan-Meier curves).

Importantly, these data unveil that it is sufficient to block Suv39h1 function to drive Ras-induced lymphomagenesis without compromising p53 function *in vivo*. In addition, the results show that control lymphomas from the early death group retain Suv39h1 expression and p53 on a genomic level.

3.3.2 Role of Suv39h1 in the Ras-pathway

Suv39h1 acts downstream of p16

Previous experiments showed that Suv39h1 is a crucial mediator of Ras-induced tumorigenesis and loss of the histone methyltransferase can even compensate for an additional p53 LOH. This places Suv39h1, like p53, as a regulator protein in the Ras-signaling cascade.
Latest research revealed the INK4aArf gene products p16 and ARF as important players in the Ras-signaling pathway. They are activated in response to oncogenic Ras and transfer the signal downstream to the p53 protein. As a consequence, loss of p53 leads to the accumulation of p16 and ARF.

To evaluate the role of Suv39h1 in the Ras-signaling cascade upstream or downstream of those players, protein expression levels of p16 and ARF were determined. In addition, the selective enrichment for those proteins was tested in a Suv39h1 proficient and deficient background. p53 null lymphoma cells were taken for comparison and N-Ras control lymphomas from the early death group served as cell type control.

Suv39h1 null lymphomas tolerate high p16 levels, but select against ARF

To test for endogenous p16 expression, whole cell protein lysates were isolated from low-passage lymphoma cells of the respective genotype and evaluated in a Western blot analysis, while endogenous ARF levels were assessed performing immunohistochemistry on infiltrated lung sections of terminally sick mice.
Data in Figure 20 (top) unveil particularly high p16 levels in Ras Suv39h1 null or p53 lymphomas compared to quite modest expression profiles in control samples. Contrarily, in Suv39h1 deficient entities and in controls, ARF levels were almost undetectable in paraffin-embedded sections of the lung *(Loddenkemper et al)*. In contrast and in line with previously published data, ARF is highly overexpressed in p53 nulls (Figure 20; middle).

This already underlines the potential role of p16 acting upstream of Suv39h1 in oncogenic Ras-signaling, whereas the ARF protein does not seem to act in the putative Ras-p16-Suv39h1 axis.

Similar results were obtained when p16 and ARF were retrovirally introduced into lymphomas of different genetic background and checked for the selective enrichment after a distinct time period *(Soyoung Lee)*. For this, control, Suv39h1 or p53 deficient cells were retrovirally transduced with either a MSCV-p16-IRES-GFP or a MSCV-ARF-IRES-GFP construct, set to 10% GFP positivity and monitored for GFP levels after 48 hours by flow cytometry.
The results (Figure 20, middle) support previous findings that Suv39h1 null cells tolerate supra-physiological levels of p16 and even enrich for the protein during the two days period comparable to p53 deficient lymphomas. In contrast, Ras control cells did not enrich for p16 and maintained stable levels after 48 hours arguing for an active p16 signaling pathway. On the other hand, high levels of ARF were not tolerated in Suv39h1 null cells and lymphomas selected against the protein - like in Ras control lymphomas where the GFP fraction decreased after 48 hours. Again, this is in line with the Western blot analysis and the immunohistochemistry results.

These results give a deeper insight into the signaling pathways Suv39h1 is involved during Ras-induced tumorigenesis in this model – likely acting downstream of p16. However, it seems that a functional ARF-p53 axis is retained in Suv39h1 null lymphomas since they remain highly susceptible to p53 inducing triggers like ARF overexpression.

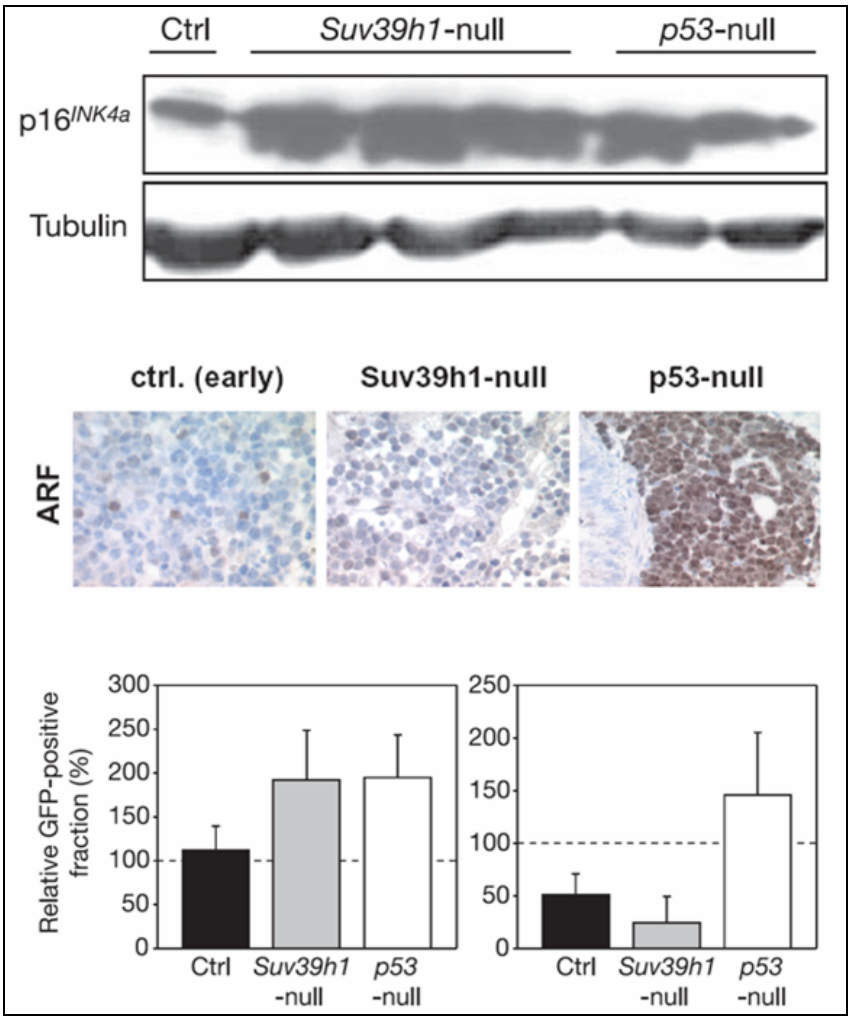

Figure 20: Role of p16 and p19ARF in Suv39h1 null lymphoma. Top: Western blot analysis of Ras-driven lymphoma cells of the indicated genotypes. Whole cell lysates (80 µg) of low-passage lymphoma cells were separated with a 15% SDS-PAGE and the membrane probed with an anti-p16 antibody (1:500) detecting murine p16 (16 kDa) or anti-tubulin (1:8000) of 50 kDa as a loading control. **Middle:** Immunohistochemistry for p19 ARF in Ras-induced lymphomas of the indicated genotypes were stained for ARF. Formalin-fixed and paraffin-embedded sections (7 µm) of infiltrated lung were probed with an anti-ARF antibody (1:10) *(Loddenkemper et al)*. **Bottom:** GFP-enrichment assay in lymphoma cells of different genotypes. Suv39h1 null (n=8), p53 null (n=3) and control lymphomas (n=5) were transduced retrovirally with either a MSCV-p16-IRES-GFP (left) or a MSCV-ARF-IRES-GFP construct (right). After transduction cell population was set to 10% GFP positivity and measured after 48 hours for relative GFP levels by FACS analysis. Error bars denote sd *(main part done by S. Lee)*.

3.4 Molecular defects in Suv39h1 compromised lymphomas

As previously shown, Suv39h1 represents a crucial mediator of Ras-induced tumor formation in the Eμ-N-Ras model. Loss of the histone methyltransferase likely controls, on the one hand, a mechanism that normally prevents lymphomagenesis or, on the other hand, supports secondary defects that promote lymphoma formation.

In the following section, the molecular defects in Suv39h1 deficient cells will be addressed and evaluated. In all experiments performed, N-Ras control lymphomas from the early death group were taken as cell type control.

3.4.1 Ras levels, p53 status and numeric aberrations

Unequal Ras levels, mutated p53 or polyploidy do not drive lymphomagenesis in a Suv39h1 null background

Ras protein expression and p53 gene sequencing analysis

Oncogenic Ras involves the activation of the Raf-MAP-Kinase pathway and the upregulation of proteins such as p53 or the INK4aArf gene products. This likely enhances the pressure to inactivate one of those key regulators during tumorigenesis. Especially p53 as gatekeeper of cell integrity might be mutated in Suv39h1 defective lymphomas and contribute to the phenotype.

Hence, evaluation of the p53 status is one crucial aspect that needs to be addressed. Therefore, RNA from Suv39h1 null and control lymphomas was isolated and used for amplifying p53 specific cDNA for further sequencing of the DNA binding domain (exon 4-8), a hotspot region for pointmutations in the p53 gene.
Representative sequencing analysis is outlined in Figure 21. In all of the samples tested (5/5 each genotype) sequencing analysis unveiled wildtype p53 of the DNA binding domain. Consequently, this assumes a functional p53 that is active in N-Ras Suv39h1 defective lymphomas as well as in controls (Details see appendix).

N-Ras control: forward p53 seq exon 4-8

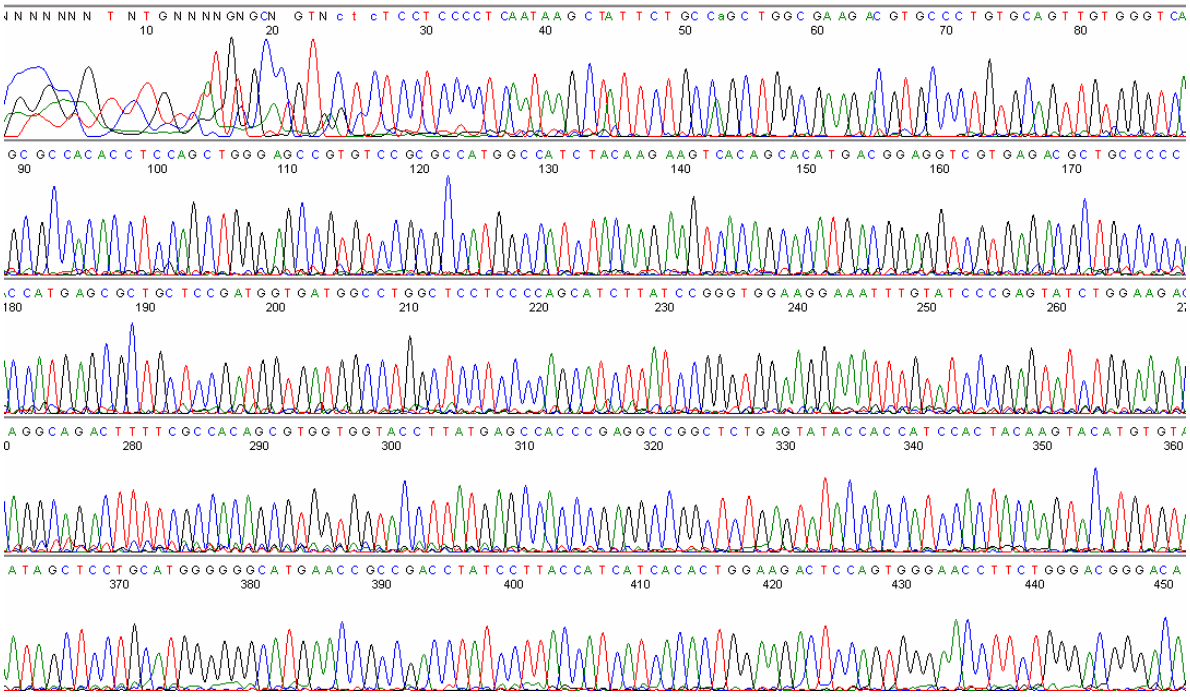

N-Ras Suv39h1 null: forward p53 seq exon 4-8

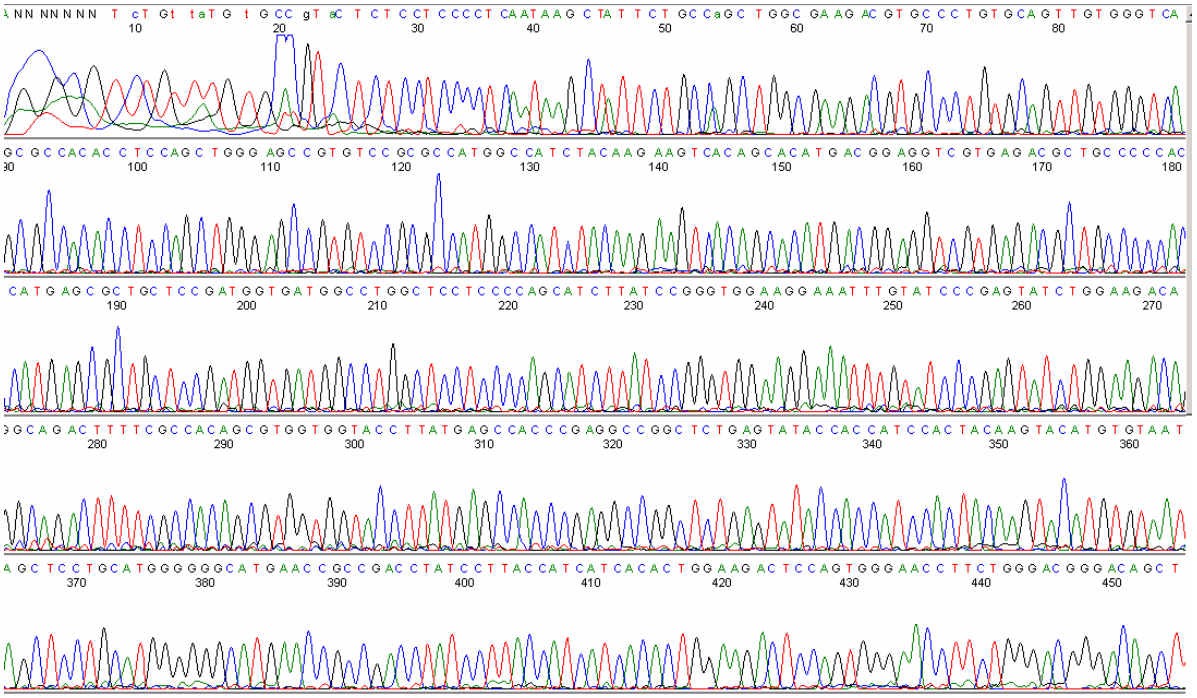

Figure 21: N-Ras control and Suv39h1 deficient lymphomas retain wildtype p53 exon 4-8. RNA of low-passage lymphoma cells (N-Ras controls; N-Ras Suv39h1 null; each genotype n=5) was isolated and cDNA was amplified using a p53 specific primer. Polymerase chain reaction was performed using a 5´- (exon 4) and a 3´-specific primer (exon 8) and sequenced in both directions (forward and reverse) using the respective primer. Representative sequencing analysis in 5´ direction of N-Ras controls (top) or Suv39h1 nulls (bottom); for 3´sequencing see appendix.

The observation that N-Ras Suv39h1 null animals die significantly earlier of an aggressive lymphoma compared to control mice suggests that those Suv39h1 deficient animals might select for hematopoietic cells expressing extremely high levels of oncogenic Ras. This likely accelerates tumorigenesis as a response to enhanced Ras-signaling and provokes an early phenotype.

To check for Ras expression levels, lymphoma cells of the respective genotypes were tested in an immunoblot analysis for their expression of Ras. For this, protein samples from whole cell lysates of low-passage lymphoma cells (N-Ras controls, Suv39h1 or p53 deficient) were separated by SDS-PAGE and probed with an anti-N-Ras antibody. Data outlined in Figure 22 (left; top) showed that all samples showed a similar, but highly varying expression pattern of oncogenic N-Ras that is driven by the Eμ promoter. This variability is found throughout the genotypes.

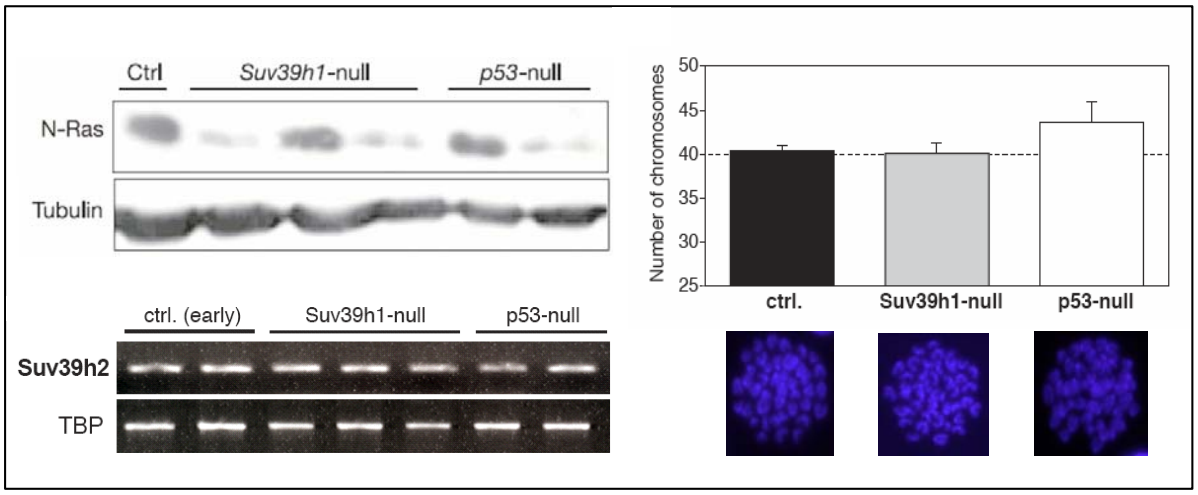

Figure 22: Ras levels, chromosomal instability, and Suv39h2 level in Suv39h1 null lymphoma. Left top: Western blot analysis of early passage lymphoma cells of the respective genotype. Whole cell lysates (80 µg) were loaded on a 15 % SDS-gel and the membrane was probed with an anti-N-Ras (1:500) detecting human N-Ras (21 kDa) and tubulin (1:8000) of 50 kDa size as loading control *(see also Figure 20; same membrane)* **Left bottom:** RT-PCR for Suv39h2 from N-Ras lymphomas of the indicated genotypes, TATA-box-binding protein (TBP) as an internal control. **Right:** Chromosomal metaphase spreads of N-Ras controls, Suv39h1 null and p53 null early passage lymphoma cells (5 per genotype). Colcemid arrested lymphoma cells were fixed, spread and stained with DAPI. Metaphases (12 of each lymphoma) were monitored and counted under the fluorescence microscope.

These results potentially exclude that Suv39h1 defective or p53 null lymphomas select for high Ras-expressing cells during tumorigenesis, ruling out that accelerated lymphomagenesis is due to enhanced Ras signaling in mice with defects in the Suv39h1 or p53 locus.

Suv39h1 deficient cells do not show segregation defects

Tumor formation is a multistep process that often requires the disruption of tumor suppressor proteins like p53. p53 is the gatekeeper of chromosomal integrity and since the gene is not mutated in Suv39h1 deficient lymphomas as shown in previous experiments it is rather unlikely that in those cells aneuploidy is the tumor driving force. However, it was shown that the Suv39h1/h2 knockout mouse quite frequently develops B cell lymphomas that are linked to chromosomal instability and to segregation defects ("butterfly chromosomes")[100]. Despite the fact that in those animals lymphomas develop rather late, it might be assumed that in response to oncogenic Ras mice select for defects in the Suv39h2 locus that accordingly accelerate the formation of lymphomas caused by an instable karyotype.

Metaphase spreads and Suv39h2 level

In order to exclude that loss of Suv39h2 and subsequent chromosomal instability have an impact on Ras-driven lymphomagenesis, Suv39h2 status and chromosomal integrity were assessed in N-Ras lymphomas of the respective genotypes.

To investigate Suv39h2 mRNA expression levels in Ras-induced lymphomas, RNA of low-passage lymphoma cells of wildtype, Suv39h1, or p53 null backgrounds was isolated and tested after gene-specific cDNA synthesis in a RT-polymerase chain reaction for the expression of Suv39h2. TATA-box-binding protein (TBP) served as an internal control.

As the results of the RT-PCR unveil, all lymphomas used in this approach were positive for the Suv39h2 message detecting comparable housekeeping gene levels (TBP). This excludes a functional loss of Suv39h2 during N-Ras driven lymphomagenesis and the putative molecular basis for chromosomal instability (Figure 22; left bottom).

However, since aneuploidy could be also driven by loss of the Suv39h1 protein alone, chromosomal integrity needs be evaluated in addition. To address this question, metaphase spreads of lymphoma cells (controls, Suv39h1- or p53-deficient) were performed to detect numeric aberrations or segregation defect ("butterfly chromosomes") in the manifest tumors. Therefore, low-passage lymphoma cells were arrested in the metaphase of the cell cycle using the spindle-checkpoint

toxin colcemid. After spreading the cell suspension on slides, metaphases were visualized with DAPI. To evaluate spreads at least 12 metaphases of each individual lymphoma were counted by fluorescence microscopy.
“Butterfly” chromosomes or similar figures were never detected in more that 100 metaphases of each sample tested throughout the genotypes. This already underlines that tumor formation is not related to a segregation defect (see representative pictures in Figure 22; right).
Chromosome numbers only slightly varied in control and Suv39h1 null lymphomas from 40, whereas p53 null tumors tested for comparison showed increased chromosome numbers according to the p53´s function in chromosomal integrity and stability. The chromosome numbers were also confirmed by collaboration partners *(Dr. Cornelia Rudolph - Medical School Hannover / Department of Cytogenetics)*.

These data exclude that Suv39h1 deficiency provokes Ras-driven lymphomagenesis by segregation defects or polyploidy which was found to induce B cell lymphomas in the Suv39h1/2 knockout mice.

3.4.2 Defects in cellular failsafe programs

In the previous experiments it was shown that in response to oncogenic Ras loss of Suv39h1 leads to a rapid formation of aggressive lymphomas *in vivo* that is independent of segregation defects, selection for high Ras levels or the p53 status.
It is likely that – as it was shown for p53 - loss of Suv39h1 accelerates Ras-driven tumorigenesis by disrupting the cellular failsafe machinery that normally prevents lymphoma formation. This is possible since mice with defects in the Suv39h1 locus display the similar time-to-death data and the same phenotypical features as p53 animals. For this, it was investigated whether Suv39h1 null lymphomas are capable to respond to therapy-inducible failsafe programs like programmed cell death (apoptosis) or a terminal cell cycle arrest (senescence) *in vitro*.

Defects in apoptosis: Loss of Suv39h1 produces apoptosis-competent Ras-lymphomas

In vitro growth and drug-responsibility of Ras-induced lymphomas

The capability of a tumor cell population to expand *in vitro* and *in vivo* is characterized by a balance of growing and dying cells. Accordingly, a population that is apoptosis-incompetent grows faster, a characteristic of p53 deficient tumor cells.

To address *in vitro* growth of the isolated lymphoma cells a growth curve analysis was performed. Therefore, well growing, low-passage lymphoma cells of the indicated genotypes were plated at identical cell numbers and viability was assessed by trypan blue exclusion over time (day 1-7). p53 null lymphoma cells were taken as control. Relative cell numbers were blotted against time (days).

Data in Figure 23 (left) show that cells all grew in an exponential fashion irrespective of the genotypes and could be established in culture. Hereby, Suv39h1 null cells did not show a significant growth advantage compared to control cells while cell numbers increased approximately 10 fold after the indicated 7 days. Contrarily, results reveal that N-Ras p53 deficient lymphomas grow rapidly and faster compared to Suv39h1 null or control cells (70 fold), underlining a putative apoptotic defect in Ras-driven p53 null tumors, but not in control or Suv39h1 deficient lymphomas.

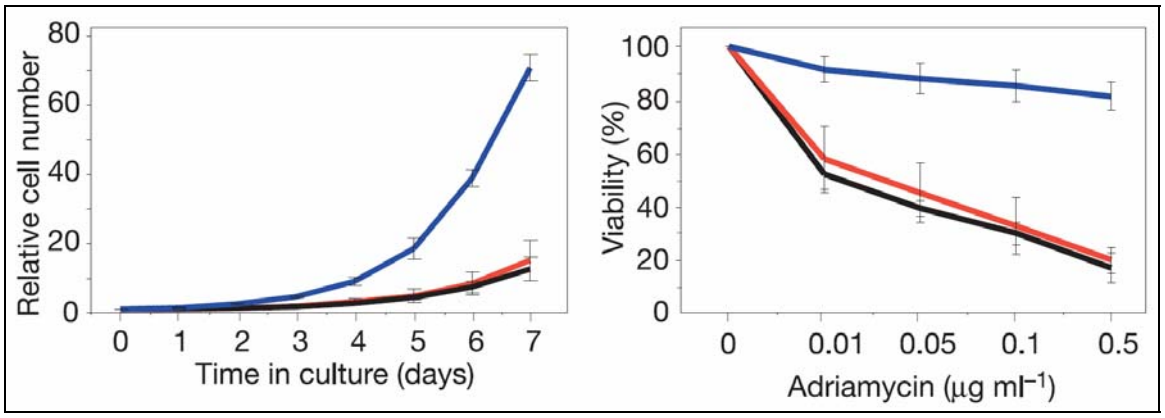

Figure 23: Suv39h1 null lymphomas are apoptosis competent. Left: Growth curve analysis of control (n=5; black), Suv39h1 null (n=14; red) and p53 null (n=4; blue) lymphoma cells. Early passage lymphoma cells of the indicated genotypes were seeded at same cell numbers and viable cells were counted each day by trypan blue exclusion. Error bars denote standard deviation (plated in duplicates). **Right:** Drug-inducability and apoptosis-competence of cells as in (a). Short term cytotoxicity of control (black), Suv39h1 null (red) and p53 null (blue) cells using the indicated Adriamycin concentrations. After 24 hours incubation time viability was assessed by trypan blue counting. Error bars reflect standard deviation.

To prove the hypothesis whether an apoptotic defect contributes to the early death phenotype in Suv39h1 deficient lymphomas, cells were exposed to the anticancer drug Adriamycin (ADR), a topoisomerase-inhibitor and DNA-damaging agent that induces p53-dependent cell death. To evaluate this model, drug-inducible apoptosis was assessed by trypan blue exclusion in a short term cytotoxicity assay.
As expected, lymphoma cells deficient for p53 did not respond to low dosages of Adriamycin and showed, even under high concentrations, almost no cell death after 24 hours. Interestingly, Suv39h1 null lymphomas remained highly sensitive to the drug displaying increased apoptosis. This was also observed in N-Ras control lymphomas displaying manifest and increasing cell death after exposure with the anticancer drug (Figure 23; right).

Those experiments clearly unveil that N-Ras driven Suv39h1 null tumors remain highly sensitive to drug-induced DNA-damage response and apoptosis competent like early death control lymphomas, whereas p53 null cells were incapable to trigger an apoptotic response.

Defects in senescence: Loss of Suv39h1 produces senescence defective Ras-lymphomas

As previous results outline, Suv39h1 null lymphomas remain highly sensitive to DNA-damaging drugs that cause a p53-depending cell death. This excludes a putative apoptotic defect that drives lymphomagenesis in response to oncogenic Ras.
Hence, it is conceivable that premature senescence as another cellular failsafe program might be disrupted in Suv39h1 null cells promoting Ras-driven lymphoma formation. Accordingly, the capability of Suv39h1 deficient cells to trigger a senescence response will be addressed in the following section.
There are several characteristics of a senescent cell population to uncover the senescent phenotype. One common feature and the gold standard to detect senescence is the upregulation of the lysosomal protein ß-galactosidase[9]. Upregulation can be visualized by an enzymatic reaction (senescence-associated ß-galactosidase assay) resulting in a blue cytoplasmic staining. In addition, the terminal cell cycle arrest can be assessed by a growth curve analysis over time. Changes in cellular morphology and granularity, further indicators of cellular senescence, can be examined by the measurement of growth in a flow-cytometry approach (FSC/SSC).

Furthermore, senescence regulators that are upregulated can be evaluated in a Western blot analysis or by immunocytochemistry.

Drug-induced senescence in Ras-driven lymphomas

To assess whether Suv39h1 deficient lymphomas are still senescence competent and can undergo a terminal growth arrest, cells were treated again with Adriamycin. However, since apoptosis is the primary response to DNA damaging agents as shown in the setting before, cells need to be protected from programmed cell death. Therefore, low-passage lymphoma cells of all genotypes were retrovirally transduced with a murine MSCV-bcl2-puro construct and selected for puromycin resistant cells in order to obtain a 100% positive population expressing Bcl2. These apoptosis protected lymphomas were exposed to a 0.1 µg/ml dose of ADR for 5 days and tested for senescence after the indicated time points. Untreated cells served as a control.

To assess the putative cell cycle arrest, ADR-treated cells and their respective controls were seeded (at identical cell numbers) on feeder plates (approximately 50% confluency). To determine growth capabilities, viable cells were counted every 24 hours. After 3 days, an aliquot was taken to measure morphological changes in a flow cytometry approach (forward sidescatter analysis). Later (day 5), treated lymphomas and their untreated counterparts were cytospun for the senescence assay (SA-ß-galactosidase) and an immunocytochemistry approach. In addition, whole cell lysates were isolated to validate expression levels of the p16 and ARF proteins.

The SA-ß-gal assay (outlined in Figure 24; top) unveils, as expected, in all untreated scenarios a SA-ß-gal negative and therefore non-senescent cell population. However, in N-Ras control lymphomas, nearly all cells turned blue (88%) after 5 days of Adriamycin treatment and forwardscatter/sidescatter analysis revealed an increase in granularity and size (inlays). Strikingly, Suv39h1 cells apparently lack a positive SA-ß-gal staining since almost no cells turned blue (9%) and retained size and granularity that is comparable to untreated cells. This observation suggests that Ras-driven Suv39h1 deficient lymphomas are incapable of undergoing a senescent phenotype in response to DNA-damaging agents *in vitro*, whereas control cells senesce under the same treatment conditions. For comparison, p53 null cells -

known to inherit a senescence defect - did not respond to the drug (7% positive SA-ß-gal; no change in size and granularity).

Expectedly, growth curve analysis (Figure 24; bottom, left) of those lymphomas uncovered that all untreated cells (UT) grew exponentially with advantages for p53 deficient lymphomas (see section before). In contrast, Adriamycin treated (ADR) N-Ras controls remained viable and cell number did not increase after 5 days, indicative of a manifest growth arrest. Remarkably and in line with the SA-ß-galactosidase staining, Suv39h1 null cells did not arrest in response to the drug and showed nearly identical cell numbers after 5 days with or without treatment.

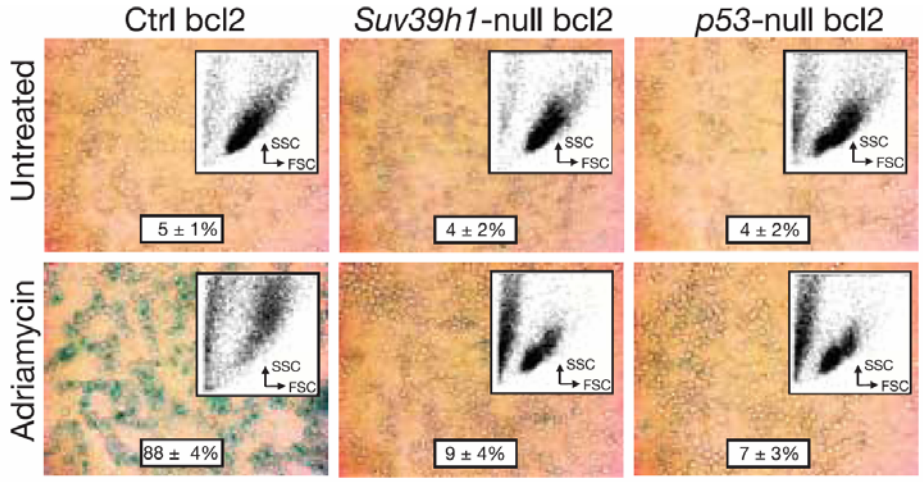

Figure 24: Suv39h1 null lymphomas are senescence defective. Top: Drug-inducible senescence in apoptosis-blocked control, Suv39h1 null and p53 null lymphoma cells. Low passage lymphoma cells were transduced retrovirally with a MSCV-bcl2-puro construct and treated after antibiotic-selection with a concentration of 0.1 µg/ml Adriamycin for five days. The respective untreated cell population was referred to as control. To assess the senescence phenotype cells were cytospun and stained for SA-ß-galactosidase at day 5 (big pictures), percentage of senescent cells were outlined including standard deviations (n=3 each sample). Morphological changes (size/granularity) were determined at day3 in a forward scatter/side scatter (FSC/SSC) FACS analysis (inlays). **Bottom:** Growth analysis (n=4 each genotype) of Adriamycin treated cells (ADR) or the untreated control (UT) as in (a). Growth was assessed by trypan blue counting of the viable fraction (d0 / d5) in controls (black), Suv39h1 null (red) and p53 null (blue) lymphomas. Error bars note standard deviation. Immunoblot (right top) analysis of Bcl2-overexpressing cells as in (a) after 5 days with (ADR) or without Adriamycin treatment (UT). Whole cell lysates (80µg) were separated on a 15% SDS-gel and the membrane was probed with either an anti-p16 (1:500, recognizes murine p16 at 16 kDa) or an anti-ARF 1:500 (detects murine p19 ARF at 19 kDa). α-tubulin (1:8000 at 50 kDa) as an internal loading control. Immunocytochemistry (right bottom) of cells after 5 days treatment with Adriamycin (ADR) or untreated cells for comparison (UT). Cytospins (right bottom) of apoptosis-blocked cells (as described above) were stained for their expression of either p16 (1:100, left) or ARF (1:10, right) *(Staining by Loddenkemper et al)*.

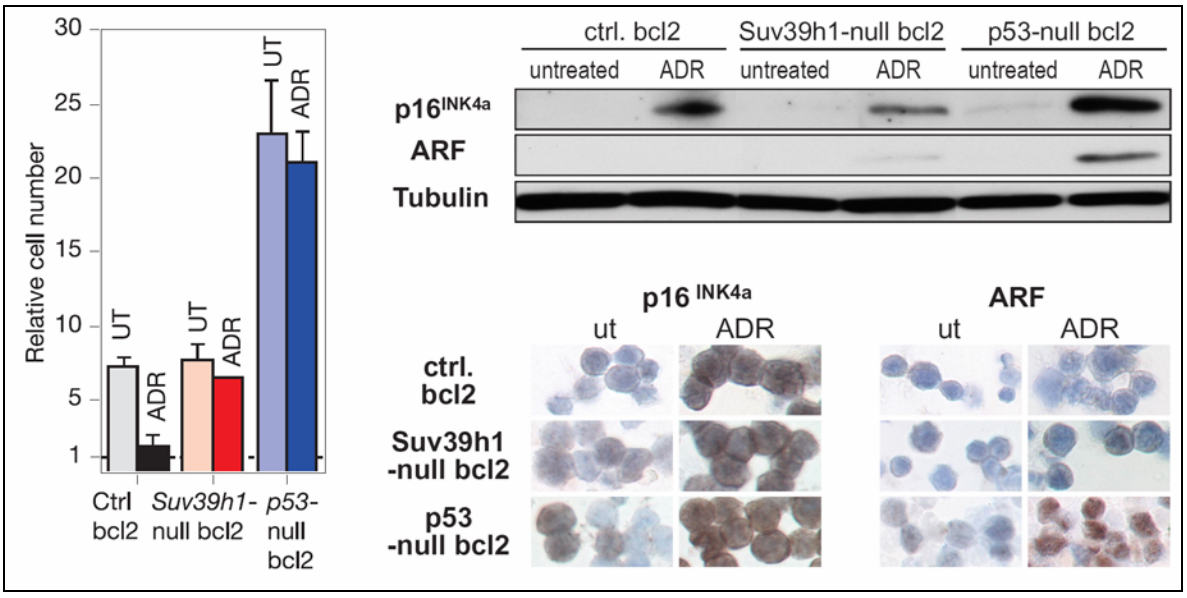

The p16 protein is a key player shown to be upregulated in Ras-induced senescence *in vitro*. To investigate p16 expression in the Adriamycin treated lymphomas, cells at day 5 were cytospun for an immunocytochemistry approach *(Loddenkemper et al)* and whole cell protein lysates were isolated to perform Western blot analysis. In parallel, also ARF levels were determined using the same test settings. Representative pictures are shown in Figure 24 (right, upper and lower pictures).
Results of both experiments clearly show that after drug exposure p16 is overexpressed in the lymphomas independent of the genotype. Nevertheless, the ARF protein was only detectable in p53 deficient lymphoma samples after treatment and only slightly increases in Suv39h1 null cells after ADR.

These data demonstrate that, in response to therapy, key regulators of the senescence machinery such as p16 are upregulated to induce a senescent phenotype. This seems to be irrespective of the genotype since p16 was found upregulated also in Suv39h1 and p53 deficient samples, assuming that the senescence machinery upstream of Suv39h1 is active and intact, but signals cannot be translated downstream.

Taken together, drug-inducible senescence can be induced in Ras control lymphoma cells displaying all features of a senescent cell population - SA-ß-gal positivity, growth arrest, morphological changes as well as the upregulation of p16. Strikingly,

Suv39h1 deficient cells are incapable of senescing upon therapy; despite the fact that proteins such as p16 are upregulated.

3.5 Molecular mechanism: Ras-induced senescence in lymphocytes and Suv39h1-dependency

3.5.1 Ras and the function of Suv39h1 in primary lymphocytes

Suv39h1 controls Ras-induced senescence by a H3K9-dependent mechanism

As it was demonstrated in the previous experiments, Ras-induced lymphoma cells that arise in the absence of Suv39h1 are still apoptosis-competent, but fail to undergo premature senescence under therapy. However, since in the Eμ-N-Ras-transgenic mouse model Ras is permanently overexpressed in the hematopoietic system, it is necessary to study the acute effect of oncogenic Ras on primary lymphocytes.

Impact of oncogenic Ras in Suv39h1 proficient and deficient primary splenocytes

To study this question, primary splenocytes were transduced with oncogenic Ras and assessed for a senescent phenotype. Splenocytes from either a non-transgenic wildtype or a Suv39h1 null mouse were isolated and retrovirally transduced with a selectable Ras vector (MSCV-H-ras-puro) and the empty vector control (MSCV-puro), respectively. After puromycin selection, cells were seeded at identical cell numbers to determine growth capabilities and senescence-associated ß-galactosidase after 6 days.

The results are outlined in Figure 25 (bottom). Growth curve analysis (Figure 25 middle) revealed that both empty vector transduced wildtype and Suv39h1 null splenocytes grew slowly, but comparably and increased in cell number about 2.5 times after 6 days, while showing only a slight background staining for the senescence marker SA-ß-gal (around 5%; upper picture).

Contrarily, H-Ras transduced wildtype splenocytes stopped proliferating while remaining viable and were nearly 80% positive for SA-ß-gal. However, in response to oncogenic Ras Suv39h1 cells still grew readily, retained viability and doubled after one week in culture, while showing only a moderate SA-ß-gal background (16%).

These data unveil that oncogenic Ras can induce a terminal cell cycle arrest in primary lymphocytes, while, remarkably, lymphocytes deficient for Suv39h1 are not entering a terminal cell cycle arrest in response to acutely overexpressed Ras.

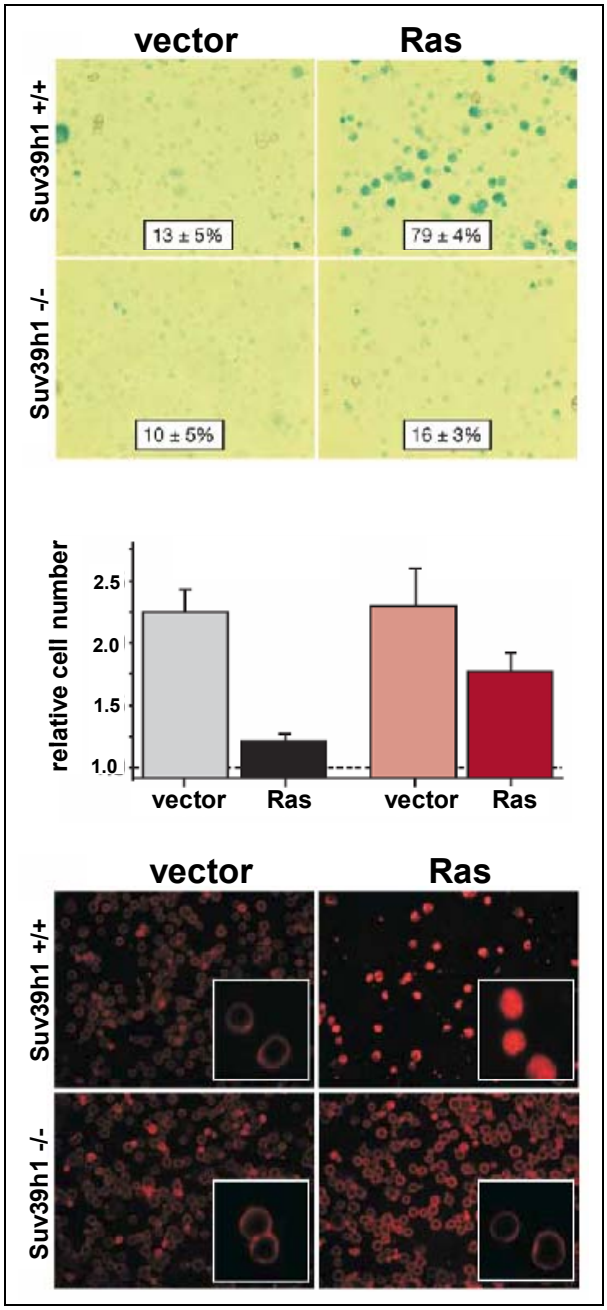

Figure 25: Ras-induced senescence in primary lymphocytes is Suv39h1/H3K9me-dependent. Primary splenocytes isolated from Suv39h1 null and wildtype mice were pooled and retrovirally transduced with either a MSCV-H-RasV12-puro construct (Ras) or the empty vector only (vector). **Right:** After antibiotic selection cells were seeded at identical cell numbers and growth was determined after day 6. Growth of Suv39h1 wildtype (Suv39h1+/+, black) and Suv39h1 null (Suv39h1-/-, red) splenocytes was assessed by trypan blue exclusion counting the viable cell fraction. Error bars denote standard deviations resulting from duplicates of two independent experiments. **Left top and**

bottom: Cytospin preparations of vector and Ras-transduced Suv39h1+/+ or Suv39h1-/- cells (see above) were plated in triplicates and stained for endogenous ß-galactosidase (b, means +/- standard deviation) and in an immunofluorescence assay (c) for trimethylated H3K9 (1:100, big pictures) and HP1-γ (1:100, inlays).

The enzymatic function of Suv39h1 is characterized by the methylation of histone H3 at lysine 9. From previous results it seems that Suv39h1 triggers a senescent phenotype in response to oncogenic Ras, however, it is not clear until now if this is accompanied with an increase in H3K9 methylation and HP1γ, a Suv39h1-linked protein associated with heterochromatin structures.

To determine whether Ras-induced senescence depends on Suv39h1 function, Ras-transduced splenocytes and their respective empty vector controls were tested for tri-methylated histone H3 (H3K9me3) and HP1γ status, respectively.

For this, splenocytes from the previous experimental setting were cytospun and tested in an immunofluorescence assay for both proteins.

Results (Figure 25; lower picture) showed that in Ras-transduced, senescent wildtype splenocytes trimethylated histone H3 is clearly increased in the nucleus compared to normal empty vector transduced cells. The same was observed for the HP1γ protein that is obviously enriched in senescent wildtype cells after Ras-induction. Remarkably, cancellation of senescence by Suv39h1 deficiency showed neither an enrichment for trimethylated histone H3 nor HP1γ in response to oncogenic Ras.

This potentially underlines that the functional loss of Suv39h1 promotes Ras-driven lymphomagenesis *in vivo* by cancelling senescence as putative failsafe machinery that is controlled by heterochromatin formation and histone methylation.

4) Discussion

Two major questions were addressed in this thesis. Firstly, does loss of the histone methyltransferase Suv39h1 have an impact on Ras-induced tumorigenesis in an *in vivo* mouse model. Secondly, if so, which underlying mechanism triggers the outcome of tumor formation, in particular, are cellular failsafe mechanisms like senescence controlled by Suv39h1 and do they counteract malignant transformation in this system. The results obtained in this study will be discussed in the following sections.

4.1 Relevance, controversial view, clinical aspect and perspectives

Since decades it has been believed that cellular senescence is a telomere-dependent phenomenon that occurs only in aging cells when a population looses the ability to divide[6,7]. However, studies of the late 90s have now demonstrated that senescence is not only restricted to cells "growing old", but is also recruited after excessive mitogenic signaling, DNA damage as well as after chemotherapy or oxidative lesions[13-16,107]. This stress-inducible, intrinsic defense mechanism terminally locks the cell in a permanent arrest while it remains metabolically active, but insensitive to any growth signals. The tumor-suppressive potential of senescence in response to oncogenic stimuli was shown several years ago when permanently activated Ras provoked a terminal cell cycle arrest *in vitro* reminiscent of senescence.

Disruption of regulators such as $p16^{INK4a}$ or p53 executed senescence and efficiently transform a cell as shown in several Ras-driven cell culture systems[15]. However, whether this failsafe program is relevant *in vivo* remained questionable. While there is clear evidence that defects in the apoptotic pathway contribute to cellular transformation *in vitro* and promote cancer formation *in vivo*, until now, premature senescence was often considered as a "culture shock" effect[108].

Limitation of the model?

A functional model to examine the role of Ras-induced senescence *in vivo* has not been addressed so far. Focussing on hematopoietic malignancies, in the present work, emphasis was based on senescence as a potential tumor suppressor mechanism to counteract Ras-provoked lymphoma formation.

Comparable approaches exist to unveil the role of failsafe programs in oncogene-driven lymphomagenesis. The Eμ-Myc transgenic mouse provides an excellent and already well established model to evaluate the impact of Myc-evoked apoptosis in lymphoma formation and treatment responses. Using this system, it was shown that disruption of tumor suppressors like p53 or INK4aArf in Eμ-Myc mice dramatically accelerates tumor formation and defects in these players significantly have an impact on treatment outcome[106,109,110].

Accordingly, we have chosen the Eμ-N-Ras transgenic mouse where oncogenic Ras is constitutively expressed in the hematopoietic compartment[104]. Despite the genetics of the N-Ras transgenic mouse model in which the oncogene is driven by the promoter of an immunoglobulin heavy chain enhancer (Eμ), mice did not succumb to B cell malignancies, but rather developed non-lymphoid sarcomas from macrophage origin, and only sporadically lymphoid tumors. However, those findings are well in line with already published data that N-Ras transgenic mice suffer from histiocytic sarcomas and quite reasonable since it was shown that the Eμ promoter indeed is active in other subpopulations of the hematopoietic compartment[104].

Markedly, defects in the Suv39h1 histone methyltransferase promote the formation of aggressive T lymphoblastic tumors in this model accompanied with significant differences in time-to-death latencies. This provides striking evidence that Ras-induced lymphomagenesis is epigenetically regulated and suggests an important role for Suv39h1. Furthermore, this is supported by the finding that lymphomas in a Suv39h1 heterozygous background select against functional Suv39h1 expression during tumor formation. According to the Lyon Hypothesis[111] this is likely since Suv39h1 is X-chromosomally linked and female mice *per se* inactivate one allele, generating a putative null scenario, therefore, it is easy to select for.

These results indicate that in response to oncogenic Ras loss of Suv39h1 likely provokes the formation of aggressive lymphoid tumors by disrupting a tumor suppressing mechanism.

Suv39h1 is an Rb-bound enzyme[102] catalyzing methylation of histone H3K9 that provides a binding site for heterochromatin proteins like HP1γ and locally provokes heterochromatin formation, also on E2F responsive S phase promoters[103]. Since methylated H3K9 was found as a characteristic feature of Rb-dependent heterochromatin foci in senescent cells, it was highly conceivable that Suv39h1 silences E2F-responsive S phase genes to suppress cell proliferation in response to cellular oncogenes and contributes to a senescent cell cycle arrest[30,93,102,112]. Indeed, as shown in the present thesis, Suv39h1 regulates senescence in response to oncogenic Ras signaling in primary lymphocytes and provides an initial barrier during lymphomagenesis.

Although the phenotype of the *in vivo* studies is quite impressive, the model itself can display a concern in this system. The Eμ-N-Ras transgenic mouse can be considered as rather not physiological since mutated N-Ras is overexpressed by an artificial promoter in the hematopoietic system. Hereby, Ras levels may not be comparable to levels in a physiological setting where endogenous Ras genes are mutated.
This is an issue of debate since varying amounts of oncogenic Ras exhibit different effects on cells and are, in addition, highly dependent on the cell type or microenviromental factors[113]. It is broadly believed that moderate levels of the oncogene induce hyperproliferation, while only higher expression levels can induce an acute arrest. For instance, freshly isolated human fibroblasts start hyperproliferating in response to oncogenic Ras and do not exhibit a senescence phenotype; unlike fibroblast celllines in culture that were shown to arrest[114]. Accordingly, it seems that cells in culture are already sensitized to exogenous stimuli by repeated passaging and overexpression of p16, while freshly isolated fibroblasts likely would reflect the scenario *in vivo*. The observation that only supraphysiological Ras levels trigger a senescence response likely supports the idea that the tumor suppressive potential might only be a culture artefact or, as in the used mouse model, the consequence of excessive overexpression due to a strong promoter.
However, together with the present thesis, hallmark studies published last year provide striking evidence that senescence indeed acts as a potential tumor suppressor mechanism *in vivo* to prevent cancer formation in human and mouse irrespective of the type of stimuli[115,116].

Constitutive activation of the Ras-signaling pathway like K-Ras^{G12V} or mutated BRAF, a downstream effector of Ras, induces senescence in pre-malignant lesion like lung adenomas or naevi cell, the benign precursor cells of melanomas. The results unveil that in different model systems either endogenous mutations in K-Ras^{G12V}, titrated expression levels of exogenous BRAF^{V600E} *in vitro* or BRAF mutations in patient samples can induce a senescence response. Together with our findings in the transgenic mouse model and the studies with overexpressed oncogenic H-Ras^{V12G} *in vitro*, it can no longer be insisted on the hypothesis that senescence is a level-dependent culture artefact. Moreover, loss of the tumor suppressor PTEN in prostate glands of the mouse induces features of cellular senescence even without any modifications in the Ras-Raf-pathway[117].
These observations show that senescence is not only inducible by activated Ras-signaling alone, but can also be triggered by regulators of the Akt-p53 axis. The papers unveil in a broad spectrum of pre-malignant entities cellular senescence as a tumor preventing program recruited in diverse tissues to counteract tumor formation.

In addition, it was also reported quite recently that permanent activation of E2F in pituitary glands of the mouse causes a hyperproliferative stimulus and led, quite unexpectedly, to a terminal arrest. Rb-connected E2F is known to drive S-phase progression and initially, permanent activation was thought to transform a cell[118]. Interestingly, it was shown in this context that deregulated E2F instead causes a cell cycle arrest linked to Rb-dependent chromatin changes reminiscent of senescence. This is well in line with the outstanding hypothesis of a stress-responsive cellular failsafe machinery that can be activated in cells at risk for transformation.

Most strikingly, we found evidence that in mice with endogenous Ras mutations lymphoma onset depends on the presence of the Suv39h1 histone methyltransferase (unpublished data, Schmitt lab), likely by controlling the same failsafe machinery as shown in the present thesis. Similar to the Eμ-N-Ras model, time-to-death data unveiled significant differences between control mice and Suv39h1 deficient animals when Ras-mutations were chemically-induced and are therefore comparable to a physiological setting.

Another issue that needs to be discussed in this model is the observation that lymphomas also form in Eμ-N-Ras control animals without any additional genetic defects. Even though control lymphomas form sporadically they need to acquire additional defects in Ras-induced signaling pathways or the cancellation of other tumor suppressing programs. However, a functional p53-pathway seems to be intact in these cells since lymphomas retain wildtype p53 transcript, show no aneuploidy and are sensitive towards exogenous p53-activating triggers such as ARF. Furthermore, Adriamycin can induce an apoptotic response and a senescent phenotype can be reiterated when cells are Bcl2-protected. Further investigation revealed that control lymphomas are unable to induce ARF protein levels in response to Adriamycin and also immunohistochemistry *in situ* showed only marginal expression of ARF, unlike in Suv39h1 and p53 deficient cells where ARF is detectable *in situ*. Preliminary data suggest that altered ARF, but not p16 expression provokes lymphoma growth in Eμ-N-Ras transgenic mice supporting the last findings (Braig and Schmitt, unpublished data). But whether ARF cancels Ras-induced senescence needs to be studied in more detail, likely by performing similar approaches described in the present thesis.

Suv39h1 and its role in senescence: a functional bias?

Recent data unveil that Ras induces cellular senescence to prevent improper proliferation and oncogenic transformation *in vitro*[15]. This includes Rb-related heterochromatin changes like methylation of histone H3K9 and the attraction of heterochromatin associated proteins like HP1 to repressive heterochromatin structures (SAHFs)[30]. Indeed, in our system, primary lymphocytes respond to the acute introduction of oncogenic Ras with a terminal cell cycle arrest that is accompanied by the up regulation of senescent markers like SA-ß-galactosidase or increased HP1γ, which can be disrupted by loss of Suv39h1. These results underscore that senescence is an epigenetically controlled process mediating a terminal cell cycle arrest changing the local chromatin status.

Suv39h1 is a histone methyltransferase that confers not only to constitutive heterochromatin formation on centromers, but also the silencing of euchromatic sites that locally repress transcriptional processes[103]. Thus, it might be able to induce

heterochromatin structures that directly or indirectly influence the repression of genes regulating an oncogene-dependent senescence response.

Accordingly, it is possible that altered expression of senescence-proteins upstream of Suv39h1 confers lymphoma formation and not Suv39h1-dependent repression of E2F responsive promoters itself. This would rather imply the regulation of $p16^{INK4a}$ or a related protein controlling the Ras-Rb-senescence axis. However, screens for H3K9-silenced promoters in tumor cells unveiled several genes of which none is p16 or another protein that controls the expression of a yet unknown senescence player. Studies on the INK4a promoter in senescent cells also showed no alteration in the acetylation status (H3K9) suggesting no change in methylation at the same histone residue. Indeed, in pre-senescent mouse embryonic fibroblasts (MEFs) oncogenic Ras was able to in induce p16 expression that does not depend on the Suv39h1 status since p16 levels did not change in the absence or presence of Suv39h1 or even when Suv39h1 is overexpressed[119].

Of note, if Suv39h1 regulates the transcription of an unknown protein that controls senescence cannot be excluded. Studies including gene array experiments or global protein analysis (e.g. a proteomics approach) in Suv39h1 proficient vs. Suv39h1 deficient scenarios should give a closer overview addressing potential target genes of Suv39h1 that might influence cell cycle progression, senescence or related mechanisms.

Can histone demethylation mimic loss of Suv39h1?

Until recently, no particular demethylase was discovered that potentially could remove the stable methyl mark on histone residues and could counter therefore Suv39h1 function. The observation that methylated lysines display the same half-life than histones supported the view that histone methylation may be a stable mark set on the nucleosome. Especially histone trimethylation, catalyzed by Suv39h1, appears to be relatively robust since trimethyl marks are stably propagated and do resist mammalian reprogramming during embryogenesis.

Surprisingly, new data using more refined technologies showed that methylation of histones can be reduced. With the latest discovery of the lysine specific demethylase 1 (LSD1) that acts specifically on mono- and dimethylated H3K4, the current view

about reverting histone methylation changed dramatically[120]. It was shown to convert H3K4me2 on active chromatin states and - when associated to another protein complex - even functionally different H3K9me2 marks on silenced chromatin regions[121]. In addition, a second demethylase (JHDM1), a JmjC domain containing protein, was found to exclusively demethylate H3K36me2[122].
Latest research on this field finally discovered JMJD2 (jumonji domain containing 2) family members, the first histone demethylases that are able to demethylate trimethylated lysines[123]. This is for particular interest since this could indeed convert the function of SU(VAR)3-9 proteins on H3K9 and counterpart its repressive function. Overexpression of such demethylases would, in principal, mimic loss of histone methyltransferases such as Suv39h1 and likely influence oncogene-induced tumor formation as well. It is clear that further work need to be investigated to uncover more details addressing the nature of reversing histone methylation, the selective interplay with HMTs and their function in cancer development. In this context it would be necessary to check for already known H3K9-related demethylases and their status in Suv39h1 deficient cells and particular their role in Ras-induced lymphomagenesis. However, the striking and reproducible phenotype observed in the tested mouse model, when Suv39h1 is genetically ablated, argues against such a mechanism.

Relevance of epigenetic regulators in tumor formation and therapy

A widely accepted hypothesis states that one alteration in a cell – like activation of Ras pathways, loss of PTEN function or permanent E2F signaling – is not sufficient to form a full-blown malignancy[1,34]. Disruption of additional key players that control cellular failsafe mechanisms is prerequisite for tumor formation. Indeed, p53 is one of the most frequent mutations in tumors; also the retinoblastoma protein is deregulated in a broad variety of cancers[1].

Contrarily, no distinct Suv39h1 modification, mutation or alteration was found in human entities so far that would emphasize its striking role protecting oncogene-induced tumorigenesis. It would be an important new piece of data linking deregulated Suv39h1 function to a human neoplasia since another Rb-linked histone methyltransferase, Riz1, was found to be mutated in human cancers[89,90]. This suggests a comparable H3K9-mediated mechanism preventing tumorigenesis in

human, likely by regulating cellular senescence or other failsafe mechanisms. On the other hand, it might not be necessary to inactivate Suv39h1 itself since related proteins such as Rb are defective in human cancer that consequently would disrupt also Suv39h1 function and releases the pressure to inactivate Suv39h1.

There is emerging evidence from different sides that histone modifications play a crucial role in cancer formation. Although a global view of disrupted histone modifications in cancer cells is still missing, plenty are already known to have an impact on malignant transformation. Mutations in genes coding for histone acetyltransferases are associated with lung or colon carcinomas, acute myeloid leukemia or epithelial cancer and HDAC1, a histone deacetylase, is overexpressed in prostate and gastric cancers[77,124]. In addition, aberrant expression of human histone methyltransferases like EZH2 is correlated with primary mammacarcinomas, Hodgkin's lymphoma and prostate cancer[125,126]. Remarkably, those epigenetic alterations raise the possibility for therapeutic intervention.

In contrast to genetic events, epigenetic changes like DNA methylation or histone modification can likely be reversed or interrupted by interfering with specific enzymes. In the last years, research has focussed on inhibitors targeting HDACs that were found to be overexpressed in a variety of human neoplasia. Combination treatments of HDAC inhibitors and DNA methylating agents are well tolerated in patients suffering from AML or the myelodisplastic syndrome and can reduce uncontrolled cell proliferation and apoptosis. However the anticancer effect remains obscure to date. Contrarily, we found that treatment of N-Ras transgenic mice with an HDAC inhibitor (Trichostatin A) and DNA demethylating agent (2-deoxy-5-azacytidine) accelerate tumor onset in those animals similar as to Suv39h1 deficiency[119]. This is well in line with the hypothesis stated in this thesis that Suv39h1 methylates histone H3K9 in Ras-induced senescent lymphocytes by silencing E2F-dependent genes. Inhibitors of histone deacetylases now potentially mimic loss of Suv39h1 in the Ras-model since hyperacetylated histones cannot be methylated in parallel, keeping transcription active on E2F-responsive promoters. This might prevent a senescent cell cycle arrest. HDAC inhibitors globally target histone acetylation; side effects on normal cells can not be excluded and whether this therapy activates a possible oncogene in another cell context still remains elusive. Accordingly, it seems that therapy based on

epigenetic alterations is highly cell-type dependent and restricted to specific tumor entities or stages.
The increasing evidence for a direct link between histone methylation and cancer together with the recent discovery of functional histone demethylases now puts the focus more on histone methylation and will be of great impact for further therapeutic intervention.

Restoring histone methylation in cancer cells could be an option to revert a malignant phenotype, likely by re-introducing a senescent growth arrest. This is quite reasonable since it was shown that pharmacological stabilization of p53 in PTEN-deficient prostate cancer cells[117] and inhibition of the ARF-repressor Tbx2 in melanoma cells directly restored cellular senescence preventing further malignant proliferation[127,128].

In close correlation with those findings, this thesis provides the first time evidence for a tight correlation between senescence as a histone-methylation governed program and lymphoma formation that raises new possibilities and strategies for cancer therapy.

5) APPENDIX

5.1 REFERENCES

1. Hanahan D, Weinberg RA. The hallmarks of cancer. Cell. 2000;100:57-70
2. Schmitt CA. Senescence, apoptosis and therapy--cutting the lifelines of cancer. Nat Rev Cancer. 2003;3:286-295
3. Schmitt CA, Lowe SW. Apoptosis and therapy. J Pathol. 1999;187:127-137
4. Schmitt CA, Lowe SW. Apoptosis is critical for drug response in vivo. Drug Resist Updat. 2001;4:132-134
5. Schmitt CA, Lowe SW. Apoptosis and chemoresistance in transgenic cancer models. J Mol Med. 2002;80:137-146
6. Hayflick L, Moorhead PS. The serial cultivation of human diploid cell strains. Exp Cell Res. 1961;25:585-621
7. Harley CB, Futcher AB, Greider CW. Telomeres shorten during ageing of human fibroblasts. Nature. 1990;345:458-460
8. Herbig U, Ferreira M, Condel L, Carey D, Sedivy JM. Cellular senescence in aging primates. Science. 2006;311:1257
9. Dimri GP, Lee X, Basile G, Acosta M, Scott G, Roskelley C, Medrano EE, Linskens M, Rubelj I, Pereira-Smith O, et al. A biomarker that identifies senescent human cells in culture and in aging skin in vivo. Proc Natl Acad Sci U S A. 1995;92:9363-9367
10. Mishima K, Handa JT, Aotaki-Keen A, Lutty GA, Morse LS, Hjelmeland LM. Senescence-associated beta-galactosidase histochemistry for the primate eye. Invest Ophthalmol Vis Sci. 1999;40:1590-1593
11. Paradis V, Youssef N, Dargere D, Ba N, Bonvoust F, Deschatrette J, Bedossa P. Replicative senescence in normal liver, chronic hepatitis C, and hepatocellular carcinomas. Hum Pathol. 2001;32:327-332
12. Chang BD, Swift ME, Shen M, Fang J, Broude EV, Roninson IB. Molecular determinants of terminal growth arrest induced in tumor cells by a chemotherapeutic agent. Proc Natl Acad Sci U S A. 2002;99:389-394
13. Chang BD, Broude EV, Dokmanovic M, Zhu H, Ruth A, Xuan Y, Kandel ES, Lausch E, Christov K, Roninson IB. A senescence-like phenotype distinguishes tumor cells that undergo terminal proliferation arrest after exposure to anticancer agents. Cancer Res. 1999;59:3761-3767
14. Chang BD, Xuan Y, Broude EV, Zhu H, Schott B, Fang J, Roninson IB. Role of p53 and p21waf1/cip1 in senescence-like terminal proliferation arrest induced in human tumor cells by chemotherapeutic drugs. Oncogene. 1999;18:4808-4818
15. Serrano M, Lin AW, McCurrach ME, Beach D, Lowe SW. Oncogenic ras provokes premature cell senescence associated with accumulation of p53 and p16INK4a. Cell. 1997;88:593-602
16. Jones CJ, Kipling D, Morris M, Hepburn P, Skinner J, Bounacer A, Wyllie FS, Ivan M, Bartek J, Wynford-Thomas D, Bond JA. Evidence for a telomere-independent "clock" limiting RAS oncogene-driven proliferation of human thyroid epithelial cells. Mol Cell Biol. 2000;20:5690-5699
17. Sherwood SW, Rush D, Ellsworth JL, Schimke RT. Defining cellular senescence in IMR-90 cells: a flow cytometric analysis. Proc Natl Acad Sci U S A. 1988;85:9086-9090

18. Shelton DN, Chang E, Whittier PS, Choi D, Funk WD. Microarray analysis of replicative senescence. Curr Biol. 1999;9:939-945
19. Harvey M, Sands AT, Weiss RS, Hegi ME, Wiseman RW, Pantazis P, Giovanella BC, Tainsky MA, Bradley A, Donehower LA. In vitro growth characteristics of embryo fibroblasts isolated from p53-deficient mice. Oncogene. 1993;8:2457-2467
20. Dimri GP, Itahana K, Acosta M, Campisi J. Regulation of a senescence checkpoint response by the E2F1 transcription factor and p14(ARF) tumor suppressor. Mol Cell Biol. 2000;20:273-285
21. Kamijo T, Zindy F, Roussel MF, Quelle DE, Downing JR, Ashmun RA, Grosveld G, Sherr CJ. Tumor suppression at the mouse INK4a locus mediated by the alternative reading frame product p19ARF. Cell. 1997;91:649-659
22. Ferbeyre G, de Stanchina E, Querido E, Baptiste N, Prives C, Lowe SW. PML is induced by oncogenic ras and promotes premature senescence. Genes Dev. 2000;14:2015-2027
23. Pearson M, Carbone R, Sebastiani C, Cioce M, Fagioli M, Saito S, Higashimoto Y, Appella E, Minucci S, Pandolfi PP, Pelicci PG. PML regulates p53 acetylation and premature senescence induced by oncogenic Ras. Nature. 2000;406:207-210
24. Hara E, Smith R, Parry D, Tahara H, Stone S, Peters G. Regulation of p16CDKN2 expression and its implications for cell immortalization and senescence. Mol Cell Biol. 1996;16:859-867
25. Alcorta DA, Xiong Y, Phelps D, Hannon G, Beach D, Barrett JC. Involvement of the cyclin-dependent kinase inhibitor p16 (INK4a) in replicative senescence of normal human fibroblasts. Proc Natl Acad Sci U S A. 1996;93:13742-13747
26. Atadja P, Wong H, Garkavtsev I, Veillette C, Riabowol K. Increased activity of p53 in senescing fibroblasts. Proc Natl Acad Sci U S A. 1995;92:8348-8352
27. Jacobs JJ, Kieboom K, Marino S, DePinho RA, van Lohuizen M. The oncogene and Polycomb-group gene bmi-1 regulates cell proliferation and senescence through the ink4a locus. Nature. 1999;397:164-168
28. Itahana K, Campisi J, Dimri GP. Mechanisms of cellular senescence in human and mouse cells. Biogerontology. 2004;5:1-10
29. Lin AW, Barradas M, Stone JC, van Aelst L, Serrano M, Lowe SW. Premature senescence involving p53 and p16 is activated in response to constitutive MEK/MAPK mitogenic signaling. Genes Dev. 1998;12:3008-3019
30. Narita M, Nunez S, Heard E, Lin AW, Hearn SA, Spector DL, Hannon GJ, Lowe SW. Rb-mediated heterochromatin formation and silencing of E2F target genes during cellular senescence. Cell. 2003;113:703-716
31. Hermeking H, Eick D. Mediation of c-Myc-induced apoptosis by p53. Science. 1994;265:2091-2093
32. Zindy F, Eischen CM, Randle DH, Kamijo T, Cleveland JL, Sherr CJ, Roussel MF. Myc signaling via the ARF tumor suppressor regulates p53-dependent apoptosis and immortalization. Genes Dev. 1998;12:2424-2433
33. Lin HJ, Eviner V, Prendergast GC, White E. Activated H-ras rescues E1A-induced apoptosis and cooperates with E1A to overcome p53-dependent growth arrest. Mol Cell Biol. 1995;15:4536-4544
34. Vogelstein B, Kinzler KW. The multistep nature of cancer. Trends Genet. 1993;9:138-141
35. Bodnar AG, Ouellette M, Frolkis M, Holt SE, Chiu CP, Morin GB, Harley CB, Shay JW, Lichtsteiner S, Wright WE. Extension of life-span by introduction of telomerase into normal human cells. Science. 1998;279:349-352

36. Kiyono T, Foster SA, Koop JI, McDougall JK, Galloway DA, Klingelhutz AJ. Both Rb/p16INK4a inactivation and telomerase activity are required to immortalize human epithelial cells. Nature. 1998;396:84-88
37. Hahn WC, Counter CM, Lundberg AS, Beijersbergen RL, Brooks MW, Weinberg RA. Creation of human tumour cells with defined genetic elements. Nature. 1999;400:464-468
38. Seger YR, Garcia-Cao M, Piccinin S, Cunsolo CL, Doglioni C, Blasco MA, Hannon GJ, Maestro R. Transformation of normal human cells in the absence of telomerase activation. Cancer Cell. 2002;2:401-413
39. Land H, Parada LF, Weinberg RA. Cellular oncogenes and multistep carcinogenesis. Science. 1983;222:771-778
40. Nowak MA, Komarova NL, Sengupta A, Jallepalli PV, Shih Ie M, Vogelstein B, Lengauer C. The role of chromosomal instability in tumor initiation. Proc Natl Acad Sci U S A. 2002;99:16226-16231
41. Weinberg RA. Oncogenes, antioncogenes, and the molecular bases of multistep carcinogenesis. Cancer Res. 1989;49:3713-3721
42. Balmain A, Pragnell IB. Mouse skin carcinomas induced in vivo by chemical carcinogens have a transforming Harvey-ras oncogene. Nature. 1983;303:72-74
43. Balmain A, Ramsden M, Bowden GT, Smith J. Activation of the mouse cellular Harvey-ras gene in chemically induced benign skin papillomas. Nature. 1984;307:658-660
44. Guerrero I, Calzada P, Mayer A, Pellicer A. A molecular approach to leukemogenesis: mouse lymphomas contain an activated c-ras oncogene. Proc Natl Acad Sci U S A. 1984;81:202-205
45. Chin L, Tam A, Pomerantz J, Wong M, Holash J, Bardeesy N, Shen Q, O'Hagan R, Pantginis J, Zhou H, Horner JW, 2nd, Cordon-Cardo C, Yancopoulos GD, DePinho RA. Essential role for oncogenic Ras in tumour maintenance. Nature. 1999;400:468-472
46. Fisher GH, Wellen SL, Klimstra D, Lenczowski JM, Tichelaar JW, Lizak MJ, Whitsett JA, Koretsky A, Varmus HE. Induction and apoptotic regression of lung adenocarcinomas by regulation of a K-Ras transgene in the presence and absence of tumor suppressor genes. Genes Dev. 2001;15:3249-3262
47. Jackson EL, Willis N, Mercer K, Bronson RT, Crowley D, Montoya R, Jacks T, Tuveson DA. Analysis of lung tumor initiation and progression using conditional expression of oncogenic K-ras. Genes Dev. 2001;15:3243-3248
48. Johnson L, Mercer K, Greenbaum D, Bronson RT, Crowley D, Tuveson DA, Jacks T. Somatic activation of the K-ras oncogene causes early onset lung cancer in mice. Nature. 2001;410:1111-1116
49. Zarbl H, Sukumar S, Arthur AV, Martin-Zanca D, Barbacid M. Direct mutagenesis of Ha-ras-1 oncogenes by N-nitroso-N-methylurea during initiation of mammary carcinogenesis in rats. Nature. 1985;315:382-385
50. Wiseman RW, Stowers SJ, Miller EC, Anderson MW, Miller JA. Activating mutations of the c-Ha-ras protooncogene in chemically induced hepatomas of the male B6C3 F1 mouse. Proc Natl Acad Sci U S A. 1986;83:5825-5829
51. Sukumar S, Notario V, Martin-Zanca D, Barbacid M. Induction of mammary carcinomas in rats by nitroso-methylurea involves malignant activation of H-ras-1 locus by single point mutations. Nature. 1983;306:658-661
52. Bos JL. ras oncogenes in human cancer: a review. Cancer Res. 1989;49:4682-4689
53. Margolis B, Skolnik EY. Activation of Ras by receptor tyrosine kinases. J Am Soc Nephrol. 1994;5:1288-1299

54. Kirsten WH, Somers KD, Mayer LA. Multiplicity of cell response to a murine erythroblastosis virus. Bibl Haematol. 1968;30:64-65
55. Harvey JJ. An Unidentified Virus Which Causes the Rapid Production of Tumours in Mice. Nature. 1964;204:1104-1105
56. Reddy EP, Reynolds RK, Santos E, Barbacid M. A point mutation is responsible for the acquisition of transforming properties by the T24 human bladder carcinoma oncogene. Nature. 1982;300:149-152
57. Tabin CJ, Bradley SM, Bargmann CI, Weinberg RA, Papageorge AG, Scolnick EM, Dhar R, Lowy DR, Chang EH. Mechanism of activation of a human oncogene. Nature. 1982;300:143-149
58. Bar-Sagi D. A Ras by any other name. Mol Cell Biol. 2001;21:1441-1443
59. Malumbres M, Barbacid M. RAS oncogenes: the first 30 years. Nat Rev Cancer. 2003;3:459-465
60. Chesa PG, Rettig WJ, Melamed MR, Old LJ, Niman HL. Expression of p21ras in normal and malignant human tissues: lack of association with proliferation and malignancy. Proc Natl Acad Sci U S A. 1987;84:3234-3238
61. Leon J, Guerrero I, Pellicer A. Differential expression of the ras gene family in mice. Mol Cell Biol. 1987;7:1535-1540
62. Muller R, Slamon DJ, Adamson ED, Tremblay JM, Muller D, Cline MJ, Verma IM. Transcription of c-onc genes c-rasKi and c-fms during mouse development. Mol Cell Biol. 1983;3:1062-1069
63. Furth ME, Aldrich TH, Cordon-Cardo C. Expression of ras proto-oncogene proteins in normal human tissues. Oncogene. 1987;1:47-58
64. Baltimore D. Our genome unveiled. Nature. 2001;409:814-816
65. Strahl BD, Allis CD. The language of covalent histone modifications. Nature. 2000;403:41-45
66. Wolffe AP, Pruss D. Deviant nucleosomes: the functional specialization of chromatin. Trends Genet. 1996;12:58-62
67. Wolffe AP, Guschin D. Review: chromatin structural features and targets that regulate transcription. J Struct Biol. 2000;129:102-122
68. Kornberg RD. Chromatin structure: a repeating unit of histones and DNA. Science. 1974;184:868-871
69. Kornberg RD, Thomas JO. Chromatin structure; oligomers of the histones. Science. 1974;184:865-868
70. Luger K, Mader AW, Richmond RK, Sargent DF, Richmond TJ. Crystal structure of the nucleosome core particle at 2.8 A resolution. Nature. 1997;389:251-260
71. Arents G, Burlingame RW, Wang BC, Love WE, Moudrianakis EN. The nucleosomal core histone octamer at 3.1 A resolution: a tripartite protein assembly and a left-handed superhelix. Proc Natl Acad Sci U S A. 1991;88:10148-10152
72. Cheung P, Allis CD, Sassone-Corsi P. Signaling to chromatin through histone modifications. Cell. 2000;103:263-271
73. Krebs JE, Fry CJ, Samuels ML, Peterson CL. Global role for chromatin remodeling enzymes in mitotic gene expression. Cell. 2000;102:587-598
74. Georgel PT, Tsukiyama T, Wu C. Role of histone tails in nucleosome remodeling by Drosophila NURF. Embo J. 1997;16:4717-4726
75. Lee KM, Sif S, Kingston RE, Hayes JJ. hSWI/SNF disrupts interactions between the H2A N-terminal tail and nucleosomal DNA. Biochemistry. 1999;38:8423-8429
76. Jenuwein T, Allis CD. Translating the histone code. Science. 2001;293:1074-1080
77. Turner BM. Histone acetylation and an epigenetic code. Bioessays. 2000;22:836-845

78. Grant PA. A tale of histone modifications. Genome Biol. 2001;2:REVIEWS0003
79. Lachner M, Jenuwein T. The many faces of histone lysine methylation. Curr Opin Cell Biol. 2002;14:286-298
80. Lachner M, O'Sullivan RJ, Jenuwein T. An epigenetic road map for histone lysine methylation. J Cell Sci. 2003;116:2117-2124
81. Bannister AJ, Kouzarides T. Histone methylation: recognizing the methyl mark. Methods Enzymol. 2004;376:269-288
82. Stallcup MR. Role of protein methylation in chromatin remodeling and transcriptional regulation. Oncogene. 2001;20:3014-3020
83. Feng Q, Wang H, Ng HH, Erdjument-Bromage H, Tempst P, Struhl K, Zhang Y. Methylation of H3-lysine 79 is mediated by a new family of HMTases without a SET domain. Curr Biol. 2002;12:1052-1058
84. Lacoste N, Utley RT, Hunter JM, Poirier GG, Cote J. Disruptor of telomeric silencing-1 is a chromatin-specific histone H3 methyltransferase. J Biol Chem. 2002;277:30421-30424
85. Ng HH, Feng Q, Wang H, Erdjument-Bromage H, Tempst P, Zhang Y, Struhl K. Lysine methylation within the globular domain of histone H3 by Dot1 is important for telomeric silencing and Sir protein association. Genes Dev. 2002;16:1518-1527
86. van Leeuwen F, Gafken PR, Gottschling DE. Dot1p modulates silencing in yeast by methylation of the nucleosome core. Cell. 2002;109:745-756
87. Waterborg JH. Dynamic methylation of alfalfa histone H3. J Biol Chem. 1993;268:4918-4921
88. Paik WK, Kim S. Protein methylation. Science. 1971;174:114-119
89. Steele-Perkins G, Fang W, Yang XH, Van Gele M, Carling T, Gu J, Buyse IM, Fletcher JA, Liu J, Bronson R, Chadwick RB, de la Chapelle A, Zhang X, Speleman F, Huang S. Tumor formation and inactivation of RIZ1, an Rb-binding member of a nuclear protein-methyltransferase superfamily. Genes Dev. 2001;15:2250-2262
90. Kim KC, Geng L, Huang S. Inactivation of a histone methyltransferase by mutations in human cancers. Cancer Res. 2003;63:7619-7623
91. Wustmann G, Szidonya J, Taubert H, Reuter G. The genetics of position-effect variegation modifying loci in Drosophila melanogaster. Mol Gen Genet. 1989;217:520-527
92. Reuter G, Spierer P. Position effect variegation and chromatin proteins. Bioessays. 1992;14:605-612
93. Rea S, Eisenhaber F, O'Carroll D, Strahl BD, Sun ZW, Schmid M, Opravil S, Mechtler K, Ponting CP, Allis CD, Jenuwein T. Regulation of chromatin structure by site-specific histone H3 methyltransferases. Nature. 2000;406:593-599
94. Firestein R, Cui X, Huie P, Cleary ML. Set domain-dependent regulation of transcriptional silencing and growth control by SUV39H1, a mammalian ortholog of Drosophila Su(var)3-9. Mol Cell Biol. 2000;20:4900-4909
95. Jenuwein T, Laible G, Dorn R, Reuter G. SET domain proteins modulate chromatin domains in eu- and heterochromatin. Cell Mol Life Sci. 1998;54:80-93
96. Deplus R, Brenner C, Burgers WA, Putmans P, Kouzarides T, de Launoit Y, Fuks F. Dnmt3L is a transcriptional repressor that recruits histone deacetylase. Nucleic Acids Res. 2002;30:3831-3838
97. Fuks F, Burgers WA, Brehm A, Hughes-Davies L, Kouzarides T. DNA methyltransferase Dnmt1 associates with histone deacetylase activity. Nat Genet. 2000;24:88-91
98. Fuks F, Hurd PJ, Deplus R, Kouzarides T. The DNA methyltransferases associate with HP1 and the SUV39H1 histone methyltransferase. Nucleic Acids Res. 2003;31:2305-2312

99. Lehnertz B, Ueda Y, Derijck AA, Braunschweig U, Perez-Burgos L, Kubicek S, Chen T, Li E, Jenuwein T, Peters AH. Suv39h-mediated histone H3 lysine 9 methylation directs DNA methylation to major satellite repeats at pericentric heterochromatin. Curr Biol. 2003;13:1192-1200
100. Peters AH, O'Carroll D, Scherthan H, Mechtler K, Sauer S, Schofer C, Weipoltshammer K, Pagani M, Lachner M, Kohlmaier A, Opravil S, Doyle M, Sibilia M, Jenuwein T. Loss of the Suv39h histone methyltransferases impairs mammalian heterochromatin and genome stability. Cell. 2001;107:323-337
101. O'Carroll D, Scherthan H, Peters AH, Opravil S, Haynes AR, Laible G, Rea S, Schmid M, Lebersorger A, Jerratsch M, Sattler L, Mattei MG, Denny P, Brown SD, Schweizer D, Jenuwein T. Isolation and characterization of Suv39h2, a second histone H3 methyltransferase gene that displays testis-specific expression. Mol Cell Biol. 2000;20:9423-9433
102. Nielsen SJ, Schneider R, Bauer UM, Bannister AJ, Morrison A, O'Carroll D, Firestein R, Cleary M, Jenuwein T, Herrera RE, Kouzarides T. Rb targets histone H3 methylation and HP1 to promoters. Nature. 2001;412:561-565
103. Vandel L, Nicolas E, Vaute O, Ferreira R, Ait-Si-Ali S, Trouche D. Transcriptional repression by the retinoblastoma protein through the recruitment of a histone methyltransferase. Mol Cell Biol. 2001;21:6484-6494
104. Haupt Y, Harris AW, Adams JM. Retroviral infection accelerates T lymphomagenesis in E mu-N-ras transgenic mice by activating c-myc or N-myc. Oncogene. 1992;7:981-986
105. Jacks T, Remington L, Williams BO, Schmitt EM, Halachmi S, Bronson RT, Weinberg RA. Tumor spectrum analysis in p53-mutant mice. Curr Biol. 1994;4:1-7
106. Schmitt CA, Fridman JS, Yang M, Baranov E, Hoffman RM, Lowe SW. Dissecting p53 tumor suppressor functions in vivo. Cancer Cell. 2002;1:289-298
107. Chang BD, Watanabe K, Broude EV, Fang J, Poole JC, Kalinichenko TV, Roninson IB. Effects of p21Waf1/Cip1/Sdi1 on cellular gene expression: implications for carcinogenesis, senescence, and age-related diseases. Proc Natl Acad Sci U S A. 2000;97:4291-4296
108. Sherr CJ, DePinho RA. Cellular senescence: mitotic clock or culture shock? Cell. 2000;102:407-410
109. Schmitt CA, Fridman JS, Yang M, Lee S, Baranov E, Hoffman RM, Lowe SW. A senescence program controlled by p53 and p16INK4a contributes to the outcome of cancer therapy. Cell. 2002;109:335-346
110. Schmitt CA, McCurrach ME, de Stanchina E, Wallace-Brodeur RR, Lowe SW. INK4a/ARF mutations accelerate lymphomagenesis and promote chemoresistance by disabling p53. Genes Dev. 1999;13:2670-2677
111. Lyon MF. Gene action in the X-chromosome of the mouse (Mus musculus L.). Nature. 1961;190:372-373
112. Ait-Si-Ali S, Guasconi V, Fritsch L, Yahi H, Sekhri R, Naguibneva I, Robin P, Cabon F, Polesskaya A, Harel-Bellan A. A Suv39h-dependent mechanism for silencing S-phase genes in differentiating but not in cycling cells. Embo J. 2004;23:605-615
113. Guerra C, Mijimolle N, Dhawahir A, Dubus P, Barradas M, Serrano M, Campuzano V, Barbacid M. Tumor induction by an endogenous K-ras oncogene is highly dependent on cellular context. Cancer Cell. 2003;4:111-120
114. Benanti JA, Galloway DA. Normal human fibroblasts are resistant to RAS-induced senescence. Mol Cell Biol. 2004;24:2842-2852

115. Collado M, Gil J, Efeyan A, Guerra C, Schuhmacher AJ, Barradas M, Benguria A, Zaballos A, Flores JM, Barbacid M, Beach D, Serrano M. Tumour biology: senescence in premalignant tumours. Nature. 2005;436:642
116. Michaloglou C, Vredeveld LC, Soengas MS, Denoyelle C, Kuilman T, van der Horst CM, Majoor DM, Shay JW, Mooi WJ, Peeper DS. BRAFE600-associated senescence-like cell cycle arrest of human naevi. Nature. 2005;436:720-724
117. Chen Z, Trotman LC, Shaffer D, Lin HK, Dotan ZA, Niki M, Koutcher JA, Scher HI, Ludwig T, Gerald W, Cordon-Cardo C, Pandolfi PP. Crucial role of p53-dependent cellular senescence in suppression of Pten-deficient tumorigenesis. Nature. 2005;436:725-730
118. Lazzerini Denchi E, Attwooll C, Pasini D, Helin K. Deregulated E2F activity induces hyperplasia and senescence-like features in the mouse pituitary gland. Mol Cell Biol. 2005;25:2660-2672
119. Braig M, Lee S, Loddenkemper C, Rudolph C, Peters AH, Schlegelberger B, Stein H, Dorken B, Jenuwein T, Schmitt CA. Oncogene-induced senescence as an initial barrier in lymphoma development. Nature. 2005;436:660-665
120. Shi Y, Lan F, Matson C, Mulligan P, Whetstine JR, Cole PA, Casero RA. Histone demethylation mediated by the nuclear amine oxidase homolog LSD1. Cell. 2004;119:941-953
121. Metzger E, Wissmann M, Yin N, Muller JM, Schneider R, Peters AH, Gunther T, Buettner R, Schule R. LSD1 demethylates repressive histone marks to promote androgen-receptor-dependent transcription. Nature. 2005;437:436-439
122. Tsukada Y, Fang J, Erdjument-Bromage H, Warren ME, Borchers CH, Tempst P, Zhang Y. Histone demethylation by a family of JmjC domain-containing proteins. Nature. 2006;439:811-816
123. Whetstine JR, Nottke A, Lan F, Huarte M, Smolikov S, Chen Z, Spooner E, Li E, Zhang G, Colaiacovo M, Shi Y. Reversal of histone lysine trimethylation by the JMJD2 family of histone demethylases. Cell. 2006;125:467-481
124. Timmermann S, Lehrmann H, Polesskaya A, Harel-Bellan A. Histone acetylation and disease. Cell Mol Life Sci. 2001;58:728-736
125. Bracken AP, Pasini D, Capra M, Prosperini E, Colli E, Helin K. EZH2 is downstream of the pRB-E2F pathway, essential for proliferation and amplified in cancer. Embo J. 2003;22:5323-5335
126. Kleer CG, Cao Q, Varambally S, Shen R, Ota I, Tomlins SA, Ghosh D, Sewalt RG, Otte AP, Hayes DF, Sabel MS, Livant D, Weiss SJ, Rubin MA, Chinnaiyan AM. EZH2 is a marker of aggressive breast cancer and promotes neoplastic transformation of breast epithelial cells. Proc Natl Acad Sci U S A. 2003;100:11606-11611
127. Jacobs JJ, Keblusek P, Robanus-Maandag E, Kristel P, Lingbeek M, Nederlof PM, van Welsem T, van de Vijver MJ, Koh EY, Daley GQ, van Lohuizen M. Senescence bypass screen identifies TBX2, which represses Cdkn2a (p19(ARF)) and is amplified in a subset of human breast cancers. Nat Genet. 2000;26:291-299
128. Vance KW, Carreira S, Brosch G, Goding CR. Tbx2 is overexpressed and plays an important role in maintaining proliferation and suppression of senescence in melanomas. Cancer Res. 2005;65:2260-2268

5.2 ATTACHMENTS

5.2.1 Summary table of mice characters

Early death group (time-to-death ≤ 180 days)

mouse	genotype		sex	time-to-death (d)	macro pathology (organs involved)				
					thymus	spleen	lymph nodes	liver	leukaemia
1	N-Ras	control	female	115	+	+	-	-	+
2	N-Ras	control	male	166	+	+	-	-	+
3	N-Ras	control	female	136	+	+	+	-	+
4	N-Ras	control	male	166	+	-	-	-	+
5	N-Ras	control	male	161	+	-	-	-	-
6	N-Ras	Suv39h1+/-	female	101	+	+	-	-	+
7	N-Ras	Suv39h1+/-	female	103	+	+	-	-	+
8	N-Ras	Suv39h1+/-	female	98	+	+	-	-	+
9	N-Ras	Suv39h1+/-	female	84	+	+	-	-	+
10	N-Ras	Suv39h1+/-	female	97	+	+	+	-	+
11	N-Ras	Suv39h1+/-	female	98	+	+	+	-	+
12	N-Ras	Suv39h1+/-	female	55	+	+	+	-	-
13	N-Ras	Suv39h1+/-	female	47	+	+	-	-	+
14	N-Ras	Suv39h1+/-	female	56	+	+	+	-	+
15	N-Ras	Suv39h1+/-	female	66	+	+	+	-	-
16	N-Ras	Suv39h1+/-	female	75	+	+	-	-	+
17	N-Ras	Suv39h1+/-	female	75	+	+	-	-	+
18	N-Ras	Suv39h1-	male	64	+	+	-	-	-
19	N-Ras	Suv39h1-	male	109	+	+	-	+	+
20	N-Ras	Suv39h1-	male	80	+	+	-	-	+
21	N-Ras	Suv39h1-	male	61	+	+	-	-	+
22	N-Ras	Suv39h1-	male	66	+	+	-	-	-
23	N-Ras	Suv39h1-	male	69	-	+	-	-	-
24	N-Ras	p53 +/-	female	78	+	-	-	-	+
25	N-Ras	p53 +/-	male	145	-	+	-	-	-
26	N-Ras	p53 +/-	male	90	+	-	-	-	+
27	N-Ras	p53 +/-	male	88	+	-	-	-	+
28	N-Ras	p53 +/-	male	147	-	+	-	-	-
29	N-Ras	p53 +/-	male	104	+	+	-	-	+
30	N-Ras	p53 +/-	female	109	+	+	-	-	+

Late death group (time-to-death > 180 days)

mouse	genotype		sex	time-to-death (d)	macro pathology (organs involved)				
					thymus	spleen	lymph nodes	liver	leukaemia
31	N-Ras	control	male	263	-	+	-	+	-
32	N-Ras	control	male	256	-	+	-	+	-
33	N-Ras	control	male	205	-	+	-	+	-
34	N-Ras	control	female	201	-	+	-	+	-
35	N-Ras	control	male	363	-	+	-	+	-
36	N-Ras	control	female	268	-	+	-	+	-
37	N-Ras	control	male	268	-	+	-	+	-
38	N-Ras	control	female	252	+	+	-	-	-
39	N-Ras	control	male	305	-	+	-	+	-
40	N-Ras	control	male	190	-	+	-	+	-

Table 2: Characteristics of terminal disease conditions in Eμ-N-Ras transgenic mice. Animals of the different genotypes were grouped according to time-do-death data (< 180 days early death; > 180 days late death). Pathological and clinical characteristics are listed.

5.2.2 p53 sequencing analysis

N-Ras controls

CS 750 p53 forward ex4:

CNCGNGNNNTGNNNNNCCGTNCTCTCCTCCCCTCaaTAAGCtaTTCTGCCagCTGGCGAAGACGTGCCCTGTGCAGTTGTG
GGTCAGCGCCACACCTCCAGCTGGGAGCCGTGTCCGCGCCATGGCCATCTACAAGAAGTCACAGCACATGACGGAGGTC
GTGAGACGCTGCCCCCACCATGAGCGCTGCTCCGATGGTGATGGCCTGGCTCCTCCCCAGCATCTTATCCGGGTGGAAG
GAAATTTGTATCCCGAGTATCTGGAAGACAGGCAGACTTTTCGCCACAGCGTGGTGGTACCTTATGAGCCACCCGAGGCC
GGCTCTgAGTATACCACCATCCACTACAAGTACATGTGTAATAGCTCCTGCATGGNGGGCATGAACCGCCGACCTATACTTA
CCATCATCACACTGGAAGACTCCAGTGGGAACCTTCTGGGACGGGACAGCTTTGAGGTTCGTGTTTGTGCCTGCCATGANA
GAGACCGCCGTACAGAAGAAGAAAATTTCAGCAAAAAGGAAGTCCTTTGTAATGAACTGCCCCCAGGGAGCGCAAAAGAGA
GCGCTGCCCACCTGCACAAGCGCATATAAACCGNNTAGAACANACCANTNGNTGGNGAGNGTNTCANACNNAAGANCNNN
GGGCGTGAACTCTTNGNGGTGGTNCGGGNGCTGNATGAGNCCTTAGAGTTAAGGNNTGCCCNNNCTANNNNNNGNGTNT
GGAGAN

CS 750 p53 reverse ex8:

NNGNNNNNAGGGCANGGCTTCCTTTTTGCGGAATTTTCTTCTTCTGTACGGCGGTCTCTCCCAGGGCAGGCACAAACACGA
ACCTCAAAGCTGTCCCGTCCCAGAAGGTTCCCACTGGAGTCTTCCAGTGTGATGATGGTAAGGATAGGTCGGCGGTTCATG
CCCCCCATGCAGGAGCTATTACACATGTACTTGTAGTGGATGGTGGTATACTCAGAGCCGGCCTCGGGTGGCTCATAAGGT
ACCACCACGCTGTGGCGAAAAGTCTGCCTGTCTTCCAGATACTCGGGATACAAATTTCCTTCCACCCGGATAAGATGCTGG
GGAGGAGCCAGGCCATCACCATCGGAGCAGCGCTCATGGTGGGGGCAGCGTCTCACGACCTCCGTCATGTGCTGTGACT
TCTTGtagATGGCCaTGGcgCgGACaCgGCTCCcAgCTNGGNGGNGNGNGCTNNCCCANAACTGCNCNGGCANNTNTTCGCC
ANNTNGNNNNNTNNTTATNGNGGGNNNNNGANNNNCCNNNAAANNNNNGNNNNNNNNNNNNNNNNNNNNNNNNANNN
NNNNNNNN

CS 746 p53 forward ex4:

NNNGNNNTNTGNNNNNNCGTNCTCTCCTCCCCTCAATAAGCTATTCTGCCaGCTGGCGAAGACGTGCCCTGTGCAGTTGTG
GGTCAGCGCCACACCTCCAGCTGGGAGCCGTGTCCGCGCCATGGCCATCTACAAGAAGTCACAGCACATGACGGAGGTC
GTGAGACGCTGCCCCCACCATGAGCGCTGCTCCGATGGTGATGGCCTGGCTCCTCCCCAGCATCTTATCCGGGTGGAAG
GAAATTTGTATCCCGAGTATCTGGAAGACAGGCAGACTTTTCGCCACAGCGTGGTGGTACCTTATGAGCCACCCGAGGCC
GGCTCTGAGTATACCACCATCCACTACAAGTACATGTGTAATAGCTCCTGCATGGGGGGCATGAACCGCCGACCTATCCTT
ACCATCATCACACTGGAAGACTCCAGTGGGAACCTTCTGGGACGGGACAGCTTTGAGGTTCGTGTTTGTGCCTGCCCTGG
GAGAGACCGCCGTACAGAAGAAGAAAATTTCCGCAAAAAGGAAGTCCTTTGCCCTGAACTGCCCCCAGGGAGCGCAAAGA
GAGCGCTGCCCACCTGCaCAAGCGCCTCTCCCCCGCAAAAGAAAAAACCACTTGATGGAGAGTATTTCACCCTCAAGATCC
GCGGGCGTaAACGCTTCGAGATGtTcCGGGagCTGaATGAGGCCTTAGagTTAAAGGaTGCCCATGCTNNANNNGNNTCTGN
NNNNAGCN

CS 746 p53 reverse ex8:

NNNNNNNANGGGCNNGNCTTCCTTTTTGCGGAATTTTCTTCTTCTGTACGGCGGTCTCTCCCAGGGCAGGCACAAACACGA
ACCTCAAAGCTGTCCCGTCCCAGAAGGTTCCCACTGGAGTCTTCCAGTGTGATGATGGTAAGGATAGGTCGGCGGTTCATG
CCCCCCATGCAGGAGCTATTACACATGTACTTGTAGTGGATGGTGGTATACTCAGAGCCGGCCTCGGGTGGCTCATAAGGT
ACCACCACGCTGTGGCGAAAAGTCTGCCTGTCTTCCAGATACTCGGGATACAAATTTCCTTCCACCCGGATAAGATGCTGG
GGAGGAGCCAGGCCATCACCATCGGAGCAGCGCTCATGGTGGGGGCAGCGTCTCACGACCTCCGTCATGTGCTGTGACT
TCTTGTAGATGGCCATGGCGCGGACACGGCTCCCAGCTGGAGGTGTGGCGCTGACCCACAACTGCACAGGGCACGTCTT
CGCCAGCTGGCAGAATAGCTTATTGAGGGGAGGAGAGTACGTGCACATAACAGACTTGGCTGTCCCAGACTGCAGGAAGC
CCAGGTGGAAGCCATAGTTGCCCTGGGTAAGACCCCACACACNANANGCGTGGTGTGGGGGGGAAAAAAAAAAAACATCT
NATGGAGAGNATTCNNNNCGGAGGANCGGNGGCTGAAAANCCTNNAGAGNNACGGGNNCTTNANNAGNNNGNNNNNTGA
ANACAGNCNCATCNCNNNNAGGNNNCTGGANNN

CS3054 p53 forward ex4:

NNNNNNNTNTGNNNNGNGCNGTNctcTCCTCCCCTCAATAAGCTATTCTGCCaGCTGGCGAAGACGTGCCCTGTGCAGTTGT
GGGTCAGCGCCACACCTCCAGCTGGGAGCCGTGTCCGCGCCATGGCCATCTACAAGAAGTCACAGCACATGACGGAGGT
CGTGAGACGCTGCCCCCACCATGAGCGCTGCTCCGATGGTGATGGCCTGGCTCCTCCCCAGCATCTTATCCGGGTGGAAG
GAAATTTGTATCCCGAGTATCTGGAAGACAGGCAGACTTTTCGCCACAGCGTGGTGGTACCTTATGAGCCACCCGAGGCC
GGCTCTGAGTATACCACCATCCACTACAAGTACATGTGTAATAGCTCCTGCATGGGGGGCATGAACCGCCGACCTATCCTT
ACCATCATCACACTGGAAGACTCCAGTGGGAACCTTCTGGGACGGGACAGCTTTGAGGTTCGTGTTTGTGCCTGCCCTGG
GAGAGACCGCCGTACAGAAGAAGAAAATTTCCGCAAAAAGGAAGTCCTTTGCCCTGAACTGCCCCCAGGGAGCGCAAAGA
GAGCGCTGcCCACCTGCACAAGCGCCTCTCCCCCGCAAAAGAAAAAACCACTTGATGGAGAGTATTTCACCCTCAAGATCC
GCGGGCGTAAACGCTTCGAGATGTTCCGGGaGCTGAATGAGGCCTTAGAGTTAAAGGATGCCCATGCTNCANNNNGAGTC
TGGAGACAGCAGGGNTCANN

CS3054 p53 reverse ex8:

TNNNGGNNNNNNNNNNCTTCCTTTTTGCGGAATTTTCTTCTTCTGTACGGCGGTCTCTCCCAGGGCAGGCACAAACACGAA
CCTCAAAGCTGTCCCGTCCCAGAAGGTTCCCACTGGAGTCTTCCAGTGTGATGATGGTAAGGATAGGTCGGCGGTTCATG
CCCCCCATGCAGGAGCTATTACACATGTACTTGTAGTGGATGGTGGTATACTCAGAGCCGGCCTCGGGTGGCTCATAAGGT
ACCACCACGCTGTGGCGAAAAGTCTGCCTGTCTTCCAGATACTCGGGATACAAATTTCCTTCCACCCGGATAAGATGCTGG
GGAGGAGCCAGGCCATCACCATCGGAGCAGCGCTCATGGTGGGGGCAGCGTCTCACGACCTCCGTCATGTGCTGTGACT
TCTTGTAGATGGCCATGGCGCGGACACGGCTCCCAGCTGGAGGTGTGGCGCTGACCCACAACTGCACAGGGCACGTCTT
CGCCAGCTGGCAGAATAGCTTATTGAGGGGAGGAGAGTACGTGCACATAACAGACTTGGCTGTCCCAGACTGCAGGAAGC
CCAGGTGGAAGCCATAGTTGCCCTGGGTAAGNNNNCACCNTCCACAANNANNACNTGCGCGGAAAAAAAAAAAAANACTT
NNTGGNNGANCTTNTNNNGNNGGGNGCGNNGNNNNNNNCANNNTCCTGNANCTACTNNTTGCTNNNTNTANGNNANNNN
CAANANCAGNNNCACCCCNNNAGNNTGGNNNNNNNN

CS3061 p53 forward ex4:

NNNNNNNTNTGNNNNGNGCNGTNctcTCCTCCCCTCAATAAGCTATTCTGCCaGCTGGCGAAGACGTGCCCTGTGCAGTTGT
GGGTCAGCGCCACACCTCCAGCTGGGAGCCGTGTCCGCGCCATGGCCATCTACAAGAAGTCACAGCACATGACGGAGGT
CGTGAGACGCTGCCCCCACCATGAGCGCTGCTCCGATGGTGATGGCCTGGCTCCTCCCCAGCATCTTATCCGGGTGGAAG
GAAATTTGTATCCCGAGTATCTGGAAGACAGGCAGACTTTTCGCCACAGCGTGGTGGTACCTTATGAGCCACCCGAGGCC

GGCTCTGAGTATACCACCATCCACTACAAGTACATGTGTAATAGCTCCTGCATGGGGGGCATGAACCGCCGACCTATCCTT
ACCATCATCACACTGGAAGACTCCAGTGGGAACCTTCTGGGACGGGACAGCTTTGAGGTTCGTGTTTGTGCCTGCCCTGG
GAGAGACCGCCGTACAGAAGAAGAAAATTTCCGCAAAAAGGAAGTCCTTTGCCCTGAACTGCCCCCAGGGAGCGCAAAGA
GAGCGCTGcCCACCTGCACAAGCGCCTCTCCCCCGCAAAAGAAAAAACCACTTGATGGAGAGTATTTCACCCTCAAGATCC
GCGGGCGTAAACGCTTCGAGATGTTCCGGGaGCTGAATGAGGCCTTAGAGTTAAAGGATGCCCATGCTNCANNNNGAGTC
TGGAGACAGCAGGGNTCANN

CS3061 p53 reverse ex8:

TNNNNNNTNGGGNNNNNTTCCTTTTTGCGgAATTTTCTTCTTCTGTACGGCGGTCTCTCCCAGGGCAGGCACAAACACGAA
CCTCAAAGCTGTCCCGTCCCAGAAGGTTCCCACTGGAGTCTTCCAGTGTGATGATGGTAAGGATAGGTCGGCGGTTCATG
CCCCCCATGCAGGAGCTATTACACATGTACTTGTAGTGGATGGTGGTATACTCAGAGCCGGCCTCGGGTGGCTCATAAGGT
ACCACCACGCTGTGGCGAAAAGTCTGCCTGTCTTCCAGATACTCGGGATACAAATTTCCTTCCACCCGGATAAGATGCTGG
GGAGGAGCCAGGCCATCACCATCGGAGCAGCGCTCATGGTGGGGGCAGCGTCTCACGACCTCCGTCATGTGCTGTGACT
TCTTGTAGATGGCCATGGCGCGGACACGGCTCCCAGCTGGAGGTGTGGCGCTGACCCACAACTGCACAGGGCACGTCTT
CGCCAGCTGGCAGAATAGCTTATTGAGGGGAGGAGAGTACGTGCACATAACAGACTTGGCTGTCCCAGACTGCAGGAAGC
CCAGGTGGAAGCCATAGTTGCNTNGTAAGACCCCCNCACNNNNNGANNAGTCTGGGNGGGAAAANAAAAAAACNANNTGN
GGGANGAGCTNNTGNNGNGGGACGCGNGNCCGANNACCNNNNNAGNTNCGGCTGNNTNATGNNNGNANAGNNNAGAAG
NNGNCNCNNNCNNNNNNNGNNNNNNN

CS2287 p53 forward ex4:

NNNNNNGTNTGNNNNNNCGTNCTCTCCTCCCCTCAATAAGCtATTCTGCCaGCTGGCGAAGACGTGCCCTGTGCAGTTGTG
GGTCAGCGCCACACCTCCAGCTGGGAGCCGTGTCCGCGCCATGGCCATCTACAAGAAGTCACAGCACATGACGGAGGTC
GTGAGACGCTGCCCCCACCATGAGCGCTGCTCCGATGGTGATGGCCTGGCTCCTCCCCAGCATCTTATCCGGGTGGAAG
GAAATTTGTATCCCGAGTATCTGGAAGACAGGCAGACTTTTCGCCACAGCGTGGTGGTACCTTATGAGCCACCCGAGGCC
GGCTCTGAGTATACCACCATCCACTACAAGTACATGTGTAATAGCTCCTGCATGGGGGGCATGAACCGCCGACCTATCCTT
ACCATCATCACACTGGAAGACTCCAGTGGGAACCTTCTGGGACGGGACAGCTTTGAGGTTCGTGTTTGTGCCTGCCCTGG
GAGAGACCGCCGTACAGAAGAAGAAAATTTCCGCAAAAAGGAAGTCCTTTGCCCTGAACTGCCCCCAGGGAGCGCAAAGA
GAGCGCTGCCCACCTGCACAAGCGCCTCTCCCCCGCAAAAGAAAAACCACTTGATGGAGAGTATTTCACCCTCAAGATCCG
CGGGCGTAAACGCTTCGaGATGTTCCGGGaGCTGAATGAGgCCTTAgaGTTAAAGGNTGCCNTGCTNNAGGNGGNGTCTGG
AGACNGCAGGCNNCANTCCNNCTACCTNNNACCAANAAGNN

CS2287 p53 reverse ex8:

NNNNNNNNNNNNNNNNNANGNNTTCCTTTTTGCGGAATTTTCTTCTTCTGTACGGCGGTCTCTCCCAGGGCAGGCACAAACA
CGAACCTCAAAGCTGTCCCGTCCCAGAAGGTTCCCACTGGAGTCTTCCAGTGTGATGATGGTAAGGATAGGTCGGCGGTT
CATGCCCCCCCATGCAGGAGCTATTACACATGTACTTGTAGTGGATGGTGGTATACTCAGAGCCGGCCTCGGGTGGCTCATA
AGGTACCACCACGCTGTGGCGAAAAGTCTGCCTGTCTTCCAGATACTCGGGATACAAATTTCCTTCCACCCGGATAAGATG
CTGGGGAGGAGCCAGGCCATCACCATCGGAGCAGCGCTCATGGTGGGGGCAGCGTCTCACGACCTCCGTCATGTGCTGT
GACTTCTTGTAGATGGCCATGGCGCGGACACGGCTCCCAGCTGGAGGTGTGGCGCTGACCCACAACTGCACAGGGCACG
TCTTCGCCAGCTGGCAGAATAGCTTATTGAGGGGAGGAGAGTACGTGCACATAACAGACTTGGCTGTCCCAGACTGCAGG
AAGCCCAGGTGGAAGCCATAGTTGCCCTGGGTTAAGANNNCCCCNCCCCANAGNGTTTTCGCGGGGAGAAAAAAANAACA
CCTNNTGGNGGGANTNTTTNCNGNNGGGTGGNGNGNNNCNNANNNNCNCNNNNGTTATGGGTGCCTGTTTTAGNGNNTG
GGNNNNNGNANAGANNNCCCNNTN

N-Ras Suv39h1 null

CS1446 p53 forward ex4:

CNNGNGNNNNGNNNTGTNNCGNCTCTCCTCCCCTCaaTAAGCtaTTCTGCCaGCTGGCGaAGACCNCCCCTGTGCTGTTGT
GGGTCAGCGCCACACCTCCAGCTGGGAGCCGTGTCCGCGCCATGGCCATCTACAAGAAGTCACAGCACATGACGGAGGT
CGTGAGACGCTGCCCCCACCATGAGCGCTGCTCCGATGGTGATGGCCTGGCTCCTCCCCAGCATCTTATCCGGGTGGAAG
GAAATTTGTATCCCGAGTATCTGGAAGACAGGCAGACTTTTCGCCACAGCGTGGTGGTACCTTATGAGCCACCCGAGGCC
GGCTCTGAGTATACCACCATCCACTACAAGTACATGTGTAATAGCTCCTGCATGGGGGGCATGAACCGCCGACCTATCCTT
ACCATCATCACACTGGAAGACTCCAGTGGGAACCTTCTGGGACGGGACAGCTTTGAGGTTCGTGTTTGTGCCTGCCCTGG
GAGAGACCGCCGTACAGAAGAAGAAAATTTCCGCAAAAAGGAAGTCCTTTGCCCTGAACTGCCCCCAGGGAGCGCAAAGA
GAGCGCTGCCCACCTGCACAAGCGCCTCTCCCCCGCAAAAGAAAAACCACTTGATGGAGAGTATTTCACCCTCAAGATCCG
CGGGCGTAAACGCTTCGAGATGTTCCGGGNGCTGAATGAGGCCTTANNGTTAAAGGNTGCCCATGCTACANNNGNGTCTG
NANNNNGCAGGGCNNNANTCCAGCTACNN

CS1446 reverse ex8:

NTNNNGTTNGGNCNNNGCTTCCTTTTTGCGGAATTTTCTTCTTCTGTACGGCGGTCTCTCCCAGGGCGGGCACAAACACGA
ACCTCAAAGCTGTCCCGTCCCAGAAGGTTCCCACTGGcGTCTTCCAGTGTGATGATGGTAAGGATAGGTCGGCGGTTCATG
CCCCCCATGCAGGAGCTATTACACATGTACTTGTAGTGGATGGTGGTATACTCAGAGCCGGCCTCGGGTGGCTCATAAGGT
ACCACCACGCTGTGGCGAAAAGTCTGCCTGTCTTCCAGATACTCGGGATACAAATTTCATTCCACCCGGATAAGATGCTGG
GGAGGAGCCAGGCCATAACCATCGGAGCAGCGCTCATGGTGGGGGCAGCGTCTCACGACCTCCGTCATGTGCTGTAACTT
CTTGTAGATGGCCATGGCGCGGACACGGCTCCCAGCTGGAGGTGTGGCGCTGACCCACAACTGCACAGGGCACGTCTTA
GCCAGCTGGCAAAATAACTTATTGAGGGGAGGAGAGTACGTGCACATCACAGACTTGgCTGTCCGAGACTGCAGAAAGCCg
AGGTGGAAGCCATAgTTGCCTGgGTAAGANAAAGAAAAACCACTTGATGGAGAGTATTTCACCCTCAAGATCCGCGGCGTA
ACNCTTCGANNTGTTCCNNNGCTGAATGANNCTTANNNTTAAGGNTGCCCATGCTACANANGAGTCTGGNNANGCAGGNTT
NANTNCAGNNNNNNTN

CS1447 p53 forward ex4:

NGCGCGTNTGTTTGNGCCGTaCTCTCCTCCCCTCAATAAGCtaTTCTGCCaGCTGGCGAAGACGTGCCCTGTGCAGTTGTG
GGTCAGCGCCACACCTCCAGCTGGGAGCCGTGTCCGCGCCATGGCCATCTACAAGAAGTCACAGCACATGACGGAGGTC
GTGAGACGCTGCCCCCACCATGAGCGCTGCTCCGATGGTGATGGCCTGGCTCCTCCCCAGCATCTTATCCGGGTGGAAG
GAAATTTGTATCCCGAGTATCTGGAAGACAGGCAGACTTTTCGCCACAGCGTGGTGGTACCTTATGAGCCACCCGAGGCC
GGCTCTGAGTATACCACCATCCACTACAAGTACATGTGTAATAGCTCCTGCATGGGGGGCATGAACCGCCGACCTATCCTT
ACCATCATCACACTGGAAGACTCCAGTGGGAACCTTCTGGGACGGGACAGCTTTGAGGTTCGTGTTTGTGCCTGCCCTGG
GAGAGACCGCCGTACAGAAGAAGAAAATTTCCGCAAAAAGGAAGTCCTTTGCCCTGAACTGCCCCCAGGGAGCGCAAAGA
GAGCGCTGCCCACCTGCACAAGCGCCTCTCCCCCGCAAAGAAAAAACCACTTGATGGAGAGTATTTCACCCTCAAGatCCG

CGGGCGTAAACGCTTCGAGATGTTCCGGGaGCTGAATGAGGCCTTAGAGTTAAAGGATGCCCNTGCTACANNNGNNNNTG
GAGNNNGCAGGGCTCANTCCAGCTACCTGAN

CS1447 p53 reverse ex8:

TNGGNGNNNNNCNNNNANNCCTTTTTGCGGAAATTTTCTTCTTCTGTACGGCGGTCTCTCCCAGGGCAGGCACAAACACGA
ACCTCAAAGCTGTCCCGTCCCAGAAGGTTCCCACTGGAGTCTTCCAGTGTGATGATGGTAAGGATAGGTCGGCGGTTCATG
CCCCCCATGCAGGAGCTATTACACATGTACTTGTAGTGGATGGTGGTATACTCAGAGCCGGCCTCGGGTGGCTCATAAGGT
ACCACCACGCTGTGGCGAAAAGTCTGCCTGTCTTCCAGATACTCGGGATACAAATTTCCTTCCACCCGGATAAGATGCTGG
GGAGGAGCCAGGCCATCACCATCGGAGCAGCGCTCATGGTGGGGGCAGCGTCTCACGACCTCCGTCATGTGCTGTGACT
TCTTGTAGATGGCCATGGCGCGGACACGGCTCCCAGCTGGAGGTGTGGCGCTGACCCACAACTGCACAGGGCACGTCTT
CGCCAGCTGGCAGAATAGCTTATTGAGGGGAGGAGAGTACGTGCACATAACAGACTTGGCTGTCCCAGACTGCAGGAAGC
CCAgGTGGAAGCCATAGTTGCCTGNNNNNNNNNNCCCCCCCCCACAAANGAGGTNGNGGGGGAAAANAAAAAAANNNNTN
NGNGACNAGTANTNNNNNNGNNNNNNNGNNNNCGNANANCCTCCAGNGCTTACGGGNTGCTGANGTAGGCCATANNNNN

CS1448 p53 forward ex4:

NNNNNNNTNNNNTTGNGCCgTaCTCTCCTCCCCTCAATAAGCtaTTCTGCCaGCTGGCGAAGACGTGCCCTGTGCAGTTGTG
GGTCAGCGCCACaCCTCCAGCTGGGAGCCGTGTCCGCGCCATGGCCATCTACAAGAAGTCACAGCACATGACGGAGGTC
GTGAGACGCTGCCCCCACCATGAGCGCTGCTCCGATGGTGATGGCCTGGCTCCTCCCCAGCATCTTATCCGGGTGGAAG
GAAATTTGTATCCCGAGTATCTGGAAGACAGGCAGACTTTTCGCCACAGCGTGGTGGTACCTTATGAGCCACCCGAGGCC
GGCTCTGAGTATACCACCATCCACTACAAGTACATGTGTAATAGCTCCTGCATGGGGGGCATGAACCGCCGACCTATCCTT
ACCATCATCACACTGGAAGACTCCAGTGGGAACCTTCTGGGACGGGACAGCTTTGAGGTTCGTGTTTGTGCCTGCCCTGG
GAGAGACCGCCGTACAGAAGAAGAAAATTTCCGCAAAAAGGAAGTCCTTTGCCCTGAACTGCCCCCAGGGAGCGCAAAGA
GAGCGCTGCCCACCTGCACAAGCGCCTCTCCCCCGCAAAAGAAAAAACCACTTGATGGAGAGTATTTCACCCTCAAGATCC
GCGGGCGTAAACGCTTCGAGATGTTCCGGGaGCTGAATGAGGCCTTAGAGTTAAAGGATGCCCATGCTACAGAGGAGTCT
GGAGNNAGCAGGGCTNNNTTCCNNCTACCNGNANNAC

CS1448 p53 reverse ex8:

NNNNNNGNNNGGNNANNNCTTCCTTTTTGCGGAAATTTTCTTCTTCTGTACGGCGGTCTCTCCCAGGGCAGGCACAAACAC
GAACCTCAAAGCTGTCCCGTCCCAGAAGGTTCCCACTGGAGTCTTCCAGTGTGATGATGGTAAGGATAGGTCGGCGGTTC
ATGCCCCCCCATGCAGGAGCTATTACACATGTACTTGTAGTGGATGGTGGTATACTCAGAGCCGGCCTCGGGTGGCTCATAA
GGTACCACCACGCTGTGGCGAAAAGTCTGCCTGTCTTCCAGATACTCGGGATACAAATTTCCTTCCACCCGGATAAGATGC
TGGGGAGGAGCCAGGCCATCACCATCGGAGCAGCGCTCATGGTGGGGGCAGCGTCTCACGACCTCCGTCATGTGCTGTG
ACTTCTTGTAGATGGCCATGGCGCGGACACGGCTCCCAGCTGGAGGTGTGGCGCTGACCCACAACTGCACAGGGCACGT
CTTCGCCAGCTGGCAGAATAGCTTATTGAGGGGAGGAGAGTACGTGCACATAACAGACTTGGCTGTCCCAGACTGCAGGA
AGCCCAGGTGGAAGCCATAGTTGCCCTGGGTAAGNNCCCCCACACACNANGGTNTNGNGGGGGNNAAANANANAANNAC
CTCGGGNCNAAACNCTTNGTGNGGGNNCCGCNNNGAANCANCNNCTNNGAGNNAAGNATNNTNNNNNAGNNNATAGNCN
NAAGNCNNNNNCTCTCNNTANN

CS1653 p53 forward ex4:

ANNNNNNNTcTGttaTGtGCCgTaCTCTCCTCCCCTCAATAAGCTATTCTGCCaGCTGGCGAAGACGTGCCCTGTGCAGTTGTG
GGTCAGCGCCACACCTCCAGCTGGGAGCCGTGTCCGCGCCATGGCCATCTACAAGAAGTCACAGCACATGACGGAGGTC
GTGAGACGCTGCCCCCACCATGAGCGCTGCTCCGATGGTGATGGCCTGGCTCCTCCCCAGCATCTTATCCGGGTGGAAG
GAAATTTGTATCCCGAGTATCTGGAAGACAGGCAGACTTTTCGCCACAGCGTGGTGGTACCTTATGAGCCACCCGAGGCC
GGCTCTGAGTATACCACCATCCACTACAAGTACATGTGTAATAGCTCCTGCATGGGGGGCATGAACCGCCGACCTATCCTT
ACCATCATCACACTGGAAGACTCCAGTGGGAACCTTCTGGGACGGGACAGCTTTGAGGTTCGTGTTTGTGCCTGCCCTGG
GAGAGACCGCCGTACAGAAGAAGAAAATTTCCGCAAAAAGGAAGTCCTTTGCCCTGAACTGCCCCCAGGGAGCGCAAAGA
GAGCGCTGCCCACCTGCACAAGCGCCTCTCCCCCGCAAAAGAAAAAACCACTTGATGGAGAGTATTTCACCCTCAAGATCCG
CGGGCGTAAACGCTTCGAGATGTTCCGGGagCTGATGAGGCCTTAGAGTTAAAGGATGCCCATGCTACAGNNGNGTCTGG
NGNCNGCAGGNNNTNACTCCNNCTACCTGNN

CS1653 p53 reverse ex8:

NTNNNNNNNNNNANNNCTTCCTTTTTTGCGGAAATTTTCTTCTTCTGTACGGCGGTCTCTCCCAGGGCAGGCACAAACACGA
ACCTCAAAGCTGTCCCGTCCCAGAAGGTTCCCACTGGAGTCTTCCAGTGTGATGATGGTAAGGATAGGTCGGCGGTTCATG
CCCCCCATGCAGGAGCTATTACACATGTACTTGTAGTGGATGGTGGTATACTCAGAGCCGGCCTCGGGTGGCTCATAAGGT
ACCACCACGCTGTGGCGAAAAGTCTGCCTGTCTTCCAGATACTCGGGATACAAATTTCCTTCCACCCGGATAAGATGCTGG
GGAGGAGCCAGGCCATCACCATCGGAGCAGCGCTCATGGTGGGGGCAGCGTCTCACGACCTCCGTCATGTGCTGTGACT
TCTTGTAGATGGCCATGGCGCGGACACGGCTCCCAGCTGGAGGTGTGGCGCTGACCCACAACTGCACAGGGCACGTCTT
CGCCAGCTGGCAGAATAGCTTATTGAGGGGAGGAGAGTACGTGCACATAACAGACTTGGCTGTCCCAGACTGCAGGAAGC
CCAGGTGGAAGCCATAGTTGCCCTGGGTAAGActNCCAACCGGCNATGGGGGTGCGGGGNAAAANANAAAACACCCGNGG
GCGAANACTCTGCGNGAGGTCNCGGCNNNNNNNACCCTCTAANTTAAAGGGTGCCGNATNATAGCATGGCNNNANANCNC
GCCNCCCCTCCTGTGNGGN

CS1654 p53 forward ex4:

NNNGNNNTcTGtTTGtGCCGTaCTCTCCTCCCCTCAATAAGCTaTTCTGCCaGCTGGCGAAGACGTGCCCTGTGCAGTTGTGG
GTCAGCGCCACACCTCCAGCTGGGAGCCGTGTCCGCGCCATGGCCATCTACAAGAAGTCACAGCACATGACGGAGGTCG
TGAGACGCTGCCCCCACCATGAGCGCTGCTCCGATGGTGATGGCCTGGCTCCTCCCCAGCATCTTATCCGGGTGGAAGGA
AATTTGTATCCCGAGTATCTGGAAGACAGGCAGACTTTTCGCCACAGCGTGGTGGTACCTTATGAGCCACCCGAGGCCGG
CTCTGAGTATACCACCATCCACTACAAGTACATGTGTAATAGCTCCTGCATGGGGGGCATGAACCGCCGACCTATCCTTAC
CATCATCACACTGGAAGACTCCAGTGGGAACCTTCTGGGACGGGACAGCTTTGAGGTTCGTGTTTGTGCCTGCCCTGGGA
GAGACCGCCGTACAGAAGAAGAAAATTTCCGCAAAAAGGAAGTCCTTTGCCCTGAACTGCCCCCAGGGAGCGCAAAGAGA
GCGCTGCCCACCTGCACAAGCGCCTCTCCCCCGCAAAAGAAAAAACCACTTGATGGAGaGTATTTCACCCTcAAGATCCGC
GGGCGTAAACGCTTCGAGATGTTCCGGagCTGAATGAGGCCTTAGAGTTAAAGGATGCCCNTGCTACAGANGGAGTCTGG
NNNNNNCAGGGCTTCACTTCCNNCTNCCTNNN

CS1654 p53 reverse ex8:

NTGNNNGNNNGGNNNNNNCTTCCTTTTTGCGGAATTTTCTTCTTCTGTACGGCGGTCTCTCCCAGGGCAGGCACAAACACG
AACCTCAAAGCTGTCCCGTCCCAGAAGGTTCCCACTGGAGTCTTCCAGTGTGATGATGGTAAGGATAGGTCGGCGGTTCAT
GCCCCCCATGCAGGAGCTATTACACATGTACTTGTAGTGGATGGTGGTATACTCAGAGCCGGCCTCGGGTGGCTCATAAG
GTACCACCACGCTGTGGCGAAAAGTCTGCCTGTCTTCCAGATACTCGGGATACAAATTTCCTTCCACCCGGATAAGATGCT
GGGGAGGAGCCAGGCCATCACCATCGGAGCAGCGCTCATGGTGGGGGCAGCGTCTCACGACCTCCGTCATGTGCTGTGA
CTTCTTGTAGATGGCCATGGCGCGGACACGGCTCCCAGCTGGAGGTGTGGCGCTGACCCACAACTGCACAGGGCACGTC

TTCGCCAGCTGGCAGAATAGCTTATTGAGGGGAGGAGAGTACGTGCACATAACAGACTTGGCTGTCCCAGACTGCAGGAA
GCCCAGGTGGAAGCCATAGTTGCCTGGGTAAGANNNNCAANNANCAGGGGGTGGGGANNNANNAAAAAAAAANATCNNNG
NNCAAANCNCATGNNGTNGNNNGGGGCNCTGAANNNNNNNNGAGTNNNNGNNGCNNTATNNNNAGCATANNNTNNAAGC
NNAGCNNCNCCNNNNNANNNN

CS1847 p53 forward ex4:

NNNNNNNNTNTGNNNTGNNNNNGTaCTCTCCTCCCCTCAATAAGCTATTCTGCCaGCTGGCGAAGACGTGCCCTGTGCAGT
TGTGGGTCAGCGCCACACCTCCAGCTGGGAGCCGTGTCCGCGCCATGGCCATCTACAAGAAGTCACAGCACATGACGGA
GGTCGTGAGACGCTGCCCCCACCATGAGCGCTGCTCCGATGGTGATGGCCTGGCTCCTCCCCAGCATCTTATCCGGGTG
GAAGGAAATTTGTATCCCGAGTATCTGGAAGACAGGCAGACTTTTCGCCACAGCGTGGTGGTACCTTATGAGCCACCCGAG
GCCGGCTCTGAGTATACCACCATCCACTACAAGTACATGTGTAATAGCTCCTGCATGGGGGGCATGAACCGCCGACCTATC
CTTACCATCATCACACTGGAAGACTCCAGTGGGAACCTTCTGGGACGGGACAGCTTTGAGGTTCGTGTTTGTGCCTGCCCT
GGGAGAGACCGCCGTACAGAAGAAGAAAATTTCCGCAAAAAGGAAGTCCTTTGCCCTGAACTGCCCCCAGGGAGCGCAAA
GAGAGCGCTGCCCACCTGCACAAGCGCCTCTCCCCCGCAAAAGAAAAAACCACTTGATGGAGAGTATTTCACCCTCAAGAT
CCGCGGGCGTAAACGCTTCGAGATGTTCCGGGaGCTGAATGAGGCCTTAgagTTAAAGGNTGCCCATGCTACNNNGNAGTC
TGGAGACAGCAGGGCTTCANTNCNNCTACCNGGAGACN

CS1847 p53 reverse ex8:

ATNNNGNNNGGNNNNNNAttCCTTTTTGCGGAAATTTTCTTCTTCTGTACGGCGGTCTCTCCCAGGGCAGGCACAAACACGA
ACCTCAAAGCTGTCCCGTCCCAGAAGGTTCCCACTGGAGTCTTCCAGTGTGATGATGGTAAGGATAGGTCGGCGGTTCATG
CCCCCCATGCAGGAGCTATTACACATGTACTTGTAGTGGATGGTGGTATACTCAGAGCCGGCCTCGGGTGGCTCATAAGGT
ACCACCACGCTGTGGCGAAAAGTCTGCCTGTCTTCCAGATACTCGGGATACAAATTTCCTTCCACCCGGATAAGATGCTGG
GGAGGAGCCAGGCCATCACCATCGGAGCAGCGCTCATGGTGGGGGCAGCGTCTCACGACCTCCGTCATGTGCTGTGACT
TCTTGTAGATGGCCATGGCGCGGACACGGCTCCCAGCTGGAGGTGTGGCGCTGACCCACAACTGCACAGGGCACGTCTT
CGCCAGCTGGCAGAATAGCTTATTGAGGGGAGGAGAGTACGTGCACATAACAGACTTGGCTGTCCCAGACTGCANGAAGC
CCAGGTGGAAGCCATAGTTGCCTGGNTAAGANNNACANNCACCNANTGNGACGGNGNNGGAGNAANAAAAAAACATCTTCG
GGNNAGACNTCTTNNNGGAGGGANCGGCGCNNGAANNNCNNCTAGAGTTANNGCTNCCNNANNTNNNCAGTAGAGNTGG
AANACNGCCNNACNNCNNNNANNNNTGCNNNAN

5.2.3 Mouse anatomy *(Modified from www.geocities.com)*

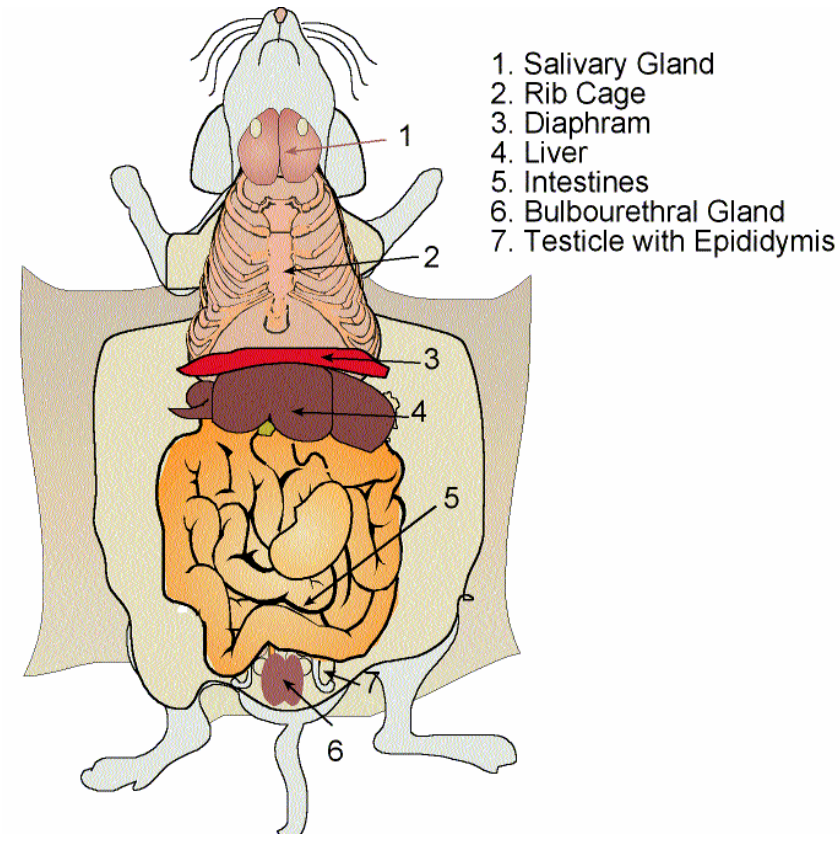

5.3 ABBREVATIONS

ARF	Alternate reading frame
APS	Ammoniumoersulfate
Bcl2	B cell lymphoma 2
Bp	Base pair
BSA	Bovine serum albumin
CDK4	Cyclin-dependent kinase 4
cDNA	Complementary DNA
dH_2O	Deionized water
DAPI	4',6-diamidino-2-phenylindole
DMEM	Dulbecco´s modified Eagle medium
DMFO	N,N-dimethylformamide
X-Gal	5-bromo-4-chloro-3-indolyl ß-D-galactoside
DMSO	Dimethylsulfoxid
DNA	Desoxyribonucleic acid
DNase	Deoxyribonuclease
DTT	Dithiothreitol
E. coli	*Escherichia coli*
EDTA	Ethylendiamintetraacetat = Titriplex III
FCS	Fetal calf serum
FITC	Fluoresceinisothiocyanat
GFP	Green-fluorescent protein
H3K9	Lysin 9 of Histone H3
H3K9met3	Tri-methylated Lysine 9 of Histone H3
HAT	Histone-Acetyltransferase
HDAC	Histone-Deacetylase
HEPES	N-2-hydroxyethylpiperazin-N'-2-ethanesulfonic acid
HMT	Histonemethyltransferase
HP1	Heterochromatin protein 1
IF	Immunofluorescence
IPT	Immunophenotyping
IL-7	Interleukin-7
IMDM	Iscove's modified Eagle's media
INK4	Inhibitor of CDK4
IRES	Internal ribosomal entry site
kb	Kilobase
LOH	Loss of heterozygosity
MAP	Mitogen-activated protein (kinase)
mRNA	Messenger-Ribonucleicacid
MSCV	Murine stem cell virus
mut	Mutated form of a gene or protein
NP-40	Nonidet P-40
PAGE	Polyacrylamid-gel electrophoresis
PBS	Phosphate Buffered Saline
PCR	Polymerase chain reaction
PML	Promyelocytic leukemia
PVDF	Poly vinylidene difluoride
Rb	Retinoblastoma protein
RNA	Ribonucleic acid
RNase	Ribonuclease

rpm	Rotations per minute
RT	Room temperature
SA-β-Gal	Senescence-associated β-galactosidase
SDS	Natriumdodecylsulfat
Su(var)3-9	Suppressor of variegation 3-9
TEMED	N,N,N´,N´-Tetramethylethylendiamin
Tris	Tris(hydroxymethyl)aminomethane
TritonX-100	Octylphenoldecaethylenglycolether
TUNEL	Terminal deoxynucleotidyl transferase mediated dUTP nick end labeling
Tween 20	Polyoxyethylensorbitanmonolaurat
wt	Wildtype form of a gene or protein

5.4 PUBLICATIONS

Ralph K. Lindemann, Melanie Braig, Pia Ballschmieter, Theresa A. Guise, Alfred Nordheim and Jürgen Dittmer:
„Protein kinase Cα regulates Ets1 transcriptional activity in invasive breast cancer cells.“
International Journal of Oncology, 2003; Volume 22: 799-805

Pia Ballschmieter, Melanie Braig, Ralph K. Lindemann, Alfred Nordheim and Jürgen Dittmer:
„Splicing variant ΔVII-Ets1 is downregulated in invasive Ets1-expressing breast cancer cells“
International Journal of Oncology, 2003; Volume 22: 849-853

Ralph K. Lindemann, Melanie Braig, Craig A. Hauser, Alfred Nordheim and Jürgen Dittmer:
„Ets2 mediates protein kinase C-induced expression of parathyroid hormone-related protein in MCF-7 breast cancer cells“
Biochemical Journal, 2003; Volume 372: 787-797

Melanie Braig, Soyoung Lee, Christoph Loddenkemper, Cornelia Rudolph, Antoine H.F.M. Peters, Brigitte Schlegelberger, Harald Stein, Bernd Dörken, Thomas Jenuwein and Clemens A. Schmitt:
„Oncogene-induced senescence as an initial barrier in lymphoma-development”
Nature, 2005; Volume 436: 660-665

Melanie Braig and Clemens A. Schmitt:
„Oncogene-induced senescence – pushing the brake of tumor development” Review.
Cancer Research, 2006; Volume 66: 2881-2884

6) ACKNOWLEDGEMENTS

An erster Stelle bedanke ich mich bei meinem Betreuer Herrn Prof. Dr. Clemens Schmitt für die Bereitstellung des Themas, die engagierte Betreuung, das fortwährende, enthusiastische Interesse an allen Experimenten und seine große Diskussionsbereitschaft.

Weiter möchte ich mich bei meinem offiziellen Doktorvater Herrn Prof. Dr. Wolfgang Uckert für die Übernahme meiner Betreuung bedanken, die Förderung bei der Zusammenstellung der Arbeit sowie die stete Gesprächs- und Hilfsbereitschaft.

Mein Dank gilt auch Prof. Dr. Reinhold Schäfer für die freundliche und unkomplizierte Übernahme des Drittgutachtens.

Herrn Prof. Dr. Bernd Dörken, Direktor der medizinischen Klinik für Hämatologie und Onkologie, danke ich für die finanzielle Unterstützung und die Möglichkeit, meine Doktorarbeit in seiner Abteilung anfertigen zu dürfen.

Prof. Dr. Lockau danke ich für die Übernahme des Vorsitzes, Prof. Leutz für die Teilnahme an der Prüfungskommission.

Ein großer Dank geht an alle derzeitigen und ehemaligen Labormitglieder der AG Schmitt. Ohne Eure Hilfe, Euren Sarkasmus und Humor hätte ich diese Zeit wohl nicht überstanden. Vielen Dank für die (schrecklichen) Mensagänge, das Ausleihen von Kleingeld zum Plündern des Süßigkeitenautomaten, etliche (sinnentleerte) Gespräche über „Grizzle“, Schuhe, den Sinn und Unsinn von SA-ß-gal und darüber dass es Schlimmer nicht sein könnte. Diese Zeit hat mir gezeigt, dass man auch auf $2m^2$ Arbeitsfläche promovieren kann, es sich lohnt immer einen alten Westerblot in der Hinterhand zu haben, es tatsächlich ein Leben nach Montag gibt und dass Superman vielleicht doch nicht die Welt rettet.

Des Weitern möchte ich mich bei Christoph Loddenkemper für eine exzellente Kooperation bedanken, seine freiwillige Umschulung zum Mauspathologen und seine unglaubliche Fähigkeit, „Dummies“ zu Füllen.

Mein größter Dank gilt meinen Freunden die stets ein großer Halt waren, meiner Familie und Stefan für Ihre Liebe und Unterstützung.

7) CURRICULUM VITAE

Melanie Braig

* 29.04.1978 (Biberach/Riß)

AUSBILDUNG

04/03-heute **Dissertation**

Charité Universitätsmedizin Berlin, Hämatologie / Onkologie / Tumor Immunologie (Prof. Clemens Schmitt) und Humboldt Universität, Abteilung Molekularbiologie (Prof. Wolfgang Uckert)
„Rolle der Histonmethyltransferase Suv39h1 in zellulärer Seneszenz und Ras-induzierter Lymphomgenese“

03/02-01/03 **Diplomarbeit**

Institut für Zellbiologie, Universität Tübingen, Abteilung Molekularbiologie (Prof. Alfred Nordheim)
„Regulation des humanen PTHrP Promotes durch Ets-Transkriptionsfaktoren und die Rolle von Proteinkinase C in nicht-invasiven Brustkrebszellen“

10/97-02/02 **Biologiestudium**

Eberhard-Karls-Universität Tübingen
Schwerpunkte: Zellbiologie, Humangenetik, Pharmakologie

08/83-06/97 **Schulbildung**

Kreisgymnasium Riedlingen / Progymnasium Bad Buchau

LABORERFAHRUNG

01/03-03/03 Universitätsklinikum Tübingen, Experimentelle Virologie (Prof. Iftner):
Quantitative real-time PCR (Taqman-Analysis) in Virus-induzierten Hautpappilomen und –karzinomen

11/01-02/02 Universitätsklinikum Tübingen, Tropenmedizin (Prof. Kremsner) und Universität Tübingen, Institut für Zellbiologie (Prof. Nordheim):
Promoterstudien und DNA/Protein-Interaktionen in EBV-infizierten B-Zelllinien

06/01-11/01 Universität Tübingen, Institut für Zellbiologie (Prof. Nordheim):
- Promoterstudien am Interleukin-5 Gen in T-Zelllinien
- Etablierung eines ChIP-Assays in Brustkrebszelllinien

SEMINARE

04/02 *ABI PRISM® 7000 Basic Training (quantitative real-time PCR)*
Applied Biosystems

09/05 *Seminar „Versuchstiere, Tierversuche und Alternativmethoden“*
Charité Universitätsmedizin & zebet Berlin
(Zertifiziert nach GV-SOLAS & FELASA Richtlinien)

VORTRÄGE UND PRÄSENTATIONEN AUF KONGRESSEN

10/04 **DGHO (Deutsche Gesellschaft für Hämatologie/Onkologie)**
Jahrestagung Innsbruck, Österreich

- Vortrag *“Impaired histone methylation promotes lymphoma development by oncogenic Ras through disruption of cellular senescence”*

12/04 **ASH (American Society of Hematology)**
Jahrestagung San Diego, USA

- Vortrag *“Impaired histone H3 methylation provokes*
- Travel Award *Ras-driven lymphomagenesis by disabling cellular senescence”*

02/07 **10th Lorne Cancer Conference**
Jahrestagung Lorne, Australien

- Poster *“Loss of the histone methyltransferase*
- Kongress-Stipendium (DFG) *Suv39h1 accelerates lymphomagenesis in response to oncogenic activation of endogenous ras alleles by N-nitroso-N-methylurea in vivo*

8) STATEMENT

Hiermit erkläre ich gemäß der Promotionsordnung der Humboldt-Universität zu Berlin vom 01. September 2005, dass ich

- die vorliegende Arbeit eigenständig und ohne Benutzung anderer als der angegebenen Hilfsmittel angefertigt habe. Alle aus anderen Quellen oder indirekt übernommenen Daten und Konzepte sowie Ergebnisse aus Kooperationsprojekten sind unter Angabe der Referenz gekennzeichnet;
- die Arbeit bisher in gleicher oder ähnlicher Form nicht in anderen Promotionsverfahren vorgelegt wurde;
- mir die geltende Promotionsordnung vom 01. September 2005 bekannt ist.

Berlin, 28.03.2007 Melanie Braig